Evaluation of Alternative Market Structure and Compensation Schemes for Incenting Transmission Reliability and Adequacy Related Investments

Final Project Report

Power Systems Engineering Research Center

A National Science Foundation
Industry/University Cooperative Research Center
since 1996

Power Systems Engineering Research Center

Evaluation of Alternative Market Structure and Compensation Schemes for Incenting Transmission Reliability and Adequacy Related Investments

Final Project Report

Research Team Faculty

Shijie Deng, Georgia Institute of Technology
Tim Mount, Cornell University
Shmuel Oren, University of California, Berkeley

Research Team Students

Haibin Sun and Jieyun Zhou, Georgia Institute of Technology
Jaeuk Ju, Cornell University
Kory Headman and Enzon Sauma, University of California, Berkeley

PSERC Publication 08-16

August 2008

Information about this project

For information about this project contact:

Shijie Deng, Ph.D.
Georgia Institute of Technology
School of Industrial and Systems Engineering
Atlanta, GA 30332
Tel: 404-894-6519
Fax: 404-894-2301
Email: deng@isye.gatech.edu

Power Systems Engineering Research Center

This is a project report from the Power Systems Engineering Research Center (PSERC). PSERC is a multi-university Center conducting research on challenges facing a restructuring electric power industry and educating the next generation of power engineers. More information about PSERC can be found at the Center's website: http://www.pserc.org.

For additional information, contact:

Power Systems Engineering Research Center
Arizona State University
577 Engineering Research Center
Box 878606
Tempe, AZ 85287-8606
Phone: 480-965-1643
Fax: 480-965-0745

Notice Concerning Copyright Material

Acknowledgements

This is the final report for the Power Systems Engineering Research Center (PSERC) research project entitled “Evaluation of Alternative Market Structure and Compensation Schemes for Incenting Transmission Reliability and Adequacy Related Investments.” (PSERC project M-11). The project began June 2005 and was completed in June 2007. We express our appreciation for the support provided by PSERC’s industrial members and by the National Science Foundation under grant NSF ECS-0134210 at Georgia Institute of Technology.

The authors thank all PSERC members for their technical advice on the project, especially Xiaoming Feng (ABB), Floyd Galvan (Entergy Corporation), Jonathan Mayo (NYISO), Mark Sanford (GE Energy), and Jianzhong Tong (PJM) who were our industry advisors.

Executive Summary

Incentives for attracting investments in transmission assets are essential to the overall success of the restructuring of the electric power industry. In general, adequate transmission capacity enhances reliability, lowers energy cost as delivered, limits market power of market participants, and provides flexibility to protect against market uncertainties such as load fluctuation, fuel price volatility, and unexpected facility outages.

Various transmission-pricing approaches have been developed for recovering transmission costs and providing incentives for future expansion or enforcement. According to the market-based investment model, a transmission investment usually expands power-transfer capability, and therefore, increases the quantity and variety of transmission rights can be issued to investors. This project tackles problems related to the evaluation of market-based schemes for compensating transmission investments.

I. Power system simulation approach for evaluating transmission reliability and adequacy related investments

First, alternative compensation mechanisms for compensating transmission network investment aimed at improving reliability and adequacy are documented. Then, the evaluation of reliability and adequacy transmission investment is performed through incorporating constraints on the transmission reliability margin (TRM) and the generation reserve margin into a fundamental power system simulation models with a Locational Marginal Price (LMP)-based market structure. Heuristic methods for identifying incremental financial transmission rights (FTRs) resulting from typical network-deepening or network-expanding transmission investment projects are illustrated.

Through a case study, we show that FTR-based compensation scheme does provide financial incentives for reliability and adequacy targeted transmission investments via allocating the incremental FTRs to investors. The magnitude of such incentives depends on the amount of incremental FTRs resulting from the investment. The quantity and value of the incremental FTRs further depend on the bid values, the transmission network topology and the initial configuration of the allocated FTRs. Thus, market-based compensation mechanisms, such as the one rewarding investors with incremental FTRs as tradable instruments for recovering sunk capital costs and hedging market risks, have the potential of adequately compensating the reliability or security constraint-relieving transmission investments.

II. Econometric modeling of the price of financial transmission rights

An econometric modeling framework for simulating the stochastic behavior of congestion costs of electricity in New York State is developed. The basic specification of the model is that the price of electricity in a specified zone (region) is a function of the corresponding load, the price of natural gas and a set of seasonal and daily variables. The estimated multivariate time-series models are then used to predict the average daily prices in various zones in New York for the summer of 2006. Since the estimated models are based on information that is available before the auction to sell the FTRs, it is appropriate to use these models to evaluate the financial risk of purchasing FTRs in the auction.

The financial risk of the FTRs in New York, namely the TCCs, for the summer of 2006 is evaluated from two different perspectives. First, the risk of hedging for a generator comes primarily from uncertainty about the actual daily temperatures next summer. Second, the risk for speculators comes from the combined uncertainty about future temperatures and future prices of natural gas. Through this process, the predicted price differences can be used as a basis for measuring the magnitude and financial riskiness of congestion costs for a specified financial transmission right. This analysis has demonstrated successfully the feasibility of using an econometric model to simulate the financial riskiness of the payout from holding FTRs using only information known prior to the FTR auction.

III. Forward price risk premium and implications for transmission investments

We examine the risk premium present in the electricity day-ahead forward price over the real-time spot price. This study establishes a quantitative model for incorporating transmission congestion into the analysis of electricity day-ahead forward risk premium.

Through simulations with a three-bus study system, it is illustrated that the more frequently transmission congestion happens, the higher the forward prices get at the load buses. Consistent with the implications of the 3-bus model, evidences from empirical studies using the New York electricity market data confirm that there exists a significant statistical relationship between the day-ahead forward risk premium and the shadow price premiums on congested transmission flowgates.

IV. Nonparametric modeling of the Hub-and-Spoke Representation of a Network

We investigated an effective non-parametric approach for identifying proxy trading hubs in an LMP-based market for the purpose of approximating correct incentives for inducing efficient capacity investment in generation and transmission through a small set of financial transmission rights such as FTRs or TCCs. We developed a non-parametric dimension reduction method for modeling the structure of the LMPs at major zones in a bulk power system. Using this model, we can identify and analyze the major factors influencing the LMPs in all zones, which may serve as explanatory variables for the pricing of FTRs.

We have applied this non-parametric model to investigate the electricity day-ahead forward price curve dynamics in the New York power market. This model performs better in forecasting short-term curves of the LMPs than do other existing time series models.

V. Inherent inefficiency of FTR auctions

Empirical studies of FTR (or, TCC) auction data from the NYISO[1] show systematic deviations between the FTR auction clearing prices and the settlement payoffs. Such

[1] Bartholomew E. S, A. S., Siddiqui, C. Marnay, and S.S. Oren "The New York Transmission Congestion Contract Market: Is it Working Efficiently", Electricity Journal, (November 2003), pp. 1-11.

deviations cannot be explained by risk aversion or by risk premiums associated with the correlation between FTRs and non diversifiable risks. As part of this project work, we have demonstrated that even with perfect foresight of the settlement payoffs, the auction clearing prices may deviate from the expected payoffs.

Our theoretical analysis and simulations show that these deviations can be explained by the fact that FTR bids quantities are limited and dispersed over a large number of FTRs since most buyers try to match the FTRs they buy to the energy transactions they wish to hedge. Such quantity limits dampen the efficiency of the auction by allocating part of the flowgate capacities to FTR bids that undervalue them.

Potential uses of the developed analytical tools

Our study documents the alternative market-based compensating schemes for creating incentives for investments in improved network reliability and adequacy. It provides a better understanding on the effectiveness of the FTR-based compensation mechanism. Based on power system simulations reflecting the competitive and volatile market environment together with the physical system operating constraints, our investigation offers a framework for analyzing the proper structure of a long-term forward contract market in a large-scale power system for increasing trading liquidity, valuing transmission assets, and providing efficient incentives for transmission capacity investment. Incentives for transmission investment from energy and capacity markets will also be identified as supplements. Through the system simulation, potential benefits of generation investment for reliability and adequacy purposes at specific locations can be quantified. Reconciling the public goods with market mechanisms, for instance, reliability enhancement may be achieved by incorporating a reliability component into LMP calculation model to create economic incentives for the investments.

The proposed power system simulation framework offers an important tool for evaluating transmission and generation investments which address the reliability and adequacy needs of a power system. For instance, this tool can be used by power merchants to evaluate opportunities in merchant transmission investments; and by system operators/regulators to examine how effective alternative incentive mechanisms are in inducing new investments for improving the system reliability and adequacy levels.

The econometric model component of our project for modeling electricity spot prices and the risk premiums in the forward prices can be commercialized into a module for existing commercial software packages to analyze the key drivers, including transmission congestion factors, which influence the price dynamics of energy and transmission rights.

Siddiqui, Afzal S., Emily S. Bartholomew Chris Marnay and Shmuel S. Oren, “On the Efficiency of the New York Independent System Operator Market for Transmission Congestion Contracts”, Journal of Managerial finance, Vol. 31, No. 1, (2005) pp. 1-45.
Seabron Adamson,Thomas Noe and Geoffrey Parker, “Efficiency of Financial Transmission Rights Markets in Centrally-Coordinated Periodic Auctions, Presented at UKERC Workshop on Financial Methods in Electricity Markets, Oxford UK, July 9-10, 2008

The price models developed in this project could form a basis for developing a method to evaluate a portfolio of FTRs and provide a framework for monitoring the behavior of participants in the FTR markets, which could be adopted by the system operators.

Future work

The identification and allocation of incremental transmission rights under a market setting with a LMP scheme will be investigated concerning configuration, quantity and maturity decisions. Alternative multivariate time-series models for the joint modeling of electricity price, load and temperature can be further investigated to better understand the stochastic behavior of locational marginal prices and the imputed value of FTRs.

Table of Contents

Table of Contents (continued)

List of Tables

List of Tables (continued)

List of Figures

List of Figures (continued)

Intentionally Blank

1. Introduction

Incentive for attracting investments in transmission assets is essential to the overall success of the restructuring of the electric power industry. In general, adequate transmission capacity enhances reliability, lowers energy cost as delivered, limits market power of market participants, and provides flexibility to protect against market uncertainties such as load fluctuation, fuel price volatility, and unexpected facility outages.

Various transmission-pricing approaches have been developed for recovering transmission costs and providing incentives for future expansion or enforcement. The embedded cost method is based on approximated power flow patterns, with transmission congestion and system externalities being smeared over all network users. In contrast, marginal cost method is based on marker values of the transmission facilities at specific locations, with transmission charges being bundled into the prices of accessible electric power and actual system dispatching in response to the ever-changing system conditions being reflected. The cost-of-service regulation and the market-based approach for inducing transmission investment have been developed under their respective contexts. Cost-of-service regulation focuses on contract path and transmission tariffs which ignore the actual economic and physical conditions[2]. Although cost-of-service regulation appears to be successful in many aspects such as balanced development of infrastructures, it results in inefficiencies such as little incentives to reduce costs, retarded innovation, and misallocation of cost and decision risk. The recently proposed market-based investment regimes rely on competition, free entry, and property-rights allocation mechanisms[3]. Price signals, as indications of where and how much to invest, and property rights, as revenue collecting instruments awarded to investors, are two essential components. Such regimes allow unfettered competition to govern investment in new transmission capacity, placing the risks of investment inefficiencies and cost overruns on invest decision-makers instead of consumers[4].

It becomes obvious that the regulatory uncertainties, lumpiness in investment, large scale of system, network externalities, and market risks have inhibited the investment incentives and caused the serious problem of transmission inadequacy. Statistics show that generation development has outpaced transmission investment in recent years[5]. The impact of the increasing lag is stressed by the market operations, where generators respond to market opportunities by transferring larger quantity of power over longer distances more frequently, while traditionally, transmission network was designed to support power transfers within electric vicinity.

According to the market-based investment model, a transmission investment usually expands power-transfer capability, and therefore, increases the quantity and variety of transmission rights can be issued to investors. It is required that the issuing of incremental transmission rights be limited by a simultaneous feasibility test, which verifies sufficiency of

---

[2] José Rotger and Frank Felder, Promoting Efficient Transmission Investment: The Role of the Market in Expanding Transmission Infrastructure, November, 2001.

3 Williams Hogan, Contract Networks for Electric Power Transmission, Journal of Regulatory Economics, 4: 211–242, 1992.

[4] William W. Hogan, Market-Based Transmission Investments and Competitive Electricity Markets, August 1999.

5 Eric Hirst, US Transmission Capacity-Present Status and Future Prospects, Prepared for Edison Electric Institute and U.S. Department of Energy, June 2004.

transmission capacity to accommodate the consolidated power injections and withdrawals corresponding to all outstanding transmission rights, taking into account thermal limits, voltage, stability, and contingency constraints[6]. It also ensures revenue adequacy, which refers to the financial solvency of the system operator in making congestion payments of physical power transactions out of the FTR revenues. However, the adequacy of incentives in terms of rewarding transmission investments is a major concern to investors [7] if the cost recovery relies solely on the values of property rights to be allocated. Economically, impact of transmission upgrades on energy price and capacity market price provides incentives to both generation companies (GENCOs) and load serving entities (LSEs). The incentives can be identified and combined with others as supplements to make transmission investment profitable and appealing to potential investors. This is one main issue that is investigated by this project based on a power system simulation model with a power pool and a locational marginal pricing (LMP) market mechanism.

In order to facilitate the efficient use of the transmission network while mitigating the volatility associated with locational marginal prices (LMPs) so as to offer price certainty to users of transmission services, tradable financial transmission rights (FTRs) are offered in most of the electricity markets in the US. The FTRs provide a mechanism for defining property rights to the transmission network and enable hedging against congestion charges to support energy trading across the network. The FTRs are defined as financial swaps entitling or obligating the holder of one MW FTR to the nodal price difference between two specified nodes over a specified time period. These rights are either allocated based on historical use or auctioned off in periodic auctions.

Based on a fundamental power system simulation model with a LMP-based market structure that we have formulated and studied in the previous PSERC project[8], we establish a framework for evaluating reliability and adequacy transmission investment through incorporating constraints on the transmission reliability margin (TRM) and the generation reserve margin into the power system simulation model. Heuristic methods for identifying incremental financial transmission rights (FTRs) resulting from typical network-deepening or network-expanding transmission investment projects are illustrated. Through a case study, we show that FTR-based compensation scheme does provide financial incentives for reliability and adequacy targeted transmission investments via allocating the incremental FTRs to investors. The magnitude of such incentives depends on the amount of incremental FTRs resulting from the investment. The quantity and value of the incremental FTRs further depend on the bid values, the transmission network topology and the initial configuration of the allocated FTRs. Thus market-based compensation mechanisms, such as the one rewarding investors with incremental FTRs as tradable instruments for recovering sunk capital costs and hedging market risks, have the potential of adequately compensating the reliability or security constraint-relieving transmission investments.

There is one inherent complexity in the FTR markets that would pose a significant challenge to the implementation of such a market-based mechanism for rewarding transmission

---

6 Bushnell, J., and S. Stoft (1996) “Electric Grid Investment under a Contract Network Regime,” Journal of Regulatory Economics, 10: 61–79.

[7] William W. Hogan, Transmission Market Design, April, 2003.

[8] Shi-Jie Deng, Sakis Meliopoulos, and Tim Mount et al. Modeling market signals for transmission adequacy issues: valuation of transmission facilities and load participation contracts in restructured electric power systems, PSERC project, ongoing.

investments in any real system with thousands of buses. For example, a point-to-point financial transmission right can be defined over any pair of buses in a bulk power system. As a result, a majority of the FTRs may experience low trading volume and poor liquidity. To address this problem, we investigated effective approaches for identifying proxy trading hubs in a LMP-based market. Specifically, we develop a non-parametric dimension reduction technique for identifying the major trading hubs and modeling the structure of all LMPs of a bulk power system in a low-dimensional space. Using this model, we can identify and analyze a relatively small set of key factors influencing the LMPs in all zones, which would serve as explanatory variables for the pricing of FTRs. We apply this non-parametric model to investigate the electricity day-ahead forward price curve dynamics in the New York power market. As we will see in Chapter 5, our model performs better in forecasting a short-term curves of the LMPs than do other existing time series models.

An econometric modeling framework for simulating the stochastic behavior of congestion costs of electricity in New York State and especially the link between NYC and the Hudson Valley is developed in Chapter 4. The basic specification of the model is that the price of electricity in a specified zone (region) is a function of the corresponding load, the price of natural gas and a set of seasonal and daily variables. Multivariate time-series models (VARMAX) are estimated for 1) the daily temperature in different locations conditional on seasonal cycles, 2) the average daily loads in different zones conditional on Heating Degree Days (HDD), Cooling Degree Days (CDD), seasonal cycles and dummy variables for days of the week, and 3) the prices of electricity in different zones conditional on the load, a polynomial lag of past prices of natural gas, seasonal cycles and dummy variables for days of the week. Daily data from 2002 to 2005 are used for the model estimation and the estimated models meet standard statistical criteria for VARMAX models (white noise residuals, etc.). The statistical specifications of these models are described in a paper that is one of the deliverables for this project (Mount, T.D. and J. Ju, 2007).

The estimated models are then used to predict the average daily prices in Western New York (Zone A), the Hudson Valley (Zone G), NYC (Zone J) and Long Island (Zone K) for the summer of 2006. The sum of the price differences for different pairs of locations from May to October represents the earnings of a six-month strip for the corresponding TCC. Since the estimated models are based on information that was available before the auction to sell the TCC, it is appropriate to use these models to evaluate the financial risk of purchasing a TCC in the auction. The financial risk of the TCC for the summer of 2006 is evaluated from two different perspectives. First, the risk of hedging for a generator comes primarily from uncertainty about the actual daily temperatures next summer. It is assumed implicitly that the generator holds a forward contract for natural gas based on the current forward prices for natural gas on the New York Mercantile Exchange (NYMEx). Second, the risk for speculators comes from the combined uncertainty about future temperatures and future prices of natural gas. Through this process, the predicted price differences can be used as a basis for measuring the magnitude and financial riskiness of congestion costs for a specified TCC.

We also investigate the risk premium present in the electricity day-ahead forward price over the real-time spot price in Chapter 6. This part of our project study establishes a quantitative model for incorporating transmission congestion into the analysis of electricity day-ahead forward risk premium. Through simulations with a three-bus study-system, it is illustrated that the more frequently transmission congestion happens, the higher the forward prices get at the

load buses. Consistent with the implications of the model, evidences from empirical studies with the New York electricity market data confirm that there exists a significant statistical relationship between the day-ahead forward risk premium and the shadow price premiums on transmission flowgates. When applied to the forecasting of next day spot prices, this model still has considerable room to improve its accuracy. One important factor is that the PTDF coefficients are inferred using historical market price data without knowledge of the transmission network structure. However, for a long-term market participant in a specific power pool, who is more familiar with the system transmission conditions, these PTDF coefficients would be known. Furthermore, additional important transmission flowgates can be identified and the corresponding shadow price premiums can be added as explanatory variables in the regression model. With these enhancements, it is foreseeable that the forecasting accuracy of the model could be improved. Given the encouraging empirical evidences from the New York electricity market, caution should still be exercised in generalizing the results to other markets where factors such as market power and regulators' price intervention may affect the market clearing process.

The dual role of the FTRs as transmission property rights backed by the physical capability of the grid and as financial hedging instruments creates some inefficiencies that we have explored in Chapter 7 as part of the project tasks. Given the liquidity of FTR market, one would expect that the expected settlement payoffs of FTRs over the duration of the contract will roughly match the FTR auction clearing prices with some random deviations attributable to uncertainty. However, empirical studies of data from the NYISO[9] show systematic deviations between the FTR auction clearing prices and the settlement payoffs. Such deviations cannot be explained by risk aversion or by risk premiums associated with the correlation between FTRs and non diversifiable risks. In our study we have demonstrated that even with perfect foresight of settlement payoffs, the auction clearing prices may deviate from the expected payoffs. Our theoretical analysis and simulations show that these deviations can be explained by the fact that FTR bids quantities are limited and dispersed over a large number of FTRs since most buyers try to match the FTRs they buy to the energy transactions they wish to hedge. Such quantity limits dampen the efficiency of the auction by allocating part of the flowgate capacities to FTR bids that undervalue them. Through a simulation study we show that the FTR bid quantities would have to be as much as 30 times the corresponding energy transactions volume for the auction prices to match the expected FTR settlements. Such inefficiencies can be reduced by segmenting the FTRs into shorter time intervals and perhaps several time-of-day segments so as to reduce the

[9] Bartholomew E. S, A. S., Siddiqui, C. Marnay, and S.S. Oren, "The New York Transmission Congestion Contract Market: Is it Working Efficiently", Electricity Journal, (November 2003), pp. 1-11.
Siddiqui, Afzal S., Emily S. Bartholomew Chris Marnay and Shmuel S. Oren, "On the Efficiency of the New York Independent System Operator Market for Transmission Congestion Contracts", Journal of Managerial finance, Vol 31, No. 1, (2005) pp. 1-45.
Seabron Adamson,Thomas Noe and Geoffrey Parker, "Efficiency of Financial Transmission Rights Markets in Centrally-Coordinated Periodic Auctions, Presented at UKERC workshop on Financial Methods in Electricity Markets, Oxford UK, July 9-10, 2008.

variability between the OPF solution used in the FTR auction clearing process and the OPF solution upon which the settlements are based.

2. Market Structures and Transmission Investments

2.1. Transmission Adequacy and Reliability Needs

Regulatory changes in the transmission system were accompanied by nationwide demand increases at an annual rate of 2-3% and substantial changes in the generation sector. New generation technologies, particularly gas-fired combined-cycle turbines, allowed electricity to be produced in more modular and flexible quantities with higher efficiency. A building boom ensued added over 200GW of new generation between the years of 1999 and 2004 (NERC, 2004). In many cases, these units were located convenient to construction or fuel resource accesses while taking adequate transmission connection capacity for granted. With the building boom reaching its end and the evolution toward competitive markets well advanced, the transmission system is becoming increasingly vital. The importance of its new role of supporting market transactions is far beyond what is indicated by the relatively small capital cost it represents in the electric power industry.

Compared with the steady increase of demand and generation, however, transmission investment declined over the same time period. In 1972 approximately 30GW generation was added, supported by $7.4billion (in year 2004 dollars) in transmission investment. In 2001, 40.6GW generation was added with only $4.6billion in transmission. By the year 2003, the numbers further diverged to having 52.4GW of new generation versus $3.9billion invested in transmission. Normalized transmission capacity measured in MW-miles/MW-demand and MW/MW-demand is declining at annual rates of 1.5% and 1.6%, respectively (see Hirst, 2004). The market environment strains the system further because merchant power plants competing for short and long-term contracts with multiple buyers are encouraged to transfer larger quantities of electricity over longer distances more frequently to capture interregional market opportunities, raising power flow patterns significantly different from the projected scenarios in system planning. As a result, transmission loading relief (TLR) procedures, which dictate a certain percentage of the power transactions that cause the monitored transmission overloading to be curtailed, have been called frequently for managing transmission utilization to prevent overload situations that put the system at risk.

It has been commonly recognized that, while considerable effort has been devoted to electricity market, development of the transmission sector has been largely overlooked. The lack of widely accepted regulation rules and absence of effective market mechanisms lead to vague signals for market participants. Potential transmission investors face physical nature, organization structure, and market risk related obstacles that complicate the projection of capital recovery. These risks include:

a. Free riding -- As a public good with non-excludable benefit sharing, typical transmission investments are haunted with the free-riding problem due to the difficulty of isolating the benefits to the investor. Market participants would choose to be free riders, expecting positive externalities induced by others' investments.

b. Market risks -- Given the ever changing electricity demands, generation portfolio, network topology, and market rules, it is impossible to predict with accuracy the future economic payoffs accrue from a transmission investment.

c. Regulation uncertainties -- One key element for the success of a transmission project is regulatory approval. In many cases, however, alignment of federal, state, and local regulations

results in project delays, and rejection is a very real possibility. Consequently, funds expended early in the project may be at substantial risk.

d. Lumpiness -- Transmission investments typically appear as additions of large blocks of capacity. The obscured linkage between expected benefit and marginal cost complicates the investment decisions. Joskow and Tirole (2003) illustrate that lumpiness leads to transmission network underinvestment.

Note that these obstacles are confounded by fragmented ownership that easily leads to sub-optimal solutions.

2.2. Transmission Investment Compensation

2.2.1 Different types of transmission investment

With the understanding of the valuation of transmission services, an efficient mechanism is needed to indicate adequate transmission investment, to lower the transmission congestion costs, and to facilitate the market based competitive electricity trading. Due to the obstacles listed in section 2.1, investment cost allocation is a complicated problem. The benefits of improving a transmission network as identified bellow are essential to understanding the problem and finding incentives for transmission investment,

a. Economic efficiency improvement -- Transmission expansion provides access to alternative power sources and additional options to meet consumption at the lowest possible social cost.

b. System reliability enhancement -- Higher transmission reliability margin and diversified fuel accesses improve interconnection by accommodating more fluctuating transactions, facility unavailability, and sudden disturbances.

c. Financial volatility reduction -- Transmission upgrades reduce system congestion and alleviate market participants' risk-hedging pressure created by volatile market prices.

d. Market power mitigation -- The electricity market is vulnerable to the exercise of market power which intentionally creates scarcity and manipulates prices. This power can be mitigated by proper transmission expansions which facilitate competition.

e. Environmental impact alleviation -- Although people are concerned about transmission facilities' right-of-ways, given the more severe environmental impact of power plants, especially in highly-populated regions, transmission connection to remote generation sources may provide a more environmentally-sound alternative to meet demand (Bloyd et al., 2002).

Corresponding to the benefits listed above, various incentives drive investment decisions or back up transmission investment cost allocations for capital recovery. Different transmission investment forms can be envisioned as follows:

a. System-wide reliability enhancing and economic efficiency improving transmission upgrades.

For a system with tight transmission capacity, transmission congestion happens frequently and out-of-merit generation units have to be called to serve demands. The inefficiency involved represents the social cost of the inadequate transmission capacity.

In addition, system reliability is impaired when a critical transmission flowgate is congested, since a subsequent contingency event may interrupt or compromise the quality of bulk power supply.

System operators usually prepare regional transmission expansion plans which consolidate reliability or improve system-wide economic efficiency. Since these projects bring widespread benefits to most market participants in the electric vicinity, it is hard to draw the beneficiary boundaries, and a regulatory process is involved to allocate costs incurred to a large group of consumers through an added service charge. A request for proposals (RFP) process is preferable since the RFP process promotes minimal cost while assigning the project's risks to the winning respondent instead of to the end consumers. Investments in this category should be limited to those projects the direct economic benefits of which are non-significant to any market participants. A potential refinement of this approach is to allocate investment costs through a cost-benefit analysis among sub-regions so that a non-uniform portion of the cost can be allocated accordingly.

b. Voluntary transmission investment

Projects in this category include generation interconnection requests to increase electricity delivery to the market, load connection requests to get access to desired resources, and capacity expansions that reduce congestion energy cost for consumers in a load pocket like, for example, New York City. The free-riders problem is less bothersome here since the economic benefits of the projects to potential investors are more exclusive, although they usually introduce more competition to mitigate the existing market power of others. A good quantitative assessment of future market opportunities is essential for the projection of economic cost-benefits analysis. Voluntary transmission investment projects are to be sponsored by those who would gain the benefits. It is necessary, however, to assure that the projects do not degrade system reliability nor create additional opportunities for market power exertion.

c. Merchant transmission projects

Merchant transmission investors rely on the LMP-based transmission service pricing mechanism and seek financial transmission rights as payoffs. Three components are essential to this category of market-motivated transmission investments. First, the spatial-differentiated electricity price signals indicate where and how much to invest; second, FTRs hedge against congestion-risks or, as tradable financial instruments, entitle investors to the right to collect revenues in the future; third, an efficient financial transmission rights identification and allocation mechanism is expected to assign proper amount of rights to appropriate investors. These rights include eliminating the opportunities of free-riding in public good benefits. Note that identification of incremental FTRs created by merchant transmission investment is guided by the SFT problem. With the revenues entitled to incremental FTRs, at least part of the cost can be recovered without resorting to the traditional regulatory charges. Bushnell and Stoft (1996) show that the transmission rights entitled revenues provide market incentives for transmission investment. The merchant investment mechanism relies on free entry and unfettered competition in the market. It places the risks of investment inefficiencies and cost overruns on investment decision-makers instead of on the involuntary end consumers.

It is notable that, due to the network externality of power flows, a transmission upgrade may affect the transfer capacity between two locations in another part of the network. As a crucial issue regarding trade-offs between cooperation and competition in the long run, the network

externality may degrade system reliability and undermine open competition. Should a transmission upgrade impair existing FTRs, the theory of public economics suggests that the investor should buy back the disabled FTRs. Another option for the system operator is to retain some transmission rights and avoid jeopardizing FTRs held by market participants when a transmission upgrade has negative impacts. However, this induces additional overheads to be socialized to all consumers.

Nevertheless, regardless of which category it belongs to, a transmission investment requires the assessment of market conditions in the future. The projection of locational market prices as the market signals is one of the most essential tasks involved. Two competing approaches are available for market price modeling: a fundamental approach that relies on system simulation; and a technical approach that directly models the randomness. While the fundamental approach provides more realistic representations under specific scenarios, it is computationally prohibitive due to the large number of scenarios to be considered. The method to be presented in this chapter is to combine the strengths of the two approaches by calibrating the stochastic price process models using probabilistic system simulation results.

2.2.2 Market-based compensation schemes

Since LMPs are volatile and cannot be foreseen with accuracy in advance, transmission usages are subject to fluctuating congestion charges. Such exposures to market price risks create strong demands for congestion-hedging among risk-averse transmission service customers. In PJM for example, the system operators identified several groups of electrically neighboring buses with active power transactions and defined them as trading hubs. The hub settlement LMPs are calculated as the average of the group of bus to provide market participants with more stable prices. Market participants can also choose to withhold transactions in case of transmission congestion to avoid congestion charges. Financial transmission rights (FTRs) also came up as sophisticated tradable market instruments to meet market participants' risk hedging demands. An FTR entitles (or obligates) its holder to collect a stream of revenues determined by LMP differences between the two underlying locations over a contractual time period specified ex ante.

Before the structuring of FTRs, physical transmission rights (PTR) were proposed at the conception of market restructuring. A PTR gives its holder the priority to access the underlying transmission facility. In the PTR-based congestion hedging mechanism, to a great extend, the allocation of PTRs through bilateral contracts or private auction markets determines the usage of scarce transmission capacity and determines the system dispatch as well. Therefore, PTR holders have market power to withhold transmission access and hamper competition. The scheduling priority of PTR holders creates perverse incentives which conflict with the bid-offer matching mechanism. Furthermore, the exclusion of the system operator's control from the withheld transmission capacity compromises the system reliability. It's been argued that the physical interpretation of transmission rights was the principal pitfall that buried the FERC's original capacity reservation tariff. In the contrast, by entitling financial congestion rents instead of priority of transmission access to FTR holders, the FTR-based congestion hedging mechanism keeps the centralized market dispatch paradigm intact. It has been adopted into the PJM system since 1998, in New York since 1999, and in New England since 2003.

As the underlying LMPs are determined by the market dispatch model which takes system operating constraints in both normal and contingent scenarios into consideration, an FTR

provides a perfect price hedge against transmission congestion for power transactions between the underlying source and sink. Assume a market participant schedules a transaction of q_{AB} MW power from source A to sink B, where the fluctuating LMPs are $\tilde{p}_A$ and $\tilde{p}_B$ during time period T, respectively. The congestion rent involved will be $q_{AB}(\tilde{p}_B - \tilde{p}_A)$. To hedge against the scenario that $\tilde{p}_B - \tilde{p}_A$ is driven very high by the ever-changing system operating conditions, the market participant can procure an FTR of q_{AB} MW from source A to sink B over time period T at a cost of C^{FTR}. It entitles him a revenue stream of $q_{AB}(\tilde{p}_B - \tilde{p}_A)$. Therefore, the total cost of the transmission service C^{Total} for the power transaction is the net of cost and revenue,

$$C^{Total} = C^{FTR} + q_{AB}(\tilde{p}_B - \tilde{p}_A) - q_{AB}(\tilde{p}_B - \tilde{p}_A) = C^{FTR} \tag{2.1}$$

Considering a random deviate Δq_{AB} of the transaction quantity in real time market from the projected q_{AB}, the total cost of uncertain transmission service $\tilde{C}^{Total}$ is,

$$\tilde{C}^{Total} = C^{FTR} + \Delta q_{AB}(\tilde{p}_B - \tilde{p}_A) \tag{2.2}$$

As long as the volume deviation Δq_{AB} is trivial, the transmission service can be secured at around the pre-determined FTR procurement cost.

Since an FTR is typically connected with an existing or projected power transaction between two locations, it represents a pair of power injection and withdrawal accordingly. To conform to the system capability and ensure the revenue solvency of the system operator, the setup of FTRs is subject to a simultaneous feasibility test (SFT) defined as follows

Definition 2.1 (**Simultaneous feasibility test**) Given a set of FTRs defined over a common time period, the system operator needs to test if the transmission network can accommodate the corresponding pairs of power injections and withdrawals $(\mathbf{P}^I, \mathbf{P}^W)$, assuming they occur simultaneously.

Using DC power flow and assuming **F** and **F'** represent the system PTDF matrix in the normal and a contingent scenario, respectively, the vectors of transmission capacity limits are **T** and **T'**, correspondingly. The SFT problem can be described as follows,

$$\mathbf{F}(\mathbf{P}^I - \mathbf{P}^W) \le \mathbf{T} \tag{2.3a}$$

$$\mathbf{F}'(\mathbf{P}^I - \mathbf{P}^W) \le \mathbf{T}' \tag{2.3b}$$

Note that constraints (2.3a) and (2.3b) represent the feasibility criteria in normal and contingency scenarios, respectively.

As a summary, the marginal cost based transmission pricing provides market incentives for transmission capacity allocation, and the FTR mechanism provides transmission service customers a transmission congestion risk hedging tool.

3. A Case Study on Effectiveness of Market-based Compensation: A Power System Simulation Model for Market Dispatch

3.1. A Market Dispatch Model: Power System Simulation

In a pool-based electricity market, market dispatch is one of the most essential functions of the system operator (called ISO or RTO). It is an establishment that coordinates the movement of wholesale electricity, acting neutrally and independently, operating the competitive wholesale electricity market and ensures the reliability in managing the regional transmission system and the wholesale electricity market. By collecting electricity supply bids and demand requests, the system operator determines the set of winning supply bids to meet the demands while observing all the system operating constraints. This centralized market dispatch can be formulated as a network constrained optimal power flow (OPF) problem, which solves a set of linear or nonlinear equations and inequalities to obtain the intended optimal operations. Alternative objectives of an OPF problem include maximizing social welfare, minimizing customer expense, minimizing system status deviation and minimizing transmission loss etc. The rational for choosing different objectives and the respective implications on market participants are discussed by Alonso et al. (1999). A primitive formulation of the market dispatch OPF that minimizes the total generation procurement cost is defined as follows,

Definition 3.1: **(The market dispatch OPF problem)** By collecting I supply bids and J demand requests, the system operator conducts the market dispatch accordingly to minimize the total generation procurement cost while accommodating all power flow balance and transmission feasibility constraints.

$$\text{Min} \qquad \mathcal{C} = \sum_{i=1}^{I} C_i(s_i) \tag{3.1a}$$

$$St. \qquad F^{Eq}(\mathbf{s}, \mathbf{d}, \mathbf{x}, \mathbf{u}) = 0 \tag{3.1b}$$

$$F^{Ineq}(\mathbf{s}, \mathbf{d}, \mathbf{x}, \mathbf{u}) \le 0 \tag{3.1c}$$

By using minimization of the total generation procurement cost as the objective, the market dispatch model actually determines the locational marginal prices. An LMP measures the incremental system generation procurement cost for a unit of incremental demand at the specific location. In addition, the settlement prices of a transmission service market are implicitly determined through this market clearing decision.

The system status variables $\mathbf{x}$ consist of magnitudes and phase angles of bus voltages, and so on. The system control variables $\mathbf{u}$ include real and reactive loads and generations, voltage settings and bounds, transformer tap settings, and so on. For example, a prescheduled multilateral transaction can be modeled as a set of power injections and withdrawals at the corresponding source and sink buses. In a system that has interface with neighboring systems and power interchanges, the interface MW limits are usually treated as required power injections or withdrawals in $\mathbf{u}$, depending on the controlled power flow directions.

The equality constraints $F^{Eq}(\mathbf{s}, \mathbf{d}, \mathbf{x}, \mathbf{u}) = 0$ are always binding at least to within a user specified tolerance. They consist of generation bus voltage setting and the power balance equations,

$$\mathbf{g}(\mathbf{s},\mathbf{d},\mathbf{x},\mathbf{u}) = 0 \tag{3.1d}$$

Specifically, according to traditional power flow formulation, considering both real and reactive power flows, the power balance equation at any bus n which matches the locational generation and load is,

$$\begin{aligned} s_n - d_n = {} & v_n \sum_{m\in\psi_n} v_m \left[G_{nm}\cos(\theta_n-\theta_m) - B_{nm}\sin(\theta_n-\theta_m)\right] \\ & + jv_n \sum_{m\in\psi_n} v_m \left[G_{nm}\sin(\theta_n-\theta_m) + B_{nm}\cos(\theta_n-\theta_m)\right] \end{aligned} \tag{3.1e}$$

Note that explicit load-flow equations are listed as essential constraints in the formal establishment of the optimal power flow problems. Instead of approximating the losses as a polynomial function of the power output of each unit (Wood and Wollenberg, 1996) and calculate a penalty factor for each generation unit, the transmission losses are accounted implicitly in the power flow equations and their market costs are imbedded in the electricity locational marginal prices.

The inequality constraints $F^{Ineq}(\mathbf{s},\mathbf{d},\mathbf{x},\mathbf{u}) \le 0$ consist of system operating limit and bound constraints. In the primitive formulation of the market dispatch OPF, generation capacity bounds

$$\mathbf{s} \le \mathbf{s}_{Max} \tag{3.1f}$$

and the transmission loading thermal limits,

$$\mathbf{h}(\mathbf{s},\mathbf{d},\mathbf{x},\mathbf{u}) \le \mathbf{T} \tag{3.1g}$$

are usually considered.

Note that the transmission loading thermal limits apply to not only single transmission lines, but also to sets of transmission facilities with certain capacity limits, defined as transmission flowgates, which constraint the power flow through the interface involved.

The Lagrange function associated with OPF problem (3.4) can be defined as,

$$\mathcal{L}(\mathbf{s},\boldsymbol{\lambda},\boldsymbol{\gamma},\boldsymbol{\eta}) = \sum_{i=1}^{I} C_i(s_i) + \boldsymbol{\lambda}\mathbf{g}(\cdot) + \boldsymbol{\gamma}(\mathbf{s}-\mathbf{s}_{\max}) + \boldsymbol{\eta}(\mathbf{h}(\cdot)-\mathbf{T}_k) \tag{3.2}$$

where, $[\boldsymbol{\lambda},\boldsymbol{\gamma},\boldsymbol{\eta}]$ are vectors of Lagrange multipliers associated with constraints (3.1d), (3.1f) and (3.1g), respectively.

In order for a point $(\mathbf{s}^*,\boldsymbol{\lambda}^*,\boldsymbol{\gamma}^*,\boldsymbol{\eta}^*)$ to be optimal, in addition to (3.1b) and (3.1c), to guarantee the gradient of $\mathcal{L}$ needs to be normal to $\mathbf{g}(\cdot)$, $\mathbf{h}(\cdot)-\mathbf{T}$, and $\mathbf{s}-\mathbf{s}_{Max}$. This requires the gradient of the objective function to be a linear combination of the gradient vectors of the active constraints $\nabla\mathbf{g}(\cdot)$, $\nabla(\mathbf{h}(\cdot)-\mathbf{T})$, and $\nabla(\mathbf{s}-\mathbf{s}_{Max})$,

$$\frac{\partial\mathcal{L}}{\partial\mathbf{s}}(\mathbf{s},\boldsymbol{\lambda},\boldsymbol{\gamma},\boldsymbol{\eta})\Big|_{\mathbf{s}=\mathbf{s}^*} = 0 \tag{3.3a}$$

plus the complementary slackness conditions,

$$\boldsymbol{\eta}^*[\mathbf{h}(\cdot)-\mathbf{T}] = 0,\ \boldsymbol{\gamma}^* \ge 0 \tag{3.3b}$$

$$\boldsymbol{\gamma}^{*}\left(\mathbf{s}^{*}-\mathbf{s}_{Max}\right)=0,\ \boldsymbol{\eta}^{*}\geq 0 \tag{3.3c}$$

In economic sense, the Lagrange multiplier λ_n associated with the real power balance at bus n can be interpreted as the locational marginal price of energy because it quantifies the cost (or value, from demand side) for supplying (or consuming) an additional MW at the bus n of the network. On the other hand, the Lagrange multiplier η_k associated with the power flow limit of the k^{th} transmission flowgate is interpreted as the variation in social generation procurement cost if the transmission capacity is relaxed, called flowgate shadow price or congestion multiplier. The Lagrange multiplier γ_i reveals the market opportunity cost associated with the scarcity of supplier i's generation capacity.

By solving (3.1), LMPs can be read off the Lagrange multipliers associated with the corresponding constraints, which measure the cost to serve the next MW of load at a specific location, using the lowest production cost of all available generation, while observing all operating constraints. In the absence of any binding constraints, all LMPs are identical. The FTR values can be readily derived from the price differences. The non-zero shadow prices of binding transmission constraints are major factors that diversify the LMPs across the system. Market uncertainties due to fluctuating system loads, varying generation bid function, and unexpected transmission circuit outages can be incorporated by using random variables $\left[\tilde{\mathbf{T}},\tilde{\mathbf{d}},\tilde{C}_i\right]$ to carry the distribution properties of the underlying coefficients, see (Sun et al. 2005). With a parametric optimal power flow formulation, sensitivity of the optimal operating conditions with respect to any parameters under interest corresponding to a market participant's input or the system operator's control can be investigated and the corresponding economic values can be interpreted.

3.2. The IEEE-RTS 24 System

Given the high dimension of a practical electric power system, analytical evaluation of the probabilistic properties of the market price behaviors requires very complicated numerical methods and procedures. A natural alternative is to resort to system simulation, through which the fundamental uncertainty factors of the system can be represented as random variables with corresponding distributions. Numerical experiments with the IEEE RTS-24 system are presented in this section. The structure of the IEEE RTS24 system is illustrated in figure 3-1,

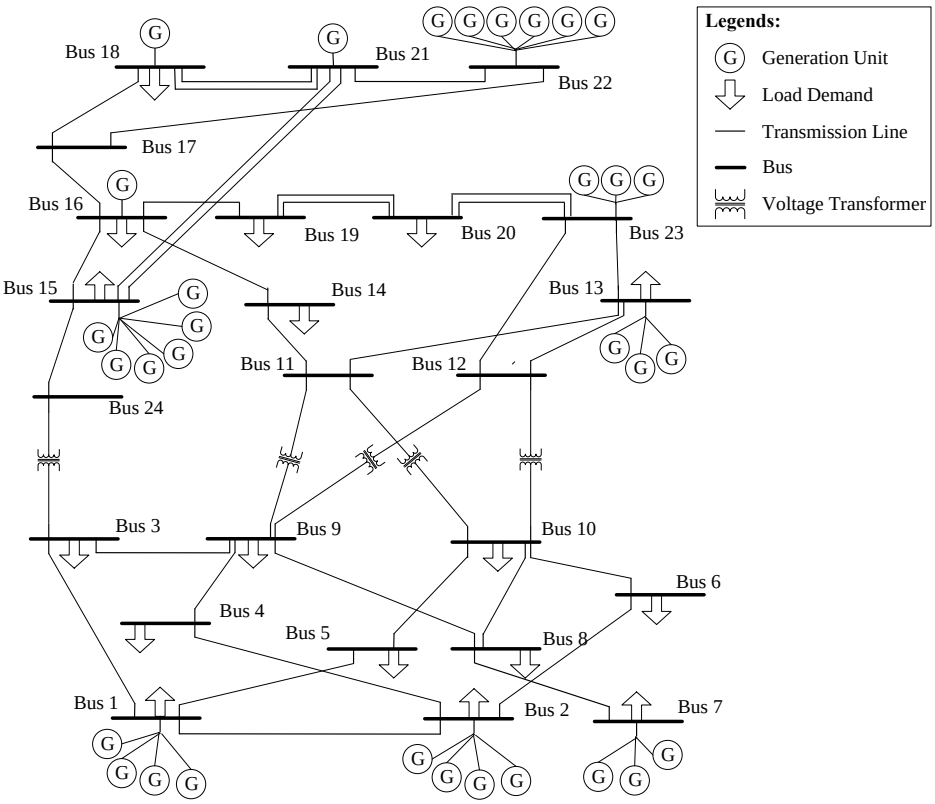

Figure 3-1 The IEEE RTS24 system

The system consists of 24 buses connected with 38 transmission lines. There are load demands at 17 of the buses, and 32 generation units connected to 10 of buses. Note that multi generation units of different capacities can reside at one bus and some buses are connected by double transmission lines. Bus 15 is the system slack bus. Most generation units reside at the upper part of the system, which consists of buses 11 - 24 and is operated at 230 kilovolt (kV). The lower part of the system is operated at 138 kV and is connected with the upper system through voltage transformers. The system has a total installed generation capacity of 3561MW. The yearly peak load D^{Peak} is 2850 MW. And the weekly, daily and hourly load peaks are given in percentages of D^{Peak}. Generation unit parameters $[\mathbf{s}_{\max}, \mathbf{Q}^{l}, \mathbf{Q}^{u}]$, transmission capacities $\mathbf{T}$ and $\mathbf{T}^{(k)}$ in contingency k, transmission parameters $[R_{mn}, X_{mn}, G_{mn}, B_{mn}]$ for each line $m-n$, the outage rates and the averaged failure-repair cycles of all types of generation and transmission equipments are referred to (Billinton and Li, 1994). The function generation procurement cost from each generation unit i is assumed to be a quadratic function of the real power output s_i, $C(s_i) = a_i + b_i s_i + c_i s_i^2$ where the coefficients $[a_i, b_i, c_i], \forall i$ are referred to (Meliopoulos et al., 1990). To reflect the increase fuel cost over the years, the values of these coefficients are doubled. We assume that the generation cost function as used in the objective function of the market dispatch include the components of a profit margin beyond the operational costs. In this case, the short-run marginal cost as used for the first best pricing can provide enough market incentives for generation suppliers.

The original IEEE RTS24 system was configured for the test of system generation adequacy related reliability analysis only, high transmission capacity was assumed in (Billinton and Li, 1994).

3.2.1 LMPs and evaluation of reliability constraints

Reliability of an electric power system is crucial to keep continuous supply of electricity at required quality. Although there has been substantial research activities on enhancing system reliability, the economic impact on market participants by imposing transmission reliability constraints in a competitive electricity market has not yet been adequately addressed. Without knowledge of the resulting market price dynamics, it is hard for system operators to estimate the economic consequences and for market participants to take proper market positions and manage risks involved. In retrospection, the unprecedented volatile California market electricity prices in 2000-2001 led to rolling blackouts and dramatic economic trauma to load serving entities. In addition to fundamental reasons such as abnormal hydro resource and high demands, the inadequacy of transmission capacity made the system vulnerable to the exercise of market power. Suppliers intentionally leveraged the generation scarcity in the dysfunctional wholesale market, since transmission bottlenecks held back the otherwise reachable alternative generation sources to the buyers. The lessons call for imposing transmission adequacy requirement to maintain a reliable environment for energy trading and to support open competition.

In an electricity market, as the competitions are getting more intensive and drive market participants to chase market opportunities, more generation units and transmission facilities are operated close to the edge for economic efficiency. This leads to higher risks of equipment contingency status and puts the failure stakes higher than ever before. A contingency event such as the forced outage of a transmission line or a generator unit may jeopardize the entire system if there lacks back up transmission capacity or generation source to support the power flows anticipated by the normal operation of the system. To prevent that a single contingency events could trigger the occurrence of cascading outages throughout the network, capacity reserves in generation and transmission should be procured and contingency analysis should be conducted.

As mentioned earlier, reliability is deemed as public good with non-excludable benefit sharing among market participants. Traditionally, the reliability enhancement and the LMP-determining market dispatch are implemented as economically separated activities. As a consequence, there lacks a market mechanism to value reliability and the costs involved are smeared among all consumers. We propose that economic values of reliability can, at least partially, be discovered with a properly designed market dispatch mechanism. A reliability-differentiated pricing scheme can be constructed correspondingly. Market dispatch OPF formulation (3.1) can be augmented to a security and adequacy constrained optimal power flow (SACOPF) problem by incorporating extra security and adequacy related constraints to address system reliability concerns.

The generation and transmission capacity reserve requirements are imposed for system adequacy concerns to ensure the existence of sufficient facilities to satisfy system disturbances. They can be imposed by allowing lower generation and transmission capacity for market dispatch. For example, replacing the constraint (3.1f) with

$$\mathbf{s} \le \left(1-\rho^{S}\right)\mathbf{s}_{Max} \tag{3.4a}$$

is equivalent to imposing a $\rho^S \cdot 100\%$ generation reserve margin. Similarly, a $\rho^T \cdot 100\%$ transmission reserve margin can be imposed by replacing the constraint (3.1g) with

$$\mathbf{h}(\mathbf{s},\mathbf{d},\mathbf{x},\mathbf{u}) \le (1-\rho^T)\mathbf{T} \tag{3.4b}$$

The unused capacity, namely, the generation reserve margin $\rho^s \mathbf{s}_{Max}$ and the transmission reserve margins $\rho^T \mathbf{T}$ can be called by contingency operating procedures when contingency events such as load surges or equipment outages happen. With such reserve margins, the systems can absorb the dynamics caused by the disturbances and remain stable. The technical problems of determining spare capacity in each generation unit and transmission facility to keep the system operation safe have been proposed by Bobo et al. (1994) and McCalley et al. (1991) respectively. By incorporating the generation and transmission reserve margin requirements as adequacy constraints into the market dispatch, their economic incentives can be revealed and passed to the corresponding beneficiaries. Therefore, an investment cost recovery mechanism can be established accordingly.

The contingency test constraints are imposed for system security, which is related to the ability of the system to respond to disturbances arising within the system. In power system operations, the N-1 criteria are widely adopted in industry for postulated contingency tests. It means that given a normal operating condition $[\mathbf{s},\mathbf{d},\mathbf{x},\mathbf{u}]$, in case a single postulated contingency event k happens, the demands $\mathbf{d}$ and the market dispatch determined supplies $\mathbf{s}$ can still be accommodated with no pressure for any immediate adjustment. However, the system control variables $\mathbf{u}$ will be changed to $\mathbf{u}^{(k)}$ and deviated system states $\mathbf{x}^{(k)}$ will be reached. The system can stand the contingency states $\mathbf{x}^{(k)}$ for a short period of time. However, to keep the safety of the system, $\mathbf{x}^{(k)}$ should not deviate out of the feasible regions and the system operator will go through certain operational procedures to put system states from the edge of feasible regions back to normal conditions. To reflect the N-1 contingency-proof criteria, for each postulated contingency event k, the following constraints should apply,

$$\mathbf{g}(\mathbf{s},\mathbf{d},\mathbf{x}^{(k)},\mathbf{u}^{(k)}) = 0 \tag{3.4c}$$

$$\mathbf{h}(\mathbf{s},\mathbf{d},\mathbf{x}^{(k)},\mathbf{u}^{(k)}) \le \mathbf{T}^{(k)} \tag{3.4d}$$

Note that under contingency event k, the transmission capacity vector may change to $\mathbf{T}^{(k)}$ correspondingly.

It is straightforward to foresee that imposing the generation and transmission capacity reserve requirements and the contingency tests leads to a more conservative market dispatch at the cost of higher generation procurement cost. The incremental cost of generation procurement incurred can be reflected by augmented market prices and passed to the corresponding market participants accordingly.

Additional practices to promote a reliable market dispatch include imposing upper and lower bounds for voltage magnitudes to keep the quality of power supply and the safety of electric equipments,

$$\mathbf{v}^l \le \mathbf{v} \le \mathbf{v}^u \tag{3.4e}$$

and imposing upper and lower bounds for reactive power outputs which reflect the corresponding generation unit's feasible operation region,

$$\mathbf{Q}^l \le \mathrm{im}(\mathbf{S}) \le \mathbf{Q}^u \tag{3.4f}$$

where $\mathrm{im}(\mathbf{S})$ denotes the reactive power outputs of generation units.

When solving the market dispatch OPF problem, as components of LMPs, marginal costs associated with various reliability constraints can be read off the corresponding Lagrange multipliers (Alvarado 2003). As more reliability constraints become active, the LMPs become further differentiated between locations across the system. By taking more conservative values for model parameters $\left[\rho^S, \rho^T, \mathbf{v}^l, \mathbf{v}^u, \mathbf{Q}^l, \mathbf{Q}^u\right]$, certain reliability criteria can be imbedded accordingly. Different model parameters can apply to different market participants according to their respective requirements. For example, for consumers expecting lower loss of load probability, higher ρ^S and ρ^T values can be determined to their generation suppliers and the corresponding transmission facilities. On the other hand, for consumers expecting a relatively stable voltage level, a higher $\mathbf{v}^l$ or a lower $\mathbf{v}^u$ should be applied to the corresponding bus. Note that such parameter-settings usually affect not individual but a group of end consumers, the decision should be based on aggregated requirements. Due to the impact on the resulting LMPs, the reliability-requirement differentiated pricing mechanism can be established.

By incorporating the reliability constraints explicitly into the market dispatch model, the openness of the market pricing mechanism can be improved since market values instead of regulation rules determine the service values and allocate the costs involved accordingly. As the restructuring continuous, further details can be incorporated into market dispatch model with evolving market mechanism.

Among various methods to reach higher reliability through market dispatch, we advocated the imposing of generation reserve margin $\rho^s \mathbf{s}_{Max}$ and the transmission reserve margin (TRM) $\rho^T \mathbf{T}$ as indicated by constraints (3.4a) and (3.4b). Here we focus on the TRM $\rho^T \mathbf{T}$ and present numerical examples in this section to show the impact of imposing constraints (3.4b).
Before jumping onto the experiments results, we start with a look at the sensitivity of LMP with respect to transmission capacity using the market dispatch model without TRM requirements. The following figure 3-2 plots the changes of system averaged LMP (equal weight for LMPs at all buses) with respect to the assumed transmission capacity limit expressed in percentage of their nominal values.

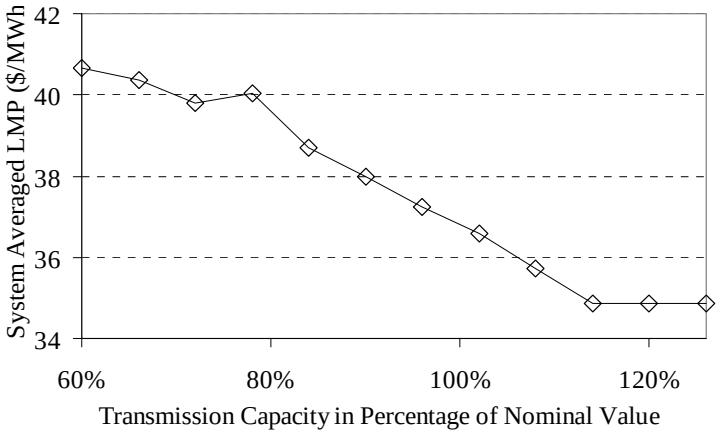

Figure 3-2 System averaged LMP with respect to transmission capacity using market dispatch without TRM requirement when the system load is 80% of peak level

From figure 3-2, we observe that the system averaged LMP decreases with the increase of available transm`ission capacity. When transmission capacity reaches a threshold point of adequacy when no transmission congestion appears throughout the system, the LMP stays constant even when more transmission capacity is invested. This is because the generation resources are dispatched in merit-order already and the increase of transmission capacity does not change the profile of winning generation supply bids. However, no more conclusions can be drawn from figure 3-2 unless that the transmission expansion increases economic efficiency in the sense of using less-costly generation to meet system demands. In order to find out the impact on distinct market participants, we pick any 2 buses (5 and 10) with pure load demands and 2 buses (18 and 22) with high installed low cost generation capacities and plot the changes of their LMPs as the available transmission capacity changes in the following figure 3-3.

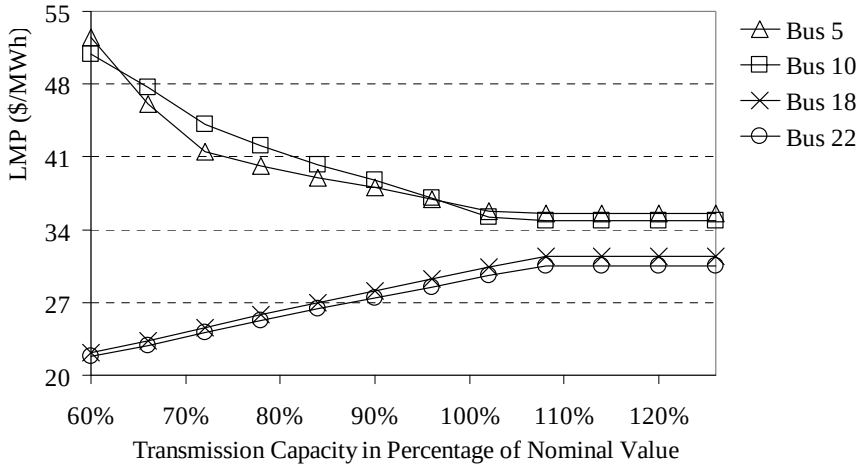

Figure 3-3 Generation and load bus LMPs with respect to transmission capacity using market dispatch without TRM requirement when the system load is 80% of peak level

As the transmission capacity increases, the change of LMPs at the 2 load buses 5 and 10 show quite similar tendency: decreases to a low value until transmission capacity reaches a certain adequacy threshold and stays the same afterwards. For generation buses 18 and 22, the

direction of the changes is the opposite: increases to a low value until transmission capacity reaches a certain adequacy threshold and stays the same afterwards. It is an interesting observation since it reveals that low-cost generation suppliers can sell more energy at higher prices given adequate transmission to support their power transactions.

Actually, similar results are observed when applying different TRMs $\rho^T \mathbf{T}$. Higher ρ^T values actually reduce the available transmission capacity for market dispatch in normal system operating conditions and reserve more capacity for contingency operating procedures. According to figure 3-3, we expect different changes of LMPs at load and low-cost generation buses when a TRM requirement is imposed. Using the given hourly load over one sample year (52 weeks), we calculate the hourly LMPs at buses 10 and 18 sequentially and plot their probability distributions in figures 3-4 and 3-5, respectively.

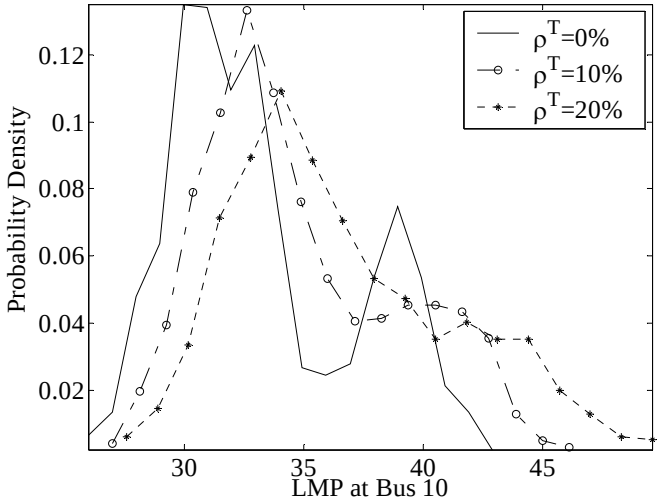

Figure 3-4 Probability distributions of LMPs at bus 10 over the sample year with different TRMs requirements

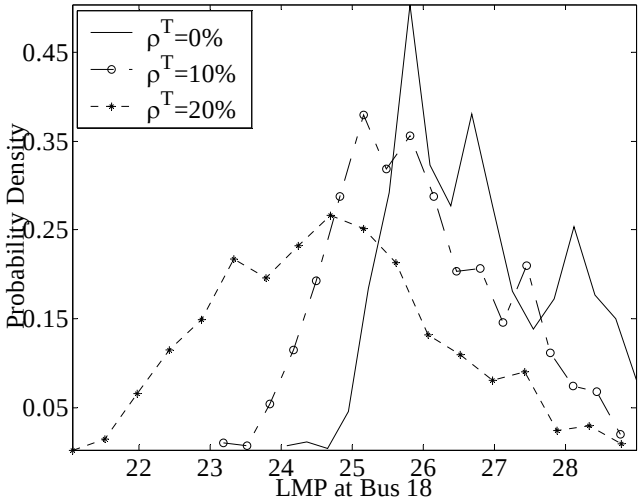

Figure 3-5 Probability distributions of LMPs at bus 18 over the sample year with different TRMs requirements

Observations from figures 3-4 and 3-5 coincide with the indication from figure 3-3: higher TRMs increase the LMP at the load bus due to transmission congestion charges and lower the LMP at the generation bus due to lower output level, while lower TRMs grant more transmission capacity for market dispatch, reduce transmission congestions and determine less differentiated LMPs between buses. The quantitative measures of averaged spatial volatility of LMPs over the sample year at different TRMs are listed in table 3-1 as follows,

Table 3-1 Averaged spatial volatility of LMPs over the sample year when imposing different TRM requirements in the market dispatch ($/MWh)

0% TRM	10% TRM	20% TRM
4.02	4.67	5.12

Identification of transmission adequacy and reliability needs

To identify transmission adequacy and reliability needs, we consider the market dispatch model without constraints (3.4a) and (3.4b). By varying the capacity of two transmission bottlenecks, the transmission lines between Bus 20 and Bus 23, between Bus 22 and Bus21, we calculate the sensitivities of reliability index for system transmission reliability margin (TRM), which is calculated as the sum over all transmission lines of the relative difference between transmission capacity and power output.

$$\sum_m \sum_n \frac{T_{mn} - \sqrt{P_{mn}^2}}{T_{mn}} \tag{3.5}$$

The simulation results for investment in transmission line between Bus 20 and Bus 23 are given by figure 3-6.

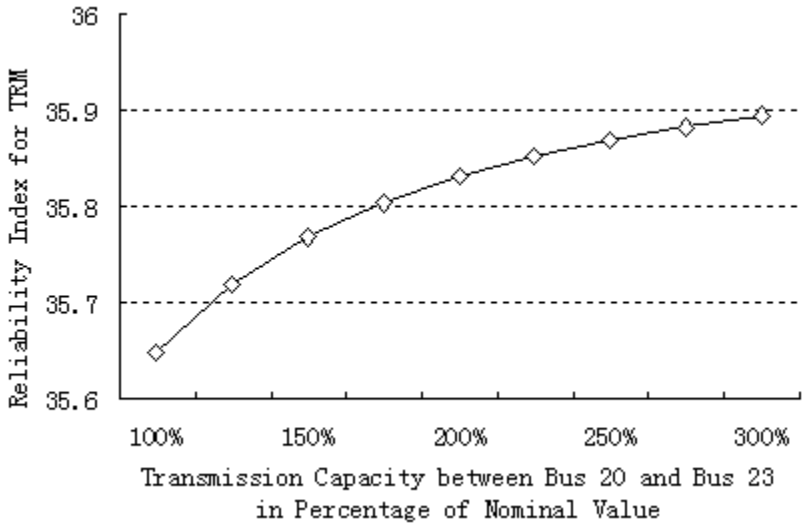

Figure 3-6 Reliability index for system TRM with respect to transmission capacity between Bus 20 and Bus 23 using market dispatch when the system load is 60% of peak level

From figure 3-6, we observe that the reliability index for TRM increases with the increase of available transmission capacity of the transmission bottleneck, though not strictly. The total generation cost decreases at the same time. The simulation results for investment in transmission line between Bus 21 and Bus 22 are given by figure 3-7.

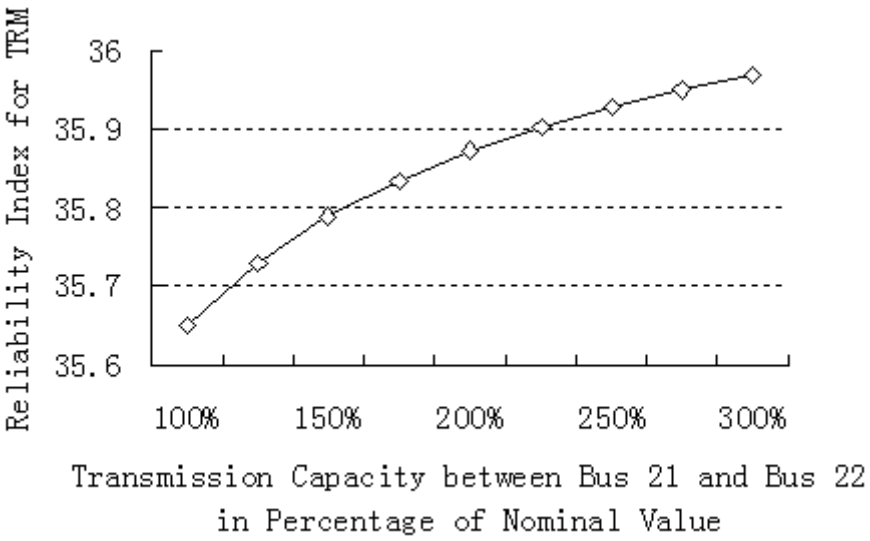

Figure 3-7 Reliability index for system TRM with respect to transmission capacity between Bus 21 and Bus 22 using market dispatch when the system load is 60% of peak level

From figure 3-7, we observe that the reliability index for TRM increases with the increase of available transmission capacity of the transmission bottleneck. The total generation cost decreases at the same time.

3.3. Effectiveness of Market-based Transmission Compensation

In 3.2.2, we illustrated how to identify the investment needed to increase transmission capacity of a transmission bottleneck to achieve certain desired reliability index level for TRM. Here we further explore the effectiveness of market-based transmission compensation. Following Kristiansen (2008), we assume there are no proxy FTRs and reward the incremental FTRs for new transmission capacity that maximizes investor's preferences. To conform to the system capability and ensure the revenue solvency of the system operator, the FTRs before and after expansion are all subject to simultaneous feasibility tests (SFT). The allocation of incremental FTRs is formulated as follows

$$\underset{\delta}{Max}\ \ b\delta$$

$$\text{s.t. } FP \le T \tag{3.6a}$$

$$F^{+}(P+\delta) \le T^{+} \tag{3.6b}$$

where

b is the bid preference parameter of the investor,

F and F^+ represent the system PTDF matrices before and after expansion,

T and T^+ are vectors of transmission capacity limits before and after expansion,

P is a vector of existing amounts of FTRs,

δ is the decision variable, amounts of incremental FTRs.

As an illustration, we expand the transmission network by increasing the capacity of transmission line between Bus 20 and Bus 23 to 150%, so that the reliability index for system TRM is above 35.87. The original IEEE RTS24 system has 1000 MW capacity on the line between Bus 20 and Bus 23. After expansion, the capacity becomes 1500 MW. Assume originally there are only two FTRs in the system: FTRs between Bus 20 and 23, Bus 22 and 21. We assume the bid values are

$b_{20,23} = 60$, $b_{22,21} = 10$,

which shows that the investor has a greater preference for incremental FTRs in transmission line between Bus 20 and Bus 23. The existing amounts of FTRs before expansion are

$P_{20,23} = 529.1$, $P_{22,21} = 300$

which are simultaneous feasible and the capacity between Bus 20 and Bus 23 are fully allocated.

The optimal incremental FTRs solved are

$\delta_{20,23} = 264.8$, $\delta_{22,21} = 57.8$

which fully allocate the expanded capacity in line between Bus 20 and Bus 23 and the capacity in line between Bus 22 and Bus 21. The FTR revenues collected from transmission lines between Bus 20 and 23, Bus 22 and 21 increase 4% and 16%, respectively.

Through this case study, we show that FTR-based compensation scheme does provide financial incentives for reliability and adequacy targeted transmission investments via allocating the incremental FTRs to investors. The magnitude of such incentives depends on the amount of incremental FTRs generated. The quantity and value of the incremental FTRs further depend on the bid values, the transmission network topology and the initial configuration of the allocated FTRs.

4. Modeling the Financial Risk of Power Transfers in the Market for Transmission Congestion Contracts in New York State

Besides FTR, another important financial instrument used to hedge against the risk of price differences between regions is Transmission Congestion Contracts (TCC). In this chapter, we use the New York State electricity market as another case study to measure the congestion costs for a specified TCC, by simulating the stochastic behavior of zonal electricity price differences.

4.1. Introduction

The electricity market in New York State (NYS) was deregulated in November 1999, and it is now operated by the New York Independent System Operator (NYISO). Even though the NYISO network is connected to the adjoining systems in New England, PJM and Canada, the NYISO market corresponds almost exactly to the geography of NYS. By 2006, the number of nodes on the NYISO network had increased to more than 400. The electricity price at each node in the wholesale market is called the nodal price. The price is determined by the system operator in an auction based on offers submitted by different generators and bids submitted by buyers. The hourly nodal prices in both the real-time and day-ahead markets are highly volatile, especially when the demand for electricity is high and the transmission network is congested.

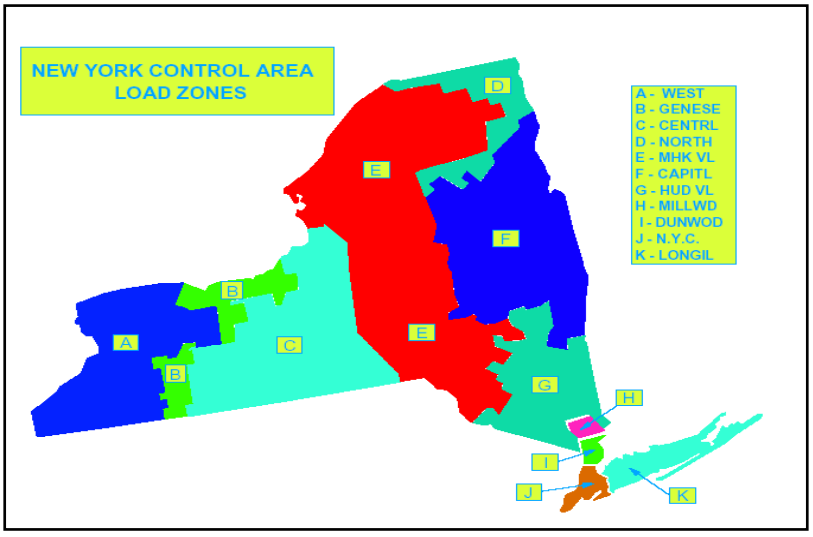

Figure 4-1 Load Zones in the Electricity Market in the New York Control Area

Source: http://www.nyiso.com/public/index.jsp

When there is no congestion on the network, the differences in the prices at different nodes are small and caused by transmission losses. Under these circumstances, all nodal prices are effectively determined by the cost (offer) of the most expensive unit generating (equivalent to a merit-order dispatch). Since the inexpensive sources of generation are mostly upstate, the network transfers power from upstate to New York City (NYC) in the SE corner of the NYISO region. When the load increases in NYC, the transmission lines linking NYC to upstate eventually become congested, and the amount of power transferred is constrained by the capacity of these lines. When the limits of transmission are reached, the market fragments into sub-regions (load pockets) and the nodal prices in a load pocket are now set by the most expensive source of generation in that load pocket. Hence, the market prices in NYC can be substantially

higher than the prices upstate. These price differences are large and are caused primarily by the cost of congestion.

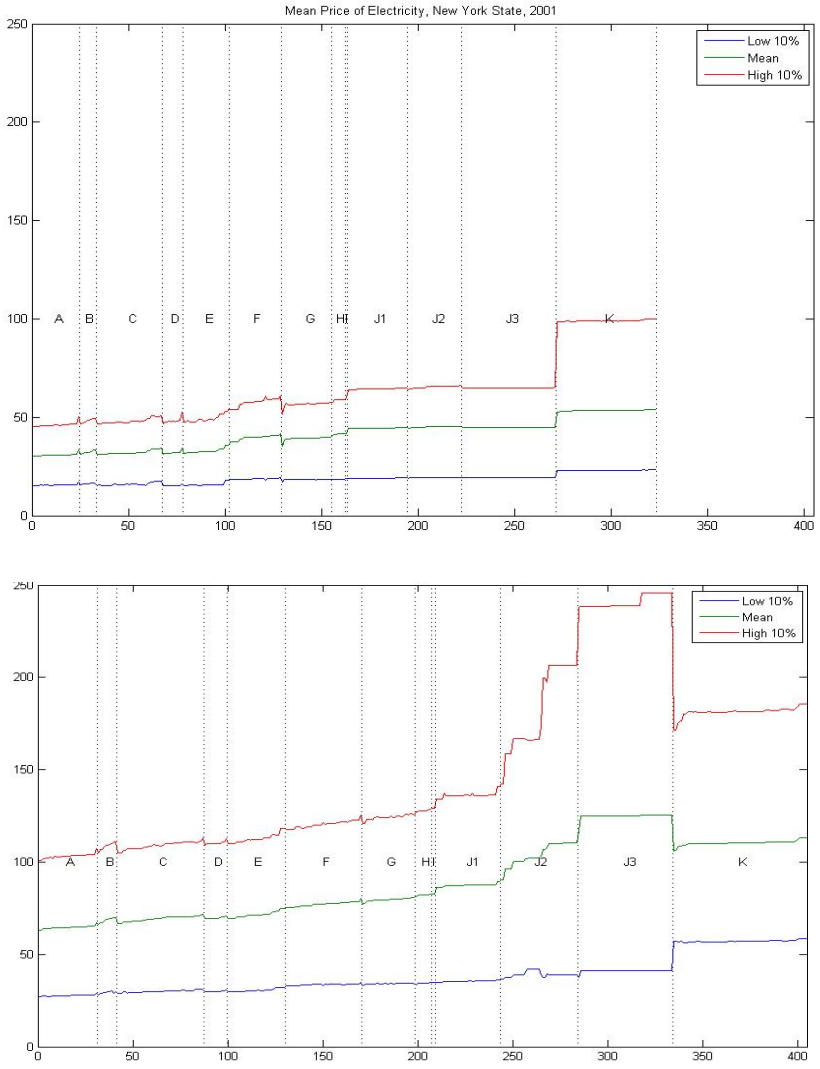

Figure 4-2 Nodal Prices of Electricity in 2001 and 2005 Ranked by Load Zone

Source: Derived from data on http://www.nyiso.com/public/index.jsp

Figure 4-1 shows the Load Zones in the New York Control Area. Most of the major sources of inexpensive generation are "upstate" in Zones A, B, C and E, and most of the load is "downstate" in New York City (Zone J) and Long Island (Zone K). The Hudson Valley (Zones G, H, and I) is the major transmission corridor for transferring power from upstate to downstate. The nodal prices in the Day-Ahead-Market (DAM) for 2001 and 2005 are shown in Figure 4-2. For each year, the mean annual price, the 90th percentile price and the 10th percentile price are computed for every node. The mean nodal prices are then ranked within each Zone and this ranking is then applied to the 90th and 10th percentile prices as well. Inspection of these two plots

shows 1) the total number of nodes increased from 2001 to 2005, 2) the nodal prices are higher downstate than upstate, 3) the differences across zones in the 10^{th} percentile prices (low load) are relatively small, 4) the differences across zones in the 90^{th} percentile prices (high load) are relatively large due to congestion, and 5) congestion has become more important over time and by 2005 there were substantial differences in nodal prices within New York City (Zone J). Note that the three sub-zones in Zone J are based on an Eigen analysis of the nodal prices and are not officially recognized by the NYISO.

If a generator in upstate wants to sell power in NYC, for example, it is not effective to use a standard bilateral contract with a buyer to hedge against price risk. When a generator holds a forward contract for fuel, the generator would typically be willing to negotiate with a local load for a fixed price contact to deliver a fixed quantity of power for specified time periods. This contract is equivalent to the type of contract-for-differences traded on the New York Mercantile Exchange (NYMEX) for different locations in the state. Hence, a generator selling into a load pocket over congested transmission lines faces additional price risk due to the volatility of congestion costs. For this reason, different kinds of financial instruments, such as Transmission Congestion Contracts (TCC) and Financial Transmission Rights (FTR), have been developed to hedge against the risk of price differences between regions. In NYS, for example, owning a TCC pays the holder the hourly price difference between a Point-of-Withdrawal and a Point-of-Injection in the day-ahead-market (adjusted for losses) for a transfer of 1MW over a specified period (for example, one month). A generator holding a forward contract for fuel combined with the appropriate TCC can hedge a fixed price contract with a buyer in a load pocket perfectly. This is the basic rationale for establishing the TCC market in NYS, and this market made it feasible for generators in upstate to adapt existing bilateral contracts with NYC to the structure of the new wholesale market. In fact, many contracts that existed before the TCC market was established have been "grandfathered" into the TCC auctions.

Since the transmission corridor between NYC and the Hudson Valley is the most important transmission bottleneck in the state, it has been a major concern of government, industry and academic analysts since the electricity market was first deregulated. The purpose of this chapter was to develop a modeling framework to simulate the stochastic behavior of congestion costs of electricity in New York State and especially the link between NYC and the Hudson Valley. Through this process, the predicted price differences can be used as a basis for measuring the magnitude and financial riskiness of congestion costs for a specified TCC.

4.2. The Econometric Results

The basic specification of the model is that the price of electricity in a specified zone (region) is a function of the corresponding load, the price of natural gas and a set of seasonal and daily variables. Multivariate time-series models (VARMAX) were estimated for 1) the daily temperature in different locations conditional on seasonal cycles, 2) the average daily loads in different zones conditional on Heating Degree Days (HDD), Cooling Degree Days (CDD), seasonal cycles and dummy variables for days of the week, and 3) the prices of electricity in different zones conditional on the load, a polynomial lag of past prices of natural gas, seasonal cycles and dummy variables for days of the week. The models were estimated using daily data from 2002 to 2005 and the estimated models meet standard statistical criteria for VARMAX models (white noise residuals, etc.). The statistical specifications of these models are described in a paper that is one of the deliverables for this project (Mount, T.D. and J. Ju, 2007).

The estimated models were then used to predict the average daily prices in Western New York (Zone A), the Hudson Valley (Zone G), NYC (Zone J) and Long Island (Zone K) for the summer of 2006. The sum of the price differences for different pairs of locations from May to October represents the earnings of a six-month strip for the corresponding TCC. Since the estimated models are based on information that was available before the auction to sell the TCC, it is appropriate to use these models to evaluate the financial risk of purchasing a TCC in the auction. The financial risk of the TCC for the summer of 2006 was evaluated from two different perspectives. First, the risk of hedging for a generator comes primarily from uncertainty about the actual daily temperatures next summer. It is assumed implicitly that the generator holds a forward contract for natural gas based on the current forward prices for natural gas on the New York Mercantile Exchange (NYMEX). Second, the risk for speculators comes from the combined uncertainty about future temperatures and future prices of natural gas.

For both hedgers and speculators, 100 different realizations of daily temperatures and loads in different zones were simulated for March to October 2006 to represent a random sample of 100 summers. For hedgers, the future daily prices of natural gas were interpolated from the forward price of natural gas on the New York Mercantile Exchange (NYMEX) for different delivery months. For speculators, 100 different realizations of the daily price of natural gas for March to October 2006 were simulated from an ARIMA model that was estimated using data for 2002 to 2005. Each realization for the daily price of natural gas was paired with one set of realizations for the daily temperatures in different zones. Given these realizations of daily temperatures and the daily price of natural gas, it is straightforward to simulate 100 sets of daily prices of electricity in different zones and compute the corresponding daily price differences. The corresponding revenues from holding a TCC for May to October 2006 can be computed by scaling and aggregating the price differences.

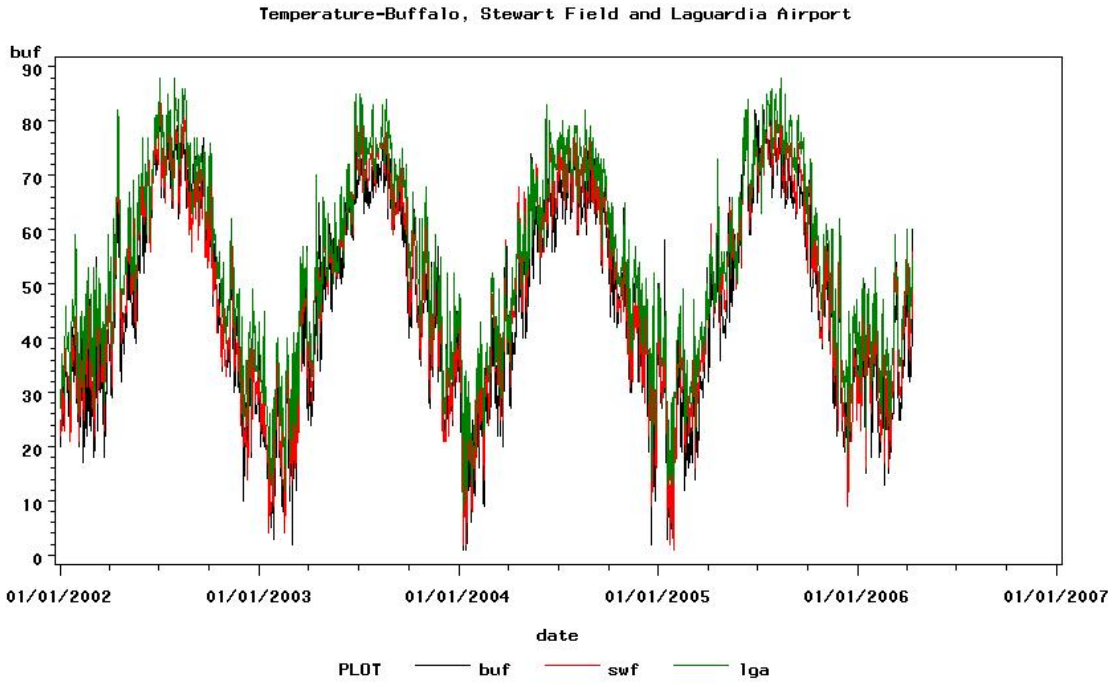

Figure 4-3 Daily Temperature Data for Three Locations in New York State

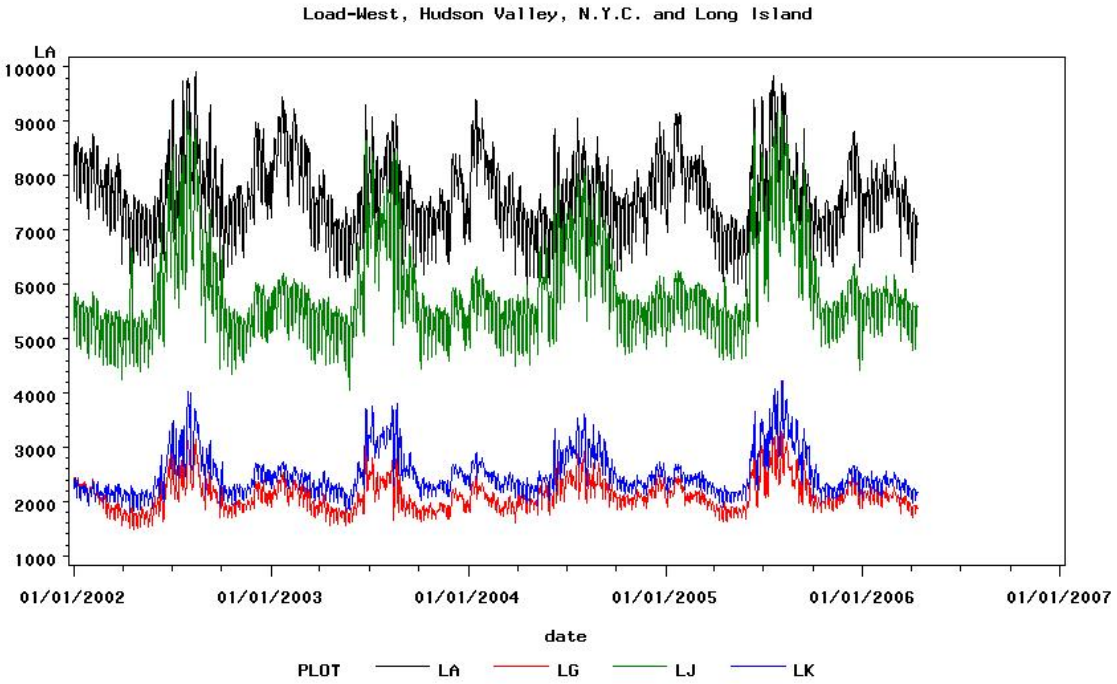

Figure 4-4 Daily Load Data for Zones A-F, G-I, J and K

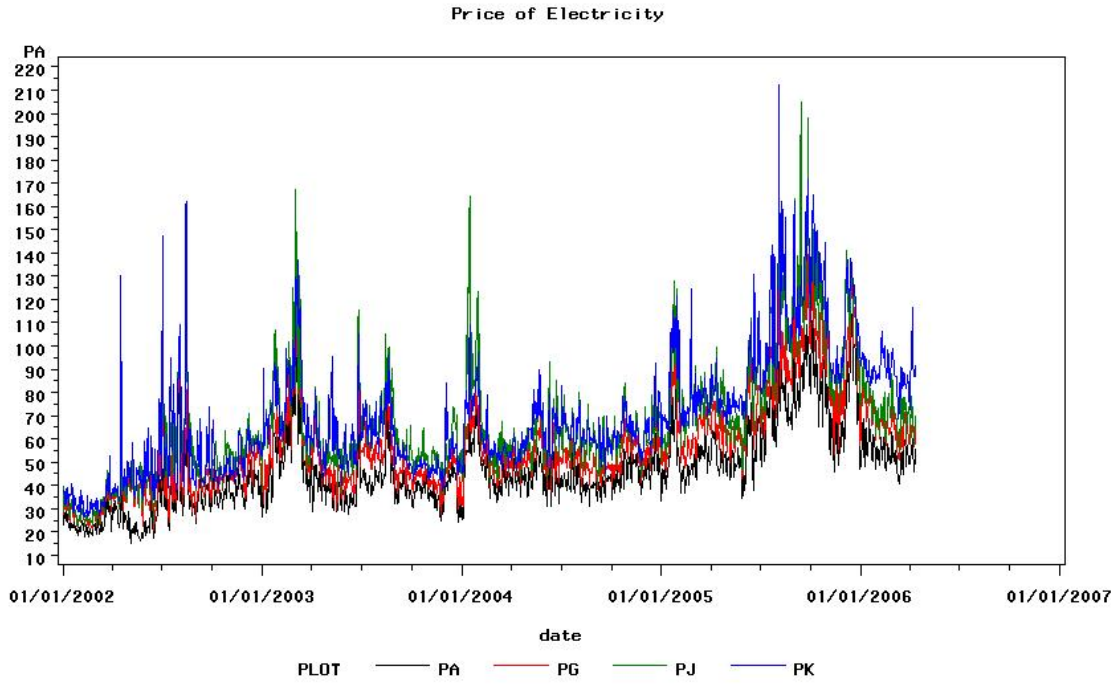

Figure 4-5 Daily Price Data for Zones A, G, J and K

The basic data used for the econometric modeling are shown in figures 4-3 to 4-5. Figure 4-3 shows the clear annual pattern of high summer temperatures and low winter temperatures. The temperatures at different locations are highly positively correlated together and this interdependence is captured by the VARMAX specification. In the simulations, the correlations among the random departures from the estimated annual cycles at different locations are incorporated and these spatial correlations have important effects on the behavior of the simulated loads and prices in the four different Zones. Figure 4-4 shows the load data for Zones A-F combined, Zones G-I combined and Zones J and K and illustrates the importance of the summer peak in NYC (Zone J) due to air conditioning (the two aggregates of the upstate Zones correspond to the main groupings in the structure of the daily nodal prices using an Eigen analysis). The summer and winter peak periods and the weekly cycles are clearly visible for load. In contrast, the behavior of the prices in figure 4-5 for Zones A, G, J, and K is more random and the annual and weekly patterns are far less obvious. In addition, prices have trended up more over time, due in part to higher prices for natural gas, compared to the loads. However, it is the variability of price differences between two locations that reflects the financial riskiness of holding a TCC. Since the prices at different locations are positively correlated together, the variability of price differences could be substantially less than the variability of the individual prices.

Using data for 2002-2005, models for temperature, load and price were estimated. The objective was to use these models to simulate the distribution of payouts from holding a TCC for the summer months in 2006. In other words, the simulated payouts were based only on information that was available before the auction to sell the TCC occurred in February 2006 (and forecasts of the price of natural gas derived from the forward prices of delivery at Henry Hub obtained from NYMEx). The main source of uncertainty in the payout from buying a TCC is that the summer temperatures in 2006 are not known. One predicted payout for May to October (the standard six month strip for a TCC) is computed by predicting the daily prices from February to October at the four locations. These daily prices are then used to compute and aggregate the corresponding price differences over the summer months. The simulation process for determining one payout of the TCC is illustrated by showing the daily realizations of temperature, load and price in figures 4-6 to 4-8. The patterns of behavior of these simulated data are similar to the observed data in figures 4-3 to 4-5, showing that the VARMAX framework captures the type of randomness that underlies the true data generating processes. The focus is now directed to evaluating the simulated price differences between NYC (Zone J) and the Hudson Valley (Zone G).

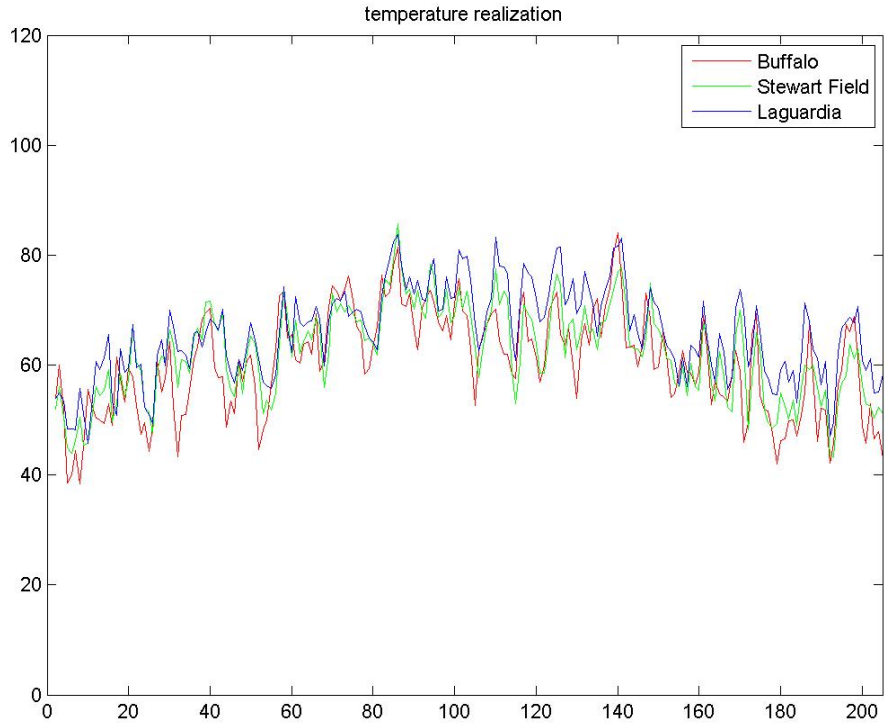

Figure 4-6 One simulated realization of daily temperatures for February to October 2006

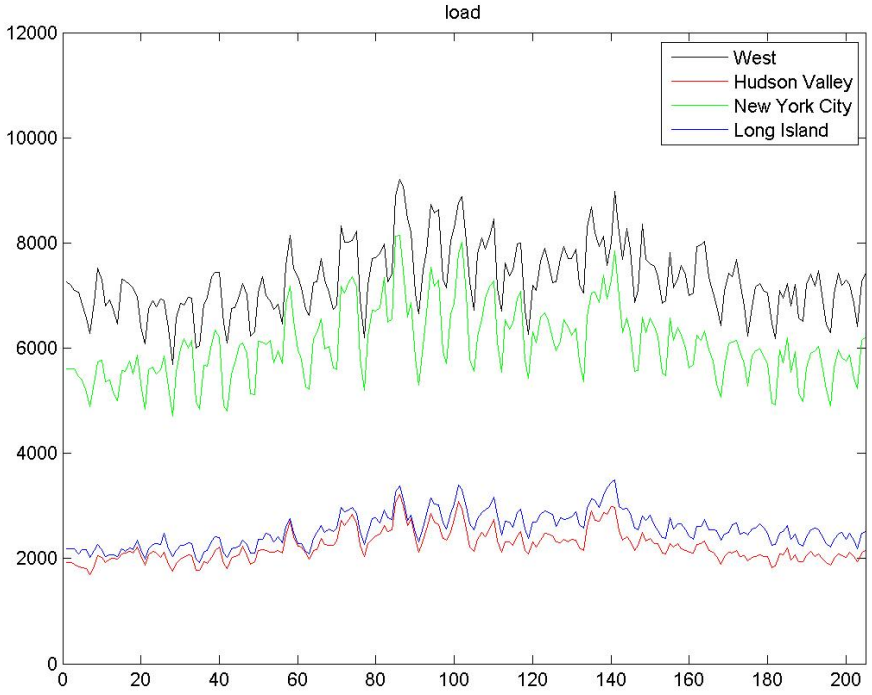

Figure 4-7 One simulated realization of daily loads for February to October 2006

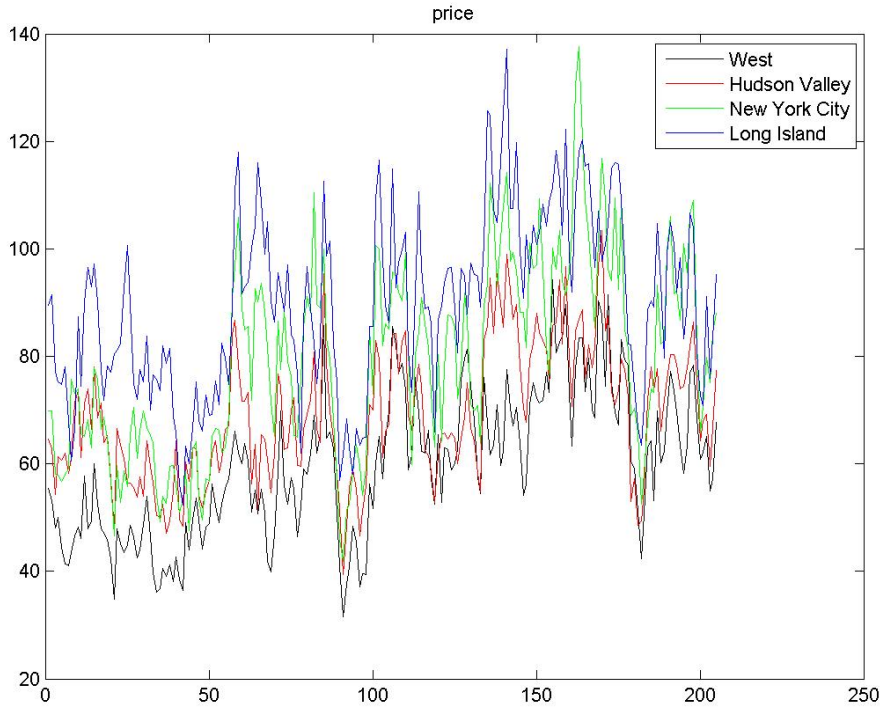

Figure 4-8 One simulated realization of daily prices for February to October 2006

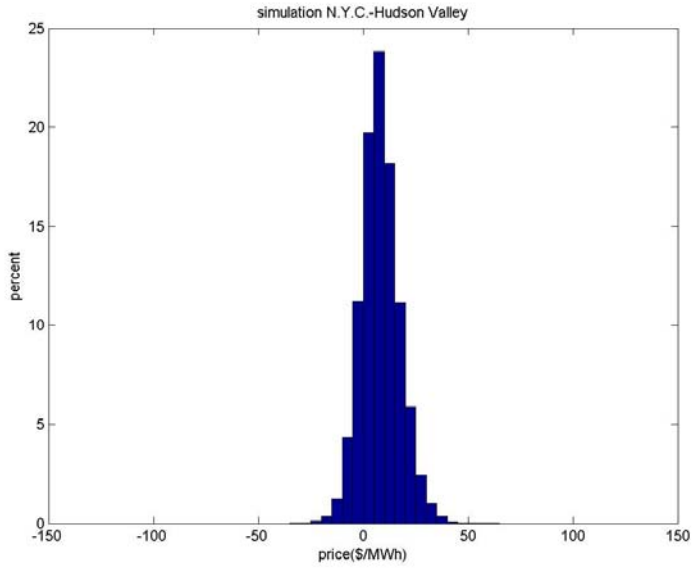

Figure 4-9 Simulated Daily Price Differences between NYC and the Hudson Valley for May-October 2006 (Hedgers using Actual Forward Prices for Natural Gas)

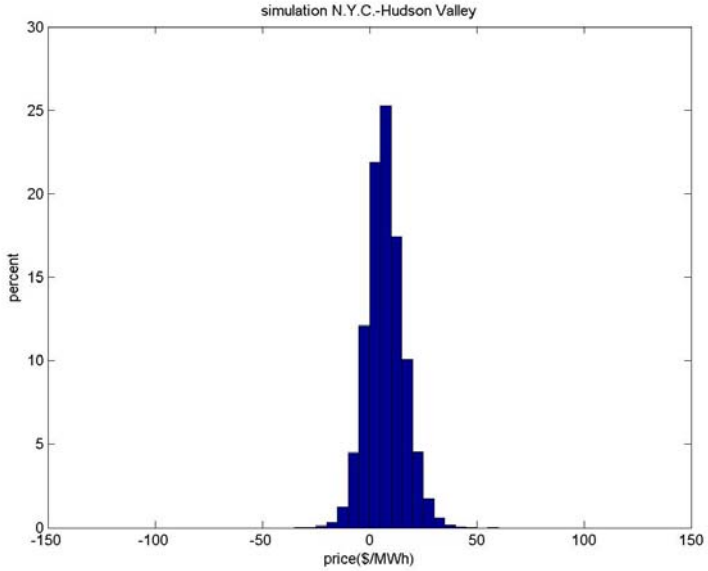

Figure 4-10 Simulated Daily Price Differences between NYC and the Hudson Valley for May-October 2006 (Speculators using Simulated Realizations of the Price for Natural Gas)

The simulated price differences in figures 4-9 and 4-10 are histograms of the simulated daily price differences between NYC and the Hudson Valley. Each histogram summarizes 100 realizations of the 184 daily price differences from May 1st to October 31st. Even though the price spikes are more likely to occur in NYC, there is no obvious skewness to the right as one might expect and the histograms are approximately normally distributed. It is interesting to note that the histogram for hedgers (using the same projection of the price of natural gas for all 100 realizations of the summer) has slightly more variability than the histogram for speculators (using different projections of the price of natural gas derived from an estimated ARIMA model). However, it is the distribution of the simulated payouts aggregated over the 184 days in a summer, corresponding to the six-month TCC, that is the main focus of this analysis.

The results for four different TCCs are summarized in table 4-1. Since the actual payout from holding a TCC is for the Congestion Component (C.C.) of the price differences only and does not include the Loss component, both two components of the actual payouts in the Summer 2006 are shown. For example, the payout from holding a TCC for a transfer from the Hudson Valley (Zone G) to NYC (Zone J) pays the total congestion costs for the 24x184 hours from May to October. The actual total congestion cost paid was $36,685.3/MW for the Zone G-J TCC but the simulations represent the differences in the Location Based Marginal Prices (LBMP, i.e. the nodal price differences). Hence, the simulated payouts correspond to the actual LBMP difference of $36,851.3/MW that includes the Loss of $166.0/MW. Comparing the actual LBMP payout with the corresponding simulated payouts shows that all of the actual LBMP payouts fall in the ranges of the simulated payouts. The actual LBMP payouts for Zones A-G, A-J and J-K are all substantially higher than the simulated mean values, and in contrast the actual LBMP payout for Zones G-J, the main focus of this analysis, is slightly less than the mean for Hedgers and slightly

above for Speculators. Overall, the actual payouts represent a realistic random selection from the simulated distributions.

Table 4-1 Simulated Payouts from Four Different Six-Month TCCs for the Summer 2006
Simulation Results ($/MW)

Sim1 (Hedgers)		Zones A-G	Zones A-J	Zones G-J	Zones J-K
Actual payout	LBMP	60,543.1	97,394.4	36,851.3	67,281.1
May-October 2006	Loss	1,698.1	1,864.1	166.0	140.3
	C.C.	58,845.0	95,530.3	36,685.3	67,140.8
Simulated payouts	max	72,021.0	108,880.8	50,574.4	74,419.7
LBMP	mean	52,000.8	89,706.5	37,705.7	48,333.1
	median	52,051.0	90,622.3	37,856.7	47,461.4
	min	37,079.5	68,974.3	17,080.3	27,908.9

Sim2 (Speculators)		A-G	A-J	G-J	J-K
Actual payout	LBMP	60,543.1	97,394.4	36,851.3	67,281.1
May-October 2006	Loss	1,698.1	1,864.1	166.0	140.3
	C.C.	58,845.0	95,530.3	36,685.3	67,140.8
Simulated payouts	max	67,501.7	100,596.8	45,393.3	74,000.7
LBMP	mean	48,907.0	82,401.0	33,494.0	49,236.2
	median	48,829.6	83,005.9	33,678.5	48,405.5
	min	34,767.9	63,205.6	14,342.5	30,194.3

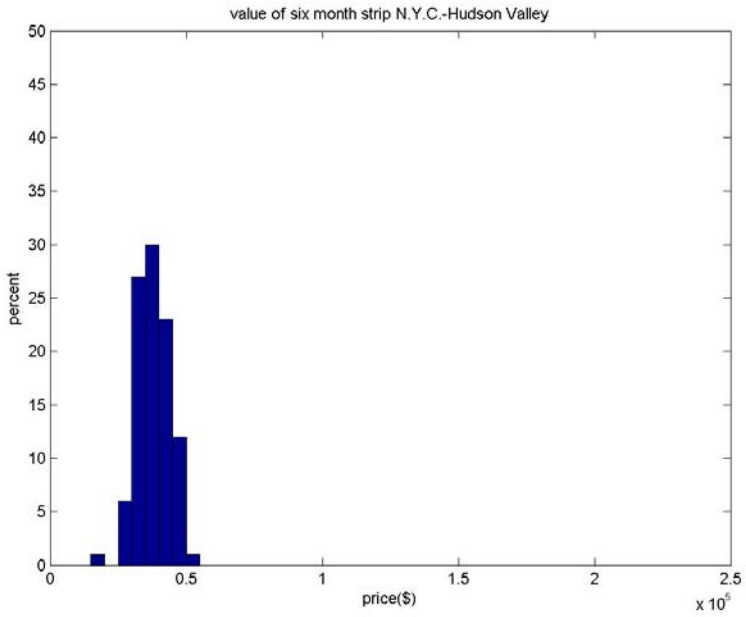

Figure 4-11 Simulated LBMP Payouts for a TCC between NYC and the Hudson Valley for May-October 2006 (Hedgers using Actual Forward Prices for Natural Gas)

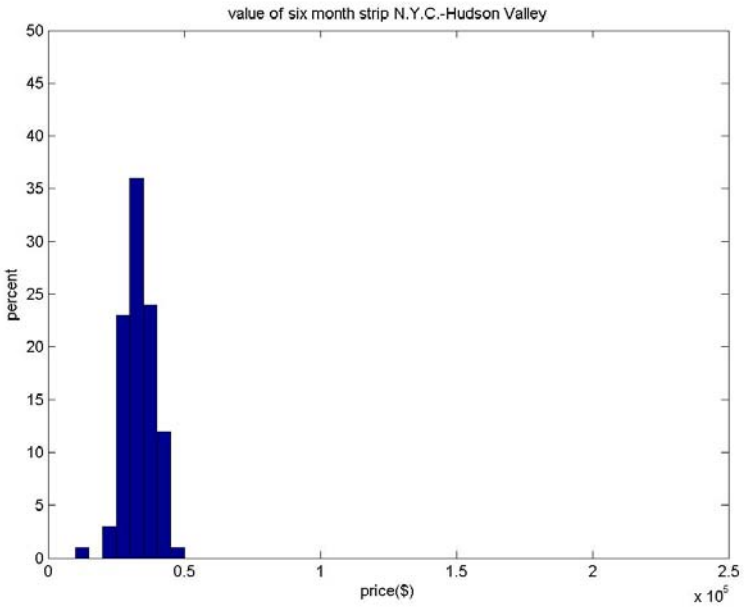

Figure 4-12 Simulated LBMP Payouts for a TCC between NYC and the Hudson Valley for May-October 2006 (Speculators using Simulated Realizations of the Price for Natural Gas)

Figures 4-11 and 4-12 show the distributions of the simulated LBMP payouts from holding a Zone G-J TCC for hedgers and speculators, respectively. These two figures are consistent with figures 4-9 and 4-10 that show the distribution of the simulated daily price differences between Zones G and J. Notice that the simulated TCC payouts are all positive even though there are a substantial number of negative price differences shown in figures 4-9 and 4-10. This is also the case for the three other TCCs presented in table 4-1. The overall conclusion is that this analysis has demonstrated successfully the feasibility of using an econometric model to simulate the financial riskiness of the payout from holding a TCC using only information known prior to the TCC auction. This method could be applied to evaluating a portfolio of TCCs, and it provides a viable framework for monitoring the behavior of participants in the TCC market that could be adopted by the NYISO.

The results show that the simulated revenues from holding a TCC between the Hudson Valley and New York City are generally close to the price paid in the auction in March. For hedgers, the auction price is 45.05 percentile of simulated revenues, and for speculators, the auction price represents the 71.27 percentile. Although this is only a single example, the results do raise questions about the effectiveness of the TCC auction as a reliable source of price discovery. This research is the first step toward understanding the stochastic behavior of transmission costs and the TCC market. Future research can look into multivariate time-series models to jointly model the price of electricity, load and temperature.

5. Reduced-form Hub-and-spoke Representation of a Power System

5.1. Introduction

We proposed to investigate effective approaches for identifying proxy trading hubs in an LMP-based market and the corresponding financial contract market structures for approximating correct incentives for inducing efficient capacity investment in generation and transmission through instruments such as FTRs or TCCs. We developed a non-parametric econometric model for modeling the structure of the LMPs at major zones in a bulk power system. Using this model, we can identify and analyze the major factors influencing the LMPs in all zones which may serve as explanatory variables for the FTR prices. We have applied this non-parametric model to investigate the electricity day-ahead forward price curve dynamics. This model performs better in short-term forecasting than existing time series models do. A paper has been completed on the non-parametric modeling of electricity forward curves and sent to a journal for publication.

5.2. Alternative Non-linear Dimension Reduction Method

5.2.1 Introduction to manifold learning

Manifold learning is a new and promising nonparametric dimension reduction approach. Many high-dimensional data sets that are encountered in real-world applications can be modeled as sets of points lying close to a low-dimensional manifold. Given a set of data points $x_1, x_2, \cdots, x_N \in R^D$, we can assume that they are sampled from a manifold with noise, i.e.,

$$x_i = f(y_i) + \varepsilon_i, i = 1, \cdots, N \tag{5.1}$$

where $y_i \in R^d, d << D$, and ε_i are noises. Integer d is also called the intrinsic dimension. The manifold based methodology offers a way to find the embedded low-dimensional feature vectors y_i from the high-dimensional data points x_i.

Many nonparametric methods were created for nonlinear manifold learning, including multidimensional scaling (MDS), locally linear embedding (LLE), Isomap, Laplacian eigenmaps, Hessian eigenmaps, local tangent space alignment (LTSA), and diffusion maps.

Among various manifold based methods, we find that locally linear embedding (LLE) works well in modeling LMPs. Our purpose is to analyze the features of cross-zonal LMPs. In next subsection, we introduce the algorithms of LLE.

5.2.2 Locally linear embedding (LLE)

Given a set of data points $x_1, x_2, \cdots, x_N \in R^D$ in the high-dimensional space, we are looking for the embedded low-dimensional feature vectors $y_1, y_2, \cdots, y_N \in R^d$. LLE is a nonparametric method that works as follows:

1. Identify the k nearest neighbors based on Euclidean distance for each data point $x_i, 1 \le i \le N$. Let N_i denote the set of the indices of the k nearest neighbors of x_i.
2. Find the optimal local convex combination of the k nearest neighbors to represent each data point x_i. That is, the following objective function (5.2) is minimized and the weights w_{ij} of the convex combinations are calculated.

$$E(w) = \sum_{i=1}^{N} \| x_i - \sum_{j \in N_i} w_{ij} x_j \|^2 \tag{5.2}$$

where $\| \cdot \|$ is the l_2 norm and $\sum_{j \in N_i} w_{ij} = 1$.

The weight w_{ij} indicates the contribution of the jth data point to the representation of the ith data point. The optimal weights can be solved as a constrained least square problem, which is finally converted into a problem of solving a linear system of equation.

3. Find the low-dimensional feature vectors $y_i, 1 \le i \le N$, which have the optimal local convex representations with weights w_{ij} obtained from the last step. That is, y_i's are computed by minimizing the following objective function:

$$\Phi(y) = \sum_{i=1}^{N} \| y_i - \sum_{j \in N_i} w_{ij} y_j \|^2 \tag{5.3}$$

It can be shown that solving the above minimization problem (5.3) is equivalent to solving an eigenvector problem with a sparse $N \times N$ matrix. The d eigenvectors associated with the d smallest nonzero eigenvalues of the matrix comprise the d-dimensional coordinates of y_i's. Thus, the coordinates of y_i's are orthogonal.

LLE does not impose any probabilistic model on the data; however, it implicitly assumes the convexity of the manifold. It can be seen later that this assumption is satisfied by the electricity price data.

5.3. Modeling of LMPs with Locally Linear Embedding Method

We used data of the day-ahead LMPs of 10am in the 15 zones of the New York Independent System Operator (NYISO): CAPITL, CENTRL, DUNWOD, GENESE, H Q, HUD VL, LONGIL, MHK VL, MILLWD, N.Y.C., NORTH, NPX, O H, PJM, and WEST. Two years (731 days) of price data from Feb 6, 2003 to Feb 5, 2005 are used as an illustration of modeling the LMPs by manifold based methodology. The data are available online (*www.nyiso.com* / *public* / *market_data* / *pricing_data.jsp*).

5.3.1 Preprocessing

LLP smoothing

The noise in (5.1) can contaminate the learning of the embedded manifold and the estimation of the intrinsic dimension. Therefore, locally linear projection (LLP) is recommended to smooth the manifold and reduce the noise. The description of the algorithm is given as follows:

ALGORITHM: LLP

For each observation $x_i, i = 1,2,\cdots,N$,

1. Find the k-nearest neighbors of x_i. The neighbors are denoted by $\tilde{x}_1, \tilde{x}_2, \cdots \tilde{x}_k$

2. Use PCA or SVD to identify the linear subspace that contains most of the information in the vectors $\tilde{x}_1, \tilde{x}_2, \cdots \tilde{x}_k$. Suppose the linear subspace is A. Let k_0 denote the assumed dimension of the embedded manifold. Then subspace A_i can be viewed as a linear subspace spanned by the singular vectors associated with the largest k_0 singular values.

3. Project x_i into the linear subspace A_i and let $x_i, i = 1, \cdots, N$, denote the projected points.

After denoising, the efficiency of manifold learning is enhanced, and the reconstruction error (TRE) of the entire calibration data set is reduced. For the illustrated data set with the intrinsic dimension being four, the TRE is 1.53% after LLP smoothing, compared to 1.72% without LLP smoothing. The choice of the two parameters in LLP, the dimension of the linear space and the number of the nearest neighbors, will be discussed in detail in subsection 5.3.4.

5.3.2 Manifold learning by LLE

LMP of 15 zones at 10am each day is considered as an observation, so the dimension of the high-dimensional space D is 15. The intrinsic dimension d is set to be four. The number of the nearest neighbors k for LLP smoothing, and LLE is selected to be a common number 16 for all the numerical studies. The details of the parameter selections are discussed in subsection 5.3.4. Due to the ease of visualization in a three-dimensional space, the low-dimensional manifold is plotted with the intrinsic dimension being three. We apply LLE to the denoised data $x_i, i = 1, \cdots, N$, which are obtained after LLP smoothing. Figure 5-1 provides the plot of the embedded three-dimensional manifold. As the low-dimensional manifold is nearly convex and uniformly distributed, LLE is an appropriate manifold based method. Figure 5-2 plots the time series of each coordinates of the feature vectors in the embedded four-dimensional manifold.

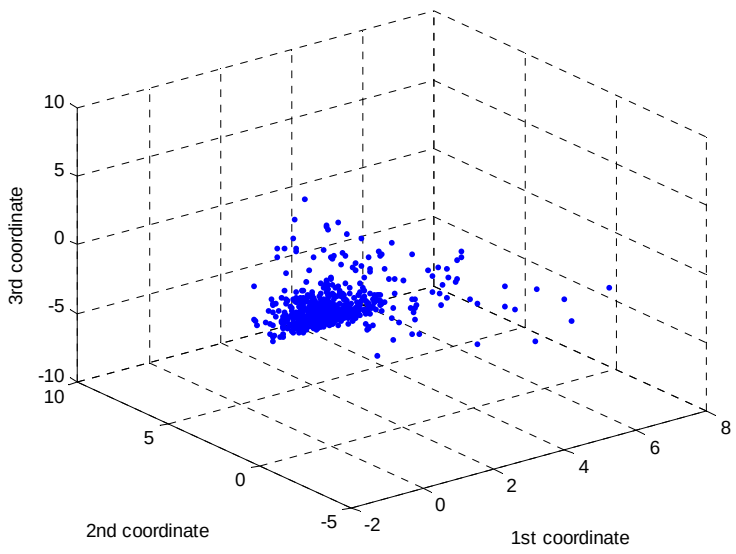

Figure 5-1 Embedded three-dimensional manifold after LLP smoothing

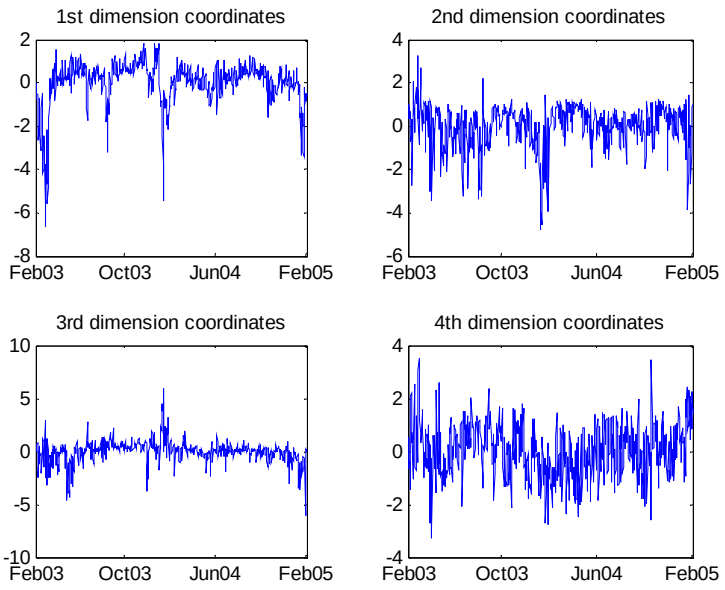

Figure 5-2 Coordinates of the embedded 4-dim manifold

5.3.3 Analysis of major factors with low-dimensional feature vectors

Interpretation of each dimension in the low-dimensional space

There are some interesting interpretations for the coordinates of the feature vectors in the low-dimensional space. The sequence of each coordinates of the low-dimensional feature vectors comprises a time series. The correlation between each time series and each FTR can be calculated. Table 5-1 shows the four FTRs, which have the maximum absolute correlations with the four-dimensional coordinates, and the corresponding correlation coefficients. It is found that the second coordinates have a very high correlation coefficient 0.8166 with the FTR from CENTRL to NYC, and the third coordinates are highly correlated with the FTR from NORTH to LONGIL with a correlation coefficient 0.7245. This also means that the second coordinates contain some other information. Table 5-1 also demonstrates that the first coordinates have a high correlation coefficient 0.684 with the FTR from CENTRL to CAPITL, and the fourth coordinates are highly correlated with the FTR from WEST to DUNWOD with a correlation coefficient -0.6208. Figure 5-3 illustrates these four FTRs in the zone map from NYISO (Source: http://www.nyiso.com/public/market_data/zone_maps.jsp).

Table 5-1 Correlation coefficient of the four-dimensional coordinates with four FTRs

Coordinate	1st	2nd	3rd	4th
FTR	CENTRL to CAPITL	CENTRL to NYC	NORTH to LONGIL	WEST to DUNWOD
Correlation Coefficient	0.684	0.8166	0.7245	-0.6208

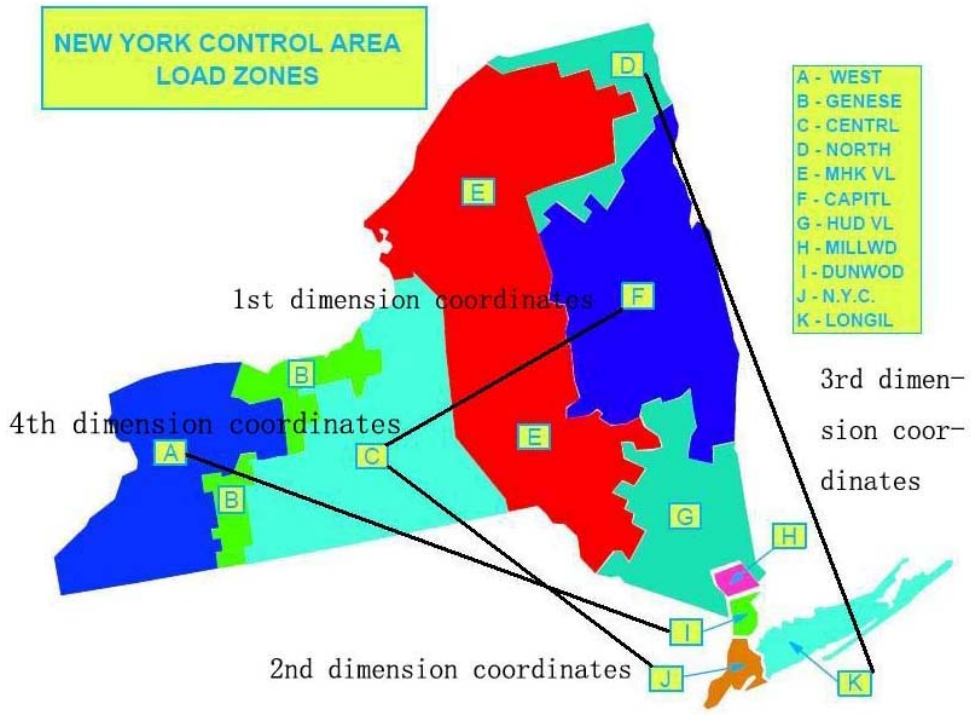

Figure 5-3 Four FTRs with the maximum absolute correlations with the 4-dim coordinates

Another interesting observation is that we could use as few as two FTRs to interpret the four-dimensional coordinates. Table 5-2 demonstrates that the FTR from WEST to DUNWOD has high correlation coefficients with the first and fourth coordinates, and the FTR between CENTRL to LONGIL has high correlation coefficients with the second and third coordinates. Figure 5-4 illustrates these two FTRs in the zone map.

Table 5-2 Correlation coefficient of the four-dimensional coordinates with two FTRs

Coordinate	1st	2nd	3rd	4th
FTR	WEST to DUNWOD	CENTRL to LONGIL	CENTRL to LONGIL	WEST to DUNWOD
Correlation Coefficient	0.6316	0.6196	0.6952	-0.6208

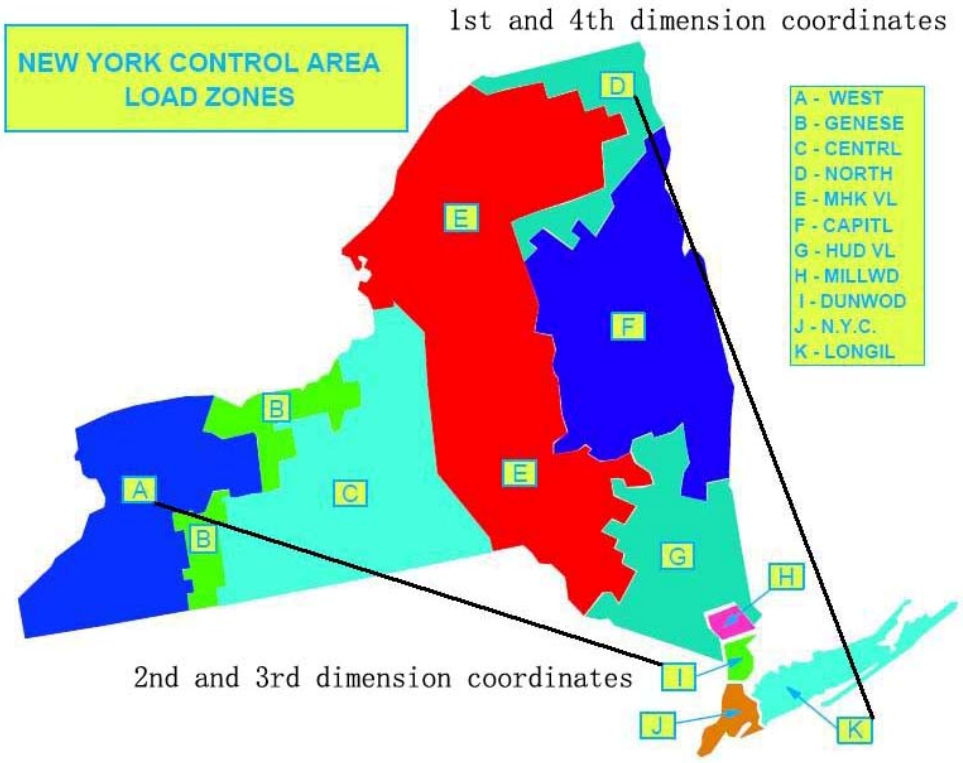

Figure 5-4 Two FTRs with high absolute correlations with the 4-dim coordinates

5.3.4 Parameter setting and sensitivity analysis

The selections of several parameters, including the number of intrinsic dimensions, the number of the nearest neighbors and the length of the calibration data, are discussed in this subsection.

Intrinsic dimension

Intrinsic dimension d is an important parameter of manifold learning. Levina (2005) and Verveer (1995) provide several approaches of estimating the intrinsic dimension. In Levina (2005), the maximum likelihood estimator of the intrinsic dimension is established. In Verveer (1995), the intrinsic dimension is estimated based on a nearest neighbor algorithm. The two methods show that the intrinsic dimension is some value around 4. Thus, it is reasonable to set the dimension of the linear space as 4 in LLP smoothing. The numerical experiments indicate that LLP smoothing can not only denoise, but also improve the efficiency of estimating the intrinsic dimension.

Another empirical way of estimating the intrinsic dimension is to analyze the sensitivity of the TRE to the different values of the intrinsic dimension. Figure 5-5 shows that the TRE is a decreasing function of the intrinsic dimension with an increasing slope. The slope of the curve in the figure has a dramatic change when the intrinsic dimension is around four. Therefore, we choose the intrinsic dimension as four.

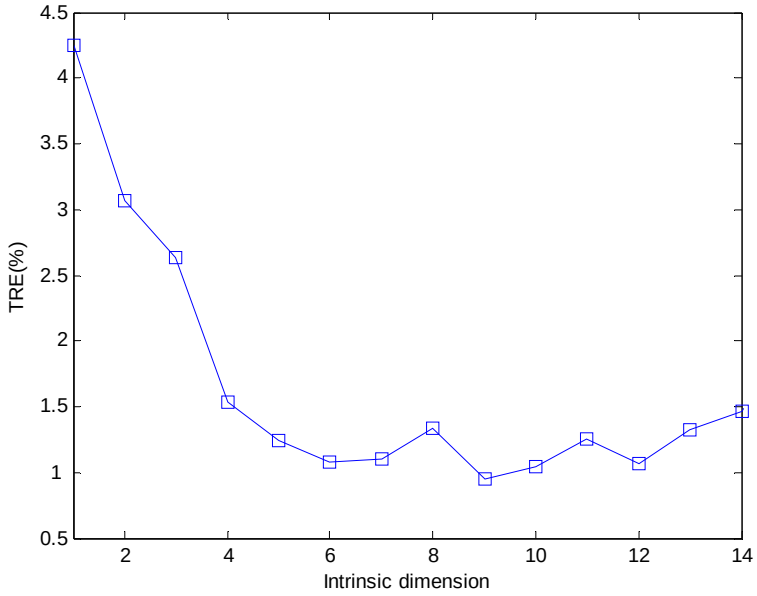

Figure 5-5 Sensitivity of TRE to the intrinsic dimension (data length = 731 days, number of the nearest neighbors = 16).

The number of the nearest neighbors

The plot of the TRE against the number of the nearest neighbors is used to select the appropriate number of the nearest neighbors. Figure 5-6 indicates the TRE first falls steeply when the number of the nearest neighbors is small, and then remains steady when the number of the nearest neighbors gets greater. We set the number of the nearest neighbors to be 16 for all the numerical studies. This is only one of the many choices as the reconstruction error is not sensitive to the number of the nearest neighbors within a range.

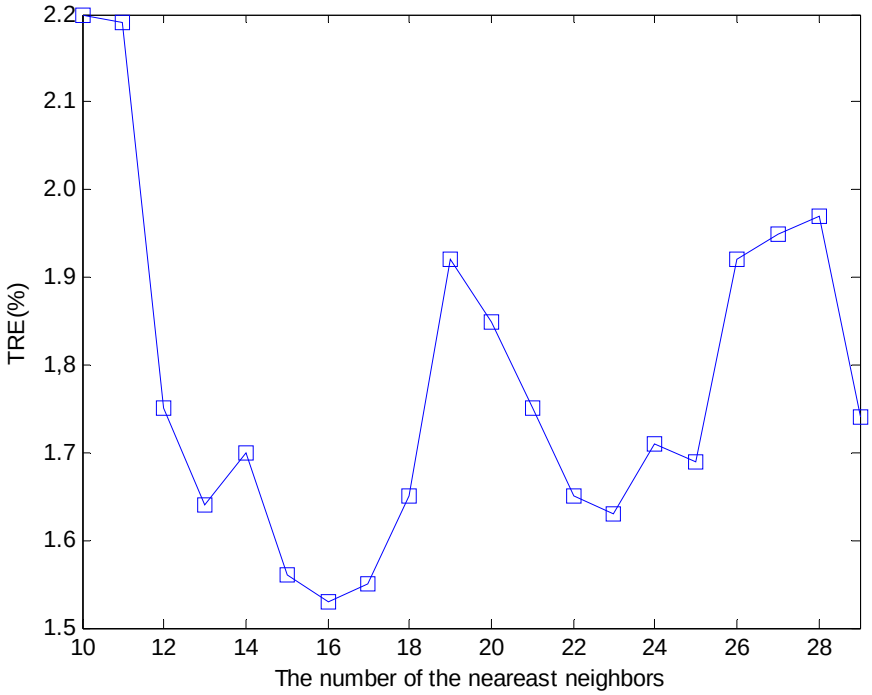

Figure 5-6 Sensitivity of TRE to the number of the nearest neighbors (data length = 731 days, intrinsic dimension = 4)

The plot of the TRE against the length of the calibration data in figure 5-7 illustrates that TRE is not very sensitive to the data length. Two years of data are applied to the manifold learning.

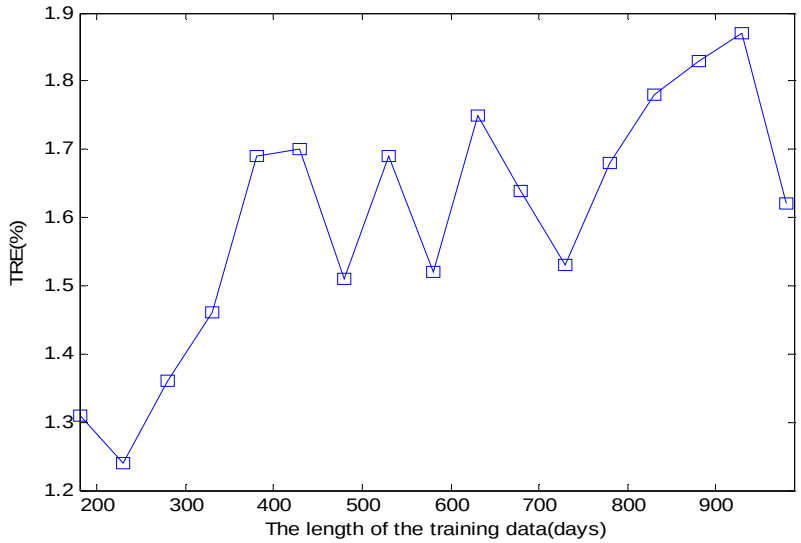

Figure 5-7 Sensitivity of TRE to the length of the calibration data (intrinsic dimension = 4, number of the nearest neighbors = 16)

5.4. Conclusions

We find that a manifold-based dimension reduction method performs very well in modeling a whole set of cross-zonal LMPs. LLE is demonstrated to be an efficient algorithm for extracting the intrinsic low-dimensional structure of electricity price curves. Using price data taken from the 15 zones of NYISO, we find that there exists a low-dimensional manifold representation of the set of day-ahead LMPs across all zones at any one single time, and specifically, the dimension of the manifold is around 4. The interpretation of each dimension in the low-dimensional space is obtained via the FTR values defined as the price differences between zonal prices to analyze the main factors that drive the cross-zonal LMP variations.

6. Day-ahead Forward Risk Premium in Electricity Markets with Transmission Network Constraints

This chapter tackles the issues of optimal hedging and equilibrium price discovering for market participants in the electricity day-ahead forward and spot wholesale markets considering transmission capacity constraints. The equilibrium prices in day-ahead forward and spot markets are derived by formulating the individual market participants' decision problems and solving them with respect to the market clearing conditions. Consequently, the locational forward risk premium, defined as the difference between the day-ahead forward price and the spot price, is expressed as a function of network topology, shadow prices of transmission flowgates, and other economic measures of the market participants. The implications of the model are illustrated through a series of numerical experiments with a three bus study-system. Empirical studies with New York electricity market data indicate that the forward risk premium determining model captures key economic features based on the hypothesis that the market prices are determined by rational risk-averse market participants.

The following notations apply to this chapter.

Acronyms

{AC, DC} {Alternating, Direct} current

GEN Generator

ISO Independent system operator

LBMP Locational based marginal price

LSE Load serving entity

MW Mega watts, unit for real power, the rate of energy consumption

MWh Mega watts hour, unit for energy consumption

NYISO New York independent system operator

NYEM New York electricity market

PTDF Power transfer distribution factor

Parameters of the transmission network

$\mathbf{F}$ Matrix of PTDFs, $\mathbf{F} = [f_{n,k}]$, where $f_{n,k}$ denotes the proportion of power flow on flowgate k for one unit of power injection into bus n paired with one unit of power ejection out of slack bus.

g_i Bus index of where the i^{th} GEN's units are connected. We assume that different GENs do not compete at the same location, i.e. if $i \neq i'$, then $g_i \neq g_{i'}$.

l_j Bus index of where the j^{th} LSE is located. We assume that all LSEs have non-overlapping franchised service area, i.e. if $j \neq j'$, then $l_j \neq l_{j'}$.

$\mathbf{T}$ Vector of transmission capacity of flowgates, $\mathbf{T} = [T_k]^T, k \in \mathcal{K}$.

$\mathcal{N}$ Set of buses, $\mathcal{N} = \{n\}, n = 1, \cdots N$.

$\mathcal{K}$ Set of flowgates, $\mathcal{K} = \{k\}, k = 1, \cdots K$.

Parameters, variables, and functions associated with market participants

$\{A_i^G, A_j^L\}$ Risk aversion coefficients of the i^{th} GEN or the j^{th} LSE, assume that $A_i^G = A_G > 0, \forall i$, and $A_j^L = A_L > 0, \forall j$.

$C(\cdot)$ Generation cost function.

$\mathbf{D}$ Vector of bus-aggregated demand of end consumers, $\mathbf{D} = [d_n]^T, n \in \mathcal{N}$.

F_i Fixed cost of the i^{th} GEN's generation cost function.

$\mathbf{G}^{\{F,S\}}$ Vector of forward/spot positions taken by GENs, $\mathbf{G}^{\{F,S\}} = [G_i^{\{F,S\}}]^T, i = 1, \cdots, I$.

$\mathbf{G}^{\{F,S\}*}$ Vector of optimal forward/spot positions of GENs, $\mathbf{G}^{\{F,S\}*} = [G_i^{\{F,S\}*}]^T, i = 1, \cdots, I$.

$\mathbf{G}$ Vector of total positions by GENs, $\mathbf{G} = [G_i]^T$, $i = 1, \cdots, I$, and $\mathbf{G} = \mathbf{G}^F + \mathbf{G}^S$.

i Index of GENs, $i = 1, \cdots, I$.

j Index of LSEs, $j = 1, \cdots, J$.

$\mathbf{L}^{\{F,S\}}$ Vector of forward/spot positions taken by LSEs, $\mathbf{L}^{\{F,S\}} = [L_j^{\{F,S\}}]^T, j = 1, \cdots, J$.

$\mathbf{L}^{\{F,S\}*}$ Vector of optimal forward/spot positions of LSEs, $\mathbf{L}^{\{F,S\}*} = [L_j^{\{F,S\}*}]^T, j = 1, \cdots, J$.

$\mathbf{L}$ Vector of total positions by LSEs, $\mathbf{L} = [L_j]^T$, $j = 1, \cdots, J$, and $\mathbf{L} = \mathbf{L}^F + \mathbf{L}^S$.

$U_{\{G,L\}}(\cdot)$ Utility function of a GEN/LSE.

$\{\rho_i^G, \rho_j^L\}$ GEN i or LSE j's profit without forward hedging.

$\pi_{\{G,L\}}^{\{F,S\}}(\cdot)$ Profit function of a GEN/LSE in forward/spot markets.

θ_i^G Parameter of GEN i's generation cost function, $\theta_i^G > 0$, assume $\theta_i^G = \theta$, $\forall i$.

α_i^G Parameter of GEN i's generation cost function, $\alpha_i^G > 0$.

ϖ A random variable representing the market uncertain which leads to load randomness and market price fluctuation.

Electricity market prices and shadow prices associated with transmission flowgates

$\mathbf{P}^{\{F,S\}}$ Vector of the LMPs in forward/spot markets, $\mathbf{P}^{\{F,S\}} = [P_n^{\{F,S\}}]^T, n \in \mathcal{N}$.

$\mathbf{P}^R$ Vector of electricity retail price for end consumer, $\mathbf{P}^R = [P_n^R]^T, n \in \mathcal{N}$.

$P_{ref}^{\{F,S\}}$ LMP at the reference bus in forward/spot markets.

$\boldsymbol{\lambda}^{\{F,S\}}$ Vector of flowgate shadow prices in forward/spot markets, $\boldsymbol{\lambda}^{\{F,S\}} = [\lambda_k^{\{F,S\}}]^T$.

6.1. Introduction

Deregulation of the electric power industry separates production and delivery of electricity as different market making functions from the previously vertically integrated monopoly. Wholesale electricity markets and retail electricity markets are established to allow trading between bulk suppliers, retailers and other financial intermediaries. As an essential commodity for national economics and household uses, electricity is traded in large quantities between these market participants. With an annual consumption of over 3.6 billion MWh, the US power market is becoming one of the most active commodity markets in the world. In the first few years following the conception of deregulation, the complexity of electricity trading and the market risks were more or less underestimated due to continuations of the power transaction contracts predetermined in the regulated regime. Until the late 1990s, electricity marketers had enjoyed substantial latitude in capital markets. However, the turmoil of the California power market in 2000-2001 and the collapse of the energy giant Enron in late 2001 created unease and reminded market participants of the harsh realism in the rapidly developing industry. The electricity trading business experienced dramatic impact although it was not the exclusive driver to such crisis. In 2002, stock depreciation and credit downgrades haunted the industry and increased the cost of capital access. The market perceptions of electricity commodities and derivatives trading associated risks came to the close attention of market participants. Stakeholders and potential investors began to appreciate the related research.

The imbedded physical nature of electricity determines the extreme volatility of its price and the illiquid of its trading. The following figure 6-1 illustrates the day-ahead (left panel) and spot (right panel) market hourly electricity prices on the reference bus in the New York power pool over the period from February 2005 through August 2006.

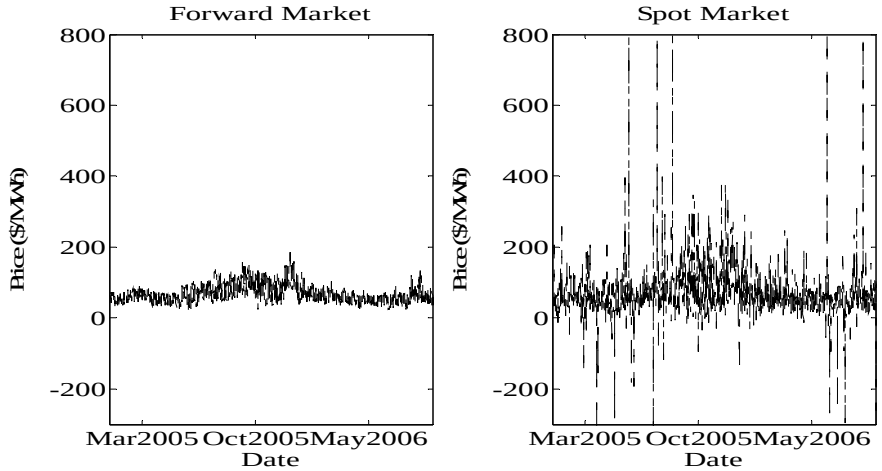

Figure 6-1 Hourly day-ahead forward and spot prices on the reference bus in NYEM

From figure 6-1, electricity price spikes are observed frequently especially in the spot market. In contrast to the general observation that in most commodity markets derivative prices are more volatile than the fundamentals, figure 6-1 shows the opposite: electricity prices in the day-ahead forward market are generally less volatile than in the underlying in the spot market.

Actually, the standard deviation of percentage changes of the hourly electricity prices as displayed in figure 6-1 is 10.7% in the day-ahead forward market (the left panel) and 121.7% in the spot market (the right panel), respectively. Compared with the stock market, the standard deviation of daily returns on the S&P 500 index during the most volatile single month in recent decades, October 1987, was 5.7% (Bessembinder and Lemmon, 2002). The extreme price volatilities put market participants at significant risk exposure in the spot market, which may lead to serious financial difficulties. It leads to the future trading of bulk electricity. Soon after the conception of the electric power industry's deregulation, the market for electricity futures emerged in the New York mercantile exchange in March 1996. Financially settled monthly futures contracts for on-peak and off-peak electricity transactions provide a channel for risk transferring between market agents who have different market projections and risk preferences. Nowadays, standardized futures contract trading for electricity delivery at specific locations provides sophisticated bulk electricity suppliers and buyer opportunities to hedge against unfavorable price fluctuations. Options on the monthly futures have been structured and offer market agents additional trading opportunities and risk management tools.

Compared with electricity spot prices which clear the transactions in the spot market, electricity forward prices clear the forward transactions and reflect the pricing of the corresponding forward contracts. There usually exist forward risk premiums which measure the differences between the forward and expected spot prices. Economic theories suggest that forward premiums represent market compensation to financial market participants for bearing the systematic risk. Although classical literatures suggest that a typical forward premium is negative due to the systematic hedging-pressure effect, recent literature (e.g., Longstaff and Wang, 2004) provides examples of positive forward premiums. Routledge et al. (2000) develop an equilibrium model of term structure of forward prices for storable commodities. In their model, a competitive rational expectations model of storage is employed to study the impact of the embedded timing option of spot commodity which is absent in the future contracts. However, the results do not necessarily extend to electricity futures. The cost-of-carry relationship links spot and forward prices by the no arbitrage condition. A forward contract can be synthesized by taking a long position in the underlying asset and holding it till the maturity of the contract. Since there lacks efficient technology to store electricity economically, the buffering benefit of holding inventory to smooth temporary demand/supply imbalance does not exist. Consequently, in addition to the resulting extreme intertemporal and interspatial price volatility, the standard arbitrage-based approach cannot be applied as it is to value electricity derivatives. Therefore, electricity forward prices do not necessarily conform to the cost-of-carry relationship (Eydeland and Geman, 1999; Pirrong and Jermakyan, 1999), and the no-arbitrage approach does not apply to power derivatives valuing directly. Pirrong and Jermakyan (1999) note that electricity forward prices differ from expected delivery date spot prices due to an endogenous market price of power demand risk. However, no attempt to explicitly model the determinants of the forward market price risks is made. Eydeland and Geman (1999) focus on electricity options and note that as a consequence of non-storability, delta hedging involving the underlying asset cannot be implemented and using the spot price evolution models for pricing power options is not helpful. Their option pricing model relies on assumptions regarding the evolution of forward power prices instead. A recent study of forward price premiums in the natural gas market (Borenstein et al., 2006) argues that since gas local distribution companies (LDCs) choose to pay to guarantee access to gas at times when gas transportation capacity is expected to be constrained, positive forward price premiums exist. However, this conclusion is back up by the fact that LDCs face a

much higher penalty for inadequate gas input than for storing excessive gas. Inspired by the fact that storable natural gas can be converted into electricity in industrialized size, Routledge et al. (2001) tackle the equilibrium pricing of electricity contracts by studying the spark spreads between the natural gas and electricity markets. Their research indicates mean reversion and positive skewness of electricity prices. Also revealed is the unstable correlation between electricity and natural gas prices. These literatures suggest relying on equilibrium-based models to derive how electricity forward prices are related to spot market conditions. According to the general equilibrium model of electricity forward prices proposed by Bessembinder and Lemmon (2002), there exists a functional relationship between electricity forward prices and the expected underlying spot price and load demand. The forward price is a biased forecast of the future spot price, with the forward premium being a decreasing function of the expected variance of the wholesale spot price and an increasing function of the expected skewness of wholesale spot prices. More specifically, the forward premium is negative (termed normal backwardation) when price volatility over-dominates the positive skewness effect, and positive (termed contango) otherwise. Generally, it shows that fundamental economic factors and market participants' risk attitude determine the forward premium. Following the equilibrium model proposed by Bessembinder and Lemmon (2002), Longstaff and Wang (2004) implement empirical studies using high frequent electricity price data from the PJM (Pennsylvania, New Jersey, and Maryland) electricity market. Their study confirms the relationship between forward risk premium and the moment statistics of spot prices and finds that the forward premiums are higher in peak hours compared with non-peak hours.

In addition to the markets for long-maturity futures, in many U.S. power pools, a two-settlement mechanism has been established which involves the market clearing in a day-ahead forward market and a real-time spot-market. Assisted with market monitoring which deters market speculation behaviors, the creation of the day-ahead forward market allows the system operators to collect information and make more accurate projections of the next-day's demand and available generation supply. The opening of the day-ahead forward markets also moderates the impact of the otherwise more volatile spot market prices and provides market participants a channel to hedge the market risks involved. Since the establishment of the two-settlement mechanism, the day-ahead forward markets have grown rapidly. The price dynamics in the day-ahead forward markets and the relation between day-ahead forward and spot prices have become one of the major concerns of market participants.

Although the model proposed by Bessembinder and Lemmon (2002) provides an economic characterization of forward risk premium for monthly settled futures contracts, it implicitly assumes single forward and spot prices apply to every market participant within the broad delivery locations of their transactions with the transmission congestion related price dynamics being smeared over the model parameters. However, if applied directly to the day-ahead forward market, the same model would over-simplify the realism since limited transmission capacity leads to different LBMPs at different locations. In addition to the supply-demand balances, market prices are vulnerable to transmission network constraints. Since physics laws determine the transmission of electric power flows, given the capacity constrained transmission network, there is a significant variation in energy prices at different locations even within one market. The following figure 6-2 illustrates the day-ahead forward (left panel) and spot (right panel) market hourly LBMP differences between the zone CENTRL and the reference bus in NYEM over February 2005 through August 2006,

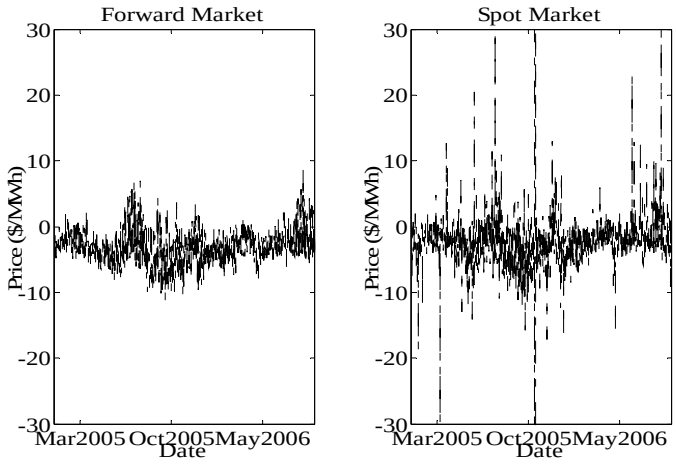

Figure 6-2 Day-ahead forward and spot price differences between zone CENTRL and the reference bus in NYEM

It illustrates the effect of network congestion resulting from limited transmission capacity. Note that spatial price differences make significant percentages of the market prices, especially in the spot market. Actually, the spatial price differences between the zone N.Y.C and the reference bus are more dramatic due to the tighter transmission capacity connection. Consequently, to understand the relationship between the day-ahead forward LBMPs and the spot LBMPs in a practical system, the model presented in (Bessembinder and Lemmon, 2002) needs to be expanded to incorporate transmission network constraints and model the interspatial price diversity.

The research work presented in this chapter investigates an equilibrium model for the pricing of electricity forward contracts in the day-ahead market while considering the impact of transmission congestion. We assume that in both the day-ahead and the spot markets, market clearing prices are determined by the supply- and demand-side participants with physical needs rather than pure speculators. We also assume that electricity bulk suppliers and retailers are risk-averse and risk-adjusted profit maximizers. An equilibrium model is formulated which leads to a regression model relating the forward risk premium to the network topology, the shadow prices of transmission flowgates, and other economic measures of the market participants. We conduct preliminary empirical analysis using historical electricity prices and transmission congestion information form the New York electricity wholesale market. The data used in this study consist of hourly day-ahead and spot electricity prices, hourly day-ahead and spot flowgate shadow prices, and hourly load level for the period from February 2005 to August 2006. The rational for using hourly data instead of daily-averaged data, as mostly adopted in other literatures, is that the occurrences of transmission congestions usually last no more than a few hours instead of days. The congestion effect may become obscured if it is scaled into daily averaged data. The observations from the empirical study are in general supportive of the relation indicated in the proposed model. They confirm that the regression model for day-ahead forward risk premium in power prices captures many of the key economic features based on the hypothesis that the market prices are determined by rational risk-averse market participants. This research

contributes to the rapidly growing literature on electricity market risks and is valuable for leading to broader insights regarding market perceptions. Although the equilibrium model considers electricity market's exclusive characteristics, the modeling framework and the insights obtained apply to other non-storable commodity markets as well.

The rest of the chapter is organized as follows. Section 6.2 describes the general setup of the day-ahead forward and spot markets for electricity wholesale. The decision problems of each market participant in the day-ahead and spot markets are formulated. Section 6.3 discusses the market clearing conditions and solves for economic determinants of market clearing prices. By maximizing each market participant's risk-adjusted profit with respect to market clearing conditions, the model gives closed form solutions for the equilibrium forward prices and optimal forward positions. The implications of the model and impacts of various system parameters on the forward risk premium are illustrated through a series of simulation studies with a 3-bus study system. A regression model for day-ahead forward risk premium, which incorporates transmission network constraints and various economic measures, is derived in section 6.4. Empirical statistical studies with New York electricity market data are conducted. The observations indicate that the proposed model captures many of the key economic features which determine the forward risk premium. The model is then used for spot market price prediction and tested against out-of-sample historical data. Finally, conclusions and directions for future research are presented in section 6.5.

6.2. Decision Problems of the Market Participants

In an open electricity pool market, the transactions of electric power are primarily driven by market participants' business incentives. End consumers' activities determine the total demand. Generators and load serving entities choose to sell or procure on either day-ahead forward or spot markets and at what quantities. They interact continuously through projected and real-time electricity transactions. There exists an independent system operator that monitors the transmission network status and dispatches the system to minimize the social energy acquisition cost. The winning electricity selling and buying bids determine the market clearing prices consequently. However, the objective of each market participant is to maximize the individual risk adjusted profit. At the market equilibrium, each market participant cannot gain profit by making unilateral moves.

Since the cost-of-carry models cannot be readily applied to price electricity derivatives, an equilibrium approach is adopted instead to assess equilibrium prices and optimal hedging positions for market participants in the day-ahead forward and spot markets. To model the two-settlement mechanism, we consider a single forward time period for electricity wholesale transactions when market participants choose their forward market positions by estimating the spot market conditions. When it comes close to the settlement of spot market, electricity load, the fundamental factor of market uncertainty, can be estimated with substantial precision in the immediate future. A same assumption in (Bessembinder and Lemmon, 2002) is made that market participants can make decisions regarding spot market positions at precisely projected spot prices.

This section presents the decision problems of major market participants. Contingency events such as outages of generation units and transmission facilities are ignored here and reserved for future researches.

6.2.1 System operator

Assume an electric power system with the transmission network consisting of a set $\mathcal{N}$ of buses and a set $\mathcal{K}$ of monitored transmission flowgates. In our analysis, three markets are considered as follows:

a. A day-ahead forward wholesale market

In the day-ahead wholesale forward market, electricity power suppliers (i.e., GENs) and buyers (i.e., LSEs) choose their forward positions $\mathbf{G}^F$ and $\mathbf{L}^F$, respectively. The market clears at the day-ahead locational marginal prices $\mathbf{P}^F$.

b. A real-time spot wholesale market

In the wholesale spot market, the suppliers and buyers choose their spot positions $\mathbf{G}^S$ and $\mathbf{L}^S$, respectively, while the market clears at the spot prices $\mathbf{P}^S$.

c. A regulated retail market

The load serving entities act as electricity buyers in the wholesale markets and sell electricity procured from the wholesale markets to the end consumers in a retail market. Although LSEs have to buy bulk electricity at time-varying competitive market clearing prices $\mathbf{P}^F$ or $\mathbf{P}^S$ in the day-ahead forward or spot market, respectively, the retail prices to end consumers are under regulation and set fixed at $\mathbf{P}^R$. Usually, the regulated retail price $\mathbf{P}^R$ to end consumers is set based on the expected spot price $\mathbf{P}^S$ plus a certain retail profit margin.

Suppose there exist I generators acting as power suppliers selling electricity into the competitive wholesale markets with J load serving entities being the wholesale buyers and suppliers in the retail market. To ensure the economical efficiency of the wholesale market, prevent discriminatory access to the transmission network, and encourage open markets competitions, an independent system operator with central dispatch authority coordinates the transmission of electricity to facilitate the transactions while monitoring against the violation of transmission network capacity. Locational marginal energy prices $\mathbf{P}^{\{F,S\}}$ and shadow prices $\boldsymbol{\lambda}^{\{F,S\}}$ associated with the congested flowgates are determined by the system dispatch and informed to the public. The aggregated electricity demands in the LSEs' franchised service territories are denoted by a vector of exogenous random variables $\mathbf{D}$, which appear as firm obligations to load serving entities.

The cost function of the i^{th} generator is assumed to be a quadratic function of the generation output G_i,

$$C(G_i) = F_i + \frac{\theta_i^G}{2\alpha_i^G} \cdot G_i^2 \tag{6.1}$$

In the model proposed in (Bessembinder and Lemmon, 2002), to account for the missed market price dynamics do to ignored transmission congestion, the term of G_i in the cost function is assumed to be higher than 2 in general. In the contrast, the transmission network constraints are modeled explicitly in the proposed model, we use quadratic functions to represent supply curves, which are, according to (Wood and Wollenberg, 1996), more realistic characterizations of the generation production.

The market participants generally optimize market decisions expecting to reach high profit on average. Suppose that the information ϖ can be viewed as a random variable with support Ω and known probability distributions, for example, with cumulative distribution function $F(\varpi)$, the profit on average can be defined as $E[\pi(\varpi)] = \int_{\varpi \in \Omega} \pi(\varpi) dF(\varpi)$.

However, for a particular realization of the system conditions, the profit resulted could be very different from the corresponding expected value. The deviation may be quite considerable if the underlying randomness has a large variance. Following the corporate risk hedging literature which argues that market agents can benefit from hedging market risks by avoiding suboptimal decisions, and given the extreme volatility of the electricity wholesale prices, electricity market participants are modeled as risk averse and willing to seek hedges in forward market against adverse real time price changes, that is, they take both expected profits and the imbedded volatilities into consideration. A utility function linear in expected value and variance of profit is chosen as follows to reflect their risk aversion,

$$E[U_{\{G,L\}}] = E[\pi_{\{G,L\}}(\omega)] - \frac{A_{\{G,L\}}}{2} Var(\pi_{\{G,L\}}(\omega)) \tag{6.2}$$

where $A_{\{G,L\}} \geq 0$ represents the weight given to the conservative part of the decision.

To simplify the problem, the forward and spot wholesale markets are modeled as closed systems where market participation is limited to generators and load serving entities with the prices determined by their physical delivery backed electricity trades. The rational for this assumption is that currently the activities of market agents, who take financial positions in the forward market and offset their positions prior to the next day delivery, are under strict regulation. Actually, due to the lack of electricity price indices (Ong, 1996), the speculative power transactions only account for a very limited percentage compared with the overall volume. Although no explicit model is built to represent market speculation, it is straightforward to envision that the unlimited costless participation of risk-neutral speculators would drive forward price converge to the expected spot price. Nevertheless, the existence of nonzero electricity forward premiums as observed from the empirical data provides incentives for financial intermediaries to create instruments, for example, power-indexed bonds, to allow outside speculators to include power positions in their portfolios (Bessembinder and Lemmon, 2002). The presence of outside speculators would be essential to market prices.

As mentioned in previous chapters, a major difference of electricity from other commodities is that electricity flow over the transmission network following the law of physics instead of flowing freely as envisioned from an economic perspective. Since electricity is priced at each distinct location, the existence of network constraints presents complications to the electricity markets. Since we are concerned with the real power only, we use the DC instead of AC power flow equations based system dispatch model in our analysis. The DC model identifies thermal limits constraints and eases the understanding of economical issues in congestion management. We have the ISO's system dispatch problems with network constraints as follows, note that the market prices can be determined based on the dispatch decisions.

Definition 6.1: (ISO's system dispatch problem in the day-ahead forward wholesale market) The ISO collects the load serving entities' electricity demands in the day-ahead forward market and dispatches the available generation resources accordingly to meet the forward

demand while minimizing the forward electricity energy acquirement cost. By clearing the supply and demand at each location with respect to the transmission capacity constraints on each monitored flowgates, the market clearing day-ahead forward location marginal prices and flowgate shadow prices are determined by solving the following optimization problem,

$$\text{Min } C(\mathbf{G}^F) = \sum_{i=1}^{I} C(G_i^F) \tag{6.3a}$$

$$\text{St. } \sum_{i=1}^{I} G_i^F = \sum_{j=1}^{J} L_j^F \tag{6.3b}$$

$$\mathbf{F}^T(\mathbf{G}^F - \mathbf{L}^F) \le \mathbf{T} \tag{6.3c}$$

$$\mathbf{G}^F \ge 0 \tag{6.3d}$$

Definition 6.2: (ISO's system dispatch problem in the spot wholesale market) The ISO collects the load serving entities' projected electricity demands in the spot market, based on the scheduled generation resources as determined in the day-ahead forward market, the ISO adjusts the available generation resources accordingly to meet the spot demand while minimizing the total electricity energy acquirement cost. By clearing the supply and demand at each location with respect to the transmission capacity constraints on each monitored flowgates, the market clearing forward location marginal prices and flowgate shadow prices are determined by solving the following optimization problem,

$$\text{Min } C(\mathbf{G}) = \sum_{i=1}^{I} C(G_i) \tag{6.4a}$$

$$\text{St. } \sum_{i=1}^{I} G_i = \sum_{j=1}^{J} L_j \tag{6.4b}$$

$$\mathbf{F}^T(\mathbf{G} - \mathbf{L}) \le \mathbf{T} \tag{6.4c}$$

$$\mathbf{G} \ge 0 \tag{6.4d}$$

Locational marginal pricing is the marginal cost of supplying the next increment of power demand at a specific location on the network, taking into account the marginal cost of generation and the physical aspects of the transmission system. Without the network constraints, electricity would be traded at a unique price wherever the physical delivery were located in the system. The demands would be met by the merit-order generations, i.e., the cheapest group of generation units, to incur the minimum social cost. However, the limited transmission network capacity may limit the transactions as congestion occurs, preventing the access to the cheapest generation resource while resorting to out of merit-order generations instead with respect to the specific location of the demands. As a consequence, the market clearing prices are differentiated across spatial locations. The optimality conditions of (6.3) and (6.4) characterize the relation between location prices and the reference bus price.

The problem (6.3), with a convex objective function and linear constraints, is a convex programming problem. The associated Lagrange function can be defined as

$$\mathcal{L}\left(\mathbf{G}^F,\boldsymbol{\lambda}^F,\gamma^F\right)=C\left(\mathbf{G}^F\right)+\gamma^F\left(\sum_{i=1}^{I}G_i^F-\sum_{j=1}^{J}L_j^F\right)+\left(\boldsymbol{\lambda}^F\right)^T\left(\mathbf{F}^T\left(\mathbf{G}^F-\mathbf{L}^F\right)-\mathbf{T}\right)$$

where γ^F is the Lagrange multiplier associated with constraints (6.3b) and $\boldsymbol{\lambda}^F$ is a vector of Lagrange multipliers – dual variables associated with constraints (6.3c).

In order for a solution $\left(\mathbf{G}^{F*},\boldsymbol{\lambda}^F,\gamma^F\right)$ to be optimal, in addition to constraints (6.3b-c), to guarantee that the gradient of $C\left(\mathbf{G}^F\right)$ is normal to $\left(\sum_{j=1}^{J}L_j^F-\sum_{i=1}^{I}G_i^F\right)$ and $\left(\mathbf{F}^T\left(\mathbf{G}^F-\mathbf{L}^F\right)-\mathbf{T}\right)$, it requires $\nabla C\left(\mathbf{G}^F\right)$ to be normal to $\nabla\left(\sum_{i=1}^{I}G_i^F-\sum_{j=1}^{J}L_j^F\right)$ and $\nabla\left(\mathbf{F}^T\left(\mathbf{G}^F-\mathbf{L}^F\right)-\mathbf{T}\right)$, that is, be linearly dependent vectors. This means the gradient of the objective function should be a linear combination of the gradients of the active constraints.

$$\frac{\partial\mathcal{L}}{\partial\mathbf{G}^F}\left(\mathbf{G}^{F*},\boldsymbol{\lambda}^F,\gamma^F\right)=0$$

plus the complementary slackness condition,

$$\left(\boldsymbol{\lambda}^F\right)^T\left(\mathbf{F}^T\left(\mathbf{G}^{F*}-\mathbf{L}^{F*}\right)-\mathbf{T}\right)=0,\ \boldsymbol{\lambda}^F\geq 0$$

Due to the convexity of (6.3a-c), the second-order optimality conditions are satisfied. In the economical sense, the Lagrange multiplier γ^{F*} associated with the system-wise power supply and demand balance can be interpreted as the locational marginal price at the reference since it quantifies the electricity procurement cost for an additional unit of load at the system reference bus. On the other hand, the Lagrange multiplier vector $\boldsymbol{\lambda}^{F*}$ associated with the power flow limit of the monitored transmission flowgate are interpreted as the variation in electricity procurement cost if the transmission capacity is relaxed, called flowgate shadow price herein below. Therefore, the necessary conditions for optimal system dispatch gives

$$\mathbf{P}^F=P_{ref}^F-\mathbf{F}\boldsymbol{\lambda}^F \tag{6.5a}$$

where for each congested transmission flowgate k, $\lambda_k^F>0$, otherwise, $\lambda_k^F=0$.

Similarly, from problem (6.4), we can get

$$\mathbf{P}^S=P_{ref}^S-\mathbf{F}\boldsymbol{\lambda}^S \tag{6.5b}$$

Note that the day-ahead forward prices $\mathbf{P}^F$ re used to settle the day-ahead forward market transactions and the settlements of spot market position deviations from the day-ahead schedules are based on the spot prices $\mathbf{P}^S$.

6.2.2 Generators and Load Serving Entities

With the consideration of transmission constraints, power suppliers cannot be deemed as homogeneous as in (Bessembinder and Lemmon, 2002). Even if they share the same production technology, their trading activities vary since they may experience diversified market prices due to their respective spatial locations. Similarly, same arguments require the LSEs been treated heterogeneously in their respective franchised service areas. With the unbundling of generation and retail services, market agents pursue their individual goals simultaneously. The market

equilibrium under the multi-agent perspective can be modeled by a set of optimization problems associated with different market participants and clears according to the market coordination conditions. A variety of models have been proposed to model market participants' behaviors in a competitive market focusing on choosing different variables to compete against their rivals. Bertrand, Cournot, and Stackelberg models have been employed in Hogan (1997), Borenstein et al. (1995), and Otero-Novas et al. (2000) to study market participants' activities. The Bertrand model takes price decision as the move of each supplier while conjecturing that the rivals will not react to its actions by changing their prices. In the Cournot model, the quantity is the driver for market equilibrium. It is also termed as Nash equilibrium and can be reached when no agent can improve individual profit by unilaterally changing equilibrium strategy. A leader is assumed in the Stackelberg model to take the first move while leaving other agents behaving as in the Cournot set up. In this section, a two-period Cournot model is employed with the DC power flow approximation of network constraints to show the interaction of strategic behaviors between different market participants in diverse locations. Specifically, we evaluate GENs' and LSEs' forward hedging and spot positions and obtain closed form solutions for the equilibrium electricity prices based on market clearing conditions. This model is extendable to include strategic behaviors in the generation reserve market.

We start with assessing the real-time spot wholesale market while taking into account the day-ahead forward positions selected beforehand. We then step back to the day-ahead forward market. The optimal decisions can be determined assuming that each GEN and LSE would behave optimally in the spot market the next day.

Spot Market

According to the aforementioned assumption of market uncertainty being cleared in the real-time spot market, market participants can make decisions regarding spot market positions at precisely projected load demand and spot prices. LSEs can procure exactly the amount of power as needed and meanwhile, GENs are able to decide spot positions contracts in the spot wholesale market at known prices.

Definition 6.3: (Generators' profit pursuing problem in the spot wholesale market) The ex post profit of a generator is the sum of revenues from electricity transactions in forward and spot markets minus the total generation cost. Therefore, given the day-ahead forward market position G_i^{F*}, GEN i's decision-making problem is to maximize the profit as follows,

$$\text{Max} \qquad \pi_G^S\left(G_i^S\right) = P_{g_i}^{F*} G_i^{F*} + P_{g_i}^S(\varpi) G_i^S - \left[F_i + \frac{\theta}{2\alpha_i^G}\left(G_i^{F*} + G_i^S\right)^2 \right] \tag{6.6}$$

The first order necessary condition

$$\frac{\partial \pi_G^S\left(G_i^S\right)}{\partial G_i^S} = P_{g_i}^S(\varpi) - \frac{\theta}{\alpha_i^G}\left(G_i^{F*} + G_i^S\right) = 0$$

gives the profit-maximizing spot market position by GEN i being,

$$G_i^{S*} = \frac{\alpha_i^G}{\theta} P_{g_i}^S(\varpi) - G_i^{F*} \tag{6.7}$$

And the second order sufficient condition satisfies

$$\frac{\partial^2 \pi_G^S\left(G_i^S\right)}{\partial G_i^{S^2}} = -\frac{\theta}{\alpha_i^G} < 0$$

Note that as implied in the generation cost function (6.1), the locational marginal price at the bus g_i defined as the marginal cost of supplying the next increment of power demand at that specific location of the network can be determined as:

$$P_{g_i} = \frac{dC\left(G_i\right)}{dG_i} = \frac{\theta}{\alpha_i^G} G_i$$

which increases with G_i and implies that the supplier can set the market price at which it sells the power. However, due to the correlations between market prices at various locations of the same system as revealed by (6.5), this price-setting cannot be decided independently of other market participants' decisions. Instead, the conformation to the market clearing conditions presented in section 6.3 combined with price relation (6.5) provides the decision environment for generators to rely on.

Definition 6.4: (Load serving entities' obligation fulfillment problems in the spot wholesale market) For LSEs, by regulation they need to fulfill the real time demand of end consumers in their franchised territory. Take LSE j as an example,

$$L_j \equiv d_{l_j} \tag{6.8}$$

Therefore, LSE j has little control over L_j^S and simply buys in the shortage of electricity power resulted from the forward contracted quantity L_j^{F*},

$$L_j^{S*} = d_{l_j} - L_j^{F*} \tag{6.9}$$

Therefore, the ex post profit of LSE j can be determined as,

$$\begin{aligned} \pi_L^S\left(L_j^S\right) &= P_{l_j}^R d_{l_j} - P_{l_j}^{F*} L_j^{F*} - P_{l_j}^S(\varpi)\left(d_{l_j} - L_j^{F*}\right) \\ &= \left(P_{l_j}^R - P_{l_j}^S(\varpi)\right) d_{l_j} + \left(P_{l_j}^S(\varpi) - P_{l_j}^{F*}\right) L_j^{F*} \end{aligned} \tag{6.10}$$

Note that the profit gain (loss) from taking day-ahead forward position L_j^{F*} is multiplied by $P_{l_j}^S(\varpi) - P_{l_j}^{F*}$. And a reduced portion of load obligation $d_{l_j} - L_j^{F*}$ of LSE j is subject to the spot market price surging risk. On the other side, the regulated retail price $P_{l_j}^R$ should be high enough to create a profit margin and keep LSE j in the market for service.

We next step back in time to formulate the day-ahead forward market decisions of market participants.

Forward Market

In the day-ahead forward market, GENs and LSEs face uncertain load demands to be revealed in the next day retail market. Given the uncertain $\mathbf{P}^S(\varpi)$ and unrevealed optimal decisions in the spot market $\mathbf{G}^S$ and $\mathbf{L}^S$, the GENs and LSEs have to rely on the projections of the spot market conditions and decide their forward market positions.

Given the subsequent optimal spot market positions $\mathbf{G}^{S*}$ as reveal in (6.7) to be taken by GEN i, his total profit with forward market position G_i^F can be determined as follows,

$$\pi_G^F\left(G_i^F\right)=P_{g_i}^F G_i^F+P_{g_i}^{S*}(\varpi)G_i^{S*}(\varpi)-\frac{\theta}{2\alpha_i^G}\left(G_i^F+G_i^{S*}(\varpi)\right)^2 \tag{6.11}$$

To facilitate the model derivation in the following sections, we define GEN i's un-hedged profit by assuming no position in forward market is taken, that is, $G_i^F=0$, that is, the profit without forward hedging is:

$$\rho_i^G(\varpi)=P_{g_i}^S(\varpi)G_i^{S*}(\varpi)-\frac{\theta}{2\alpha_i^G}\left(G_i^{S*}(\varpi)\right)^2=\frac{\alpha_i^G}{2\theta}\left(P_{g_i}^S(\varpi)\right)^2 \tag{6.12}$$

where, according to equation (6.5), $P_{g_i}^S(\varpi)=P_{Ref}^S(\varpi)-f_{g_i,k}\lambda_k^S(\varpi)$, assuming k is the only transmission flowgate which has tight capacity and non-zero associated shadow price in the system.

Taking the G_i^{S*} revealed in (6.7) and the $\rho_i^G(\varpi)$ defined in (6.12) into consideration, equation (6.11) can be transformed into the following neat form,

$$\pi_G^F\left(G_i^F\right)=\rho_i^G(\varpi)+G_i^F\left(P_{g_i}^F-P_{g_i}^S(\varpi)\right) \tag{6.13}$$

Definition 6.5: (GENs' risk-adjusted profit pursuing problem in the day-ahead forward wholesale market) With the projected overall profit (6.13), the risk-averse generator i's utility maximization problem in the form of (6.2) in the day-ahead forward market is as follows,

$$\text{Max}\qquad E\left[U_G^F\left(G_i^F\right)\right]=E\left[\pi_G^F\left(G_i^F\right)\right]-\frac{A_G}{2}Var\left(\pi_G^F\left(G_i^F\right)\right) \tag{6.14}$$

Given the rational that the un-hedged profit $\rho_i^G(\varpi)$ is calculated when no forward market position is taken, we can assume that $E\left[\rho_i^G(\varpi)\right]$ and $Var\left(\rho_i^G(\varpi)\right)$ are independent of G_i^F, which leads to explicit form of (6.14) as follows,

$$E\left[U_G^F\left(G_i^F\right)\right]=E\left[\rho_i^G(\varpi)\right]+G_i^F\left(P_{g_i}^F-E\left[P_{g_i}^S(\varpi)\right]\right)$$
$$-\frac{A_G}{2}\left[Var\left(\rho_i^G(\varpi)\right)+\left(G_i^F\right)^2Var\left(P_{g_i}^S(\varpi)\right)-2G_i^F Cov\left(\rho_i^G(\varpi),P_{g_i}^S(\varpi)\right)\right]$$

The first order necessary condition for optimality

$$\frac{\partial E\left[U_G^F\left(G_i^F\right)\right]}{\partial G_i^F}=P_{g_i}^F-E\left[P_{g_i}^{S*}(\varpi)\right]-A_G\left[G_i^F\cdot Var\left(P_{g_i}^{S*}(\varpi)\right)-Cov\left(\rho_i^G(\varpi),P_{g_i}^{S*}(\varpi)\right)\right]=0$$

gives the expected utility maximizing GEN i's forward market position being,

$$G_i^{F*}=\frac{P_{g_i}^F-E\left[P_{g_i}^{S*}(\varpi)\right]}{A_G Var\left(P_{g_i}^{S*}(\varpi)\right)}+\frac{Cov\left(\rho_i^G(\varpi),P_{g_i}^{S*}(\varpi)\right)}{Var\left(P_{g_i}^{S*}(\varpi)\right)} \tag{6.15}$$

where, according to (6.12), $Cov\left(\rho_i^G(\varpi),P_{g_i}^{S*}(\varpi)\right)=\frac{\alpha_i^G}{2\theta}Cov\left(\left(P_{g_i}^{S*}(\varpi)\right)^2,P_{g_i}^{S*}(\varpi)\right)$

And the second order sufficient condition of optimality satisfies,

$$\frac{\partial^2 E\left[U_G^F\left(G_i^F\right)\right]}{\partial {G_i^F}^2} = -A_G Var\left(P_{g_i}^{S*}(\omega)\right) < 0$$

As described in (6.15), the optimal forward position consists of two components with the first reflects the position taken in response to the bias in the forward price as compared to the expected spot prices. Note that since $\rho_i^G(\varpi)$ is positively correlated with $P_{g_i}^{S*}(\varpi)$ for $\forall i$, the second term of GEN i's forward market position accounts for the effort to reduce the total profit's risk exposure to the spot market prices as compared to without forward hedging. Note that in (6.15), the $E\left[P_{g_i}^{S*}(\varpi)\right]$ denotes the conditional expectation of $P_{g_i}^{S*}(\varpi)$, similarly, $Var\left(P_{g_i}^{S*}(\varpi)\right)$ and $Cov\left(\rho_i^G(\varpi), P_{g_i}^{S*}(\varpi)\right)$ are both conditional measures.

Taking (6.15) back into (6.7), the optimal position to take in the wholesale spot market by GEN i can be expressed as,

$$G_i^{S*} = \frac{\alpha_i^G}{\theta} P_{g_i}^S(\varpi) - \left(\frac{P_{g_i}^F - E\left[P_{g_i}^{S*}(\varpi)\right]}{A_G Var\left(P_{g_i}^{S*}(\varpi)\right)} + \frac{Cov\left(\rho_i^G(\varpi), P_{g_i}^{S*}(\varpi)\right)}{Var\left(P_{g_i}^{S*}(\varpi)\right)} \right) \tag{6.16}$$

Similarly, load serving entity j's profit function is to be determined as,

$$\begin{aligned} \pi_L^S\left(L_j^S\right) &= P_{l_j}^R L_j(\varpi) - P_{l_j}^F L_j^F - P_{l_j}^{S*}(\varpi)\left(L_j^R(\varpi) - L_j^F\right) \\ &= \left(P_{l_j}^R - P_{l_j}^{S*}(\varpi)\right) L_j(\varpi) + \left(P_{l_j}^{S*}(\varpi) - P_{l_j}^F\right) L_j^F \end{aligned} \tag{6.17}$$

By assuming no position to be taken in forward market, that is, $L_j^F = 0$, we define LSE j's profit without forward hedging as:

$$\rho_j^L(\varpi) = \left(P_{l_j}^R - P_{l_j}^{S*}(\varpi)\right) L_j(\varpi)$$

where, $P_{l_j}^S(\varpi) = P_{Ref}^S(\varpi) - f_{l_j,k} \boldsymbol{\lambda}_k^S(\varpi)$

Note that LSE j's profit without forward hedging is exposed to risks of electricity acquiring cost in wholesale spot market and revenue in the retail market. The retail revenue co-varies positively with the electricity wholesale spot price since electricity price is positively correlated with the locational demand in general. And this correlation can be amplified by the regulated retail price level. However, the cost to acquire the required electricity from wholesale market offsets the revenue.

Therefore, take in the L_j^{S*} revealed in (6.9) and the $\rho_j^L(\varpi)$ defined in (6.17) into consideration, (6.17) can be transformed into the following,

$$\pi_L^F\left(L_j^F\right) = \rho_j^L(\varpi) - L_j^F\left(P_{l_j}^F - P_{l_j}^{S*}(\varpi)\right) \tag{6.18}$$

Definition 6.6: (LSEs' risk-adjusted profit pursuing problem in the forward wholesale market) With the projected overall profit (6.18), the risk-averse load serving entity j's utility maximization problem in the form of (6.2) in the day-ahead forward market is as follows,

$$\text{Max} \qquad E\left[U_L^F\left(L_j^F\right)\right] = E\left[\pi_L^F\left(L_j^F\right)\right] - \frac{A_L}{2} Var\left(\pi_L^F\left(L_j^F\right)\right) \tag{6.19}$$

By assume $E\left[\rho_j^L(\varpi)\right]$ and $Var(\rho_j^L(\varpi))$ being independent of L_j^F, which is reasonable given that un-hedged profit $\rho_j^L(\varpi)$ considers zero L_j^F, we get,

$$E\left[U_L^F\left(L_j^F\right)\right] = E\left[\rho_j^L(\varpi)\right] - L_j^F P_{l_j}^F + L_j^F E\left[P_{l_j}^{S*}(\varpi)\right]$$

$$-\frac{A_L}{2}\cdot\left(Var\left(\rho_j^L(\varpi)\right) + \left(L_j^F\right)^2 Var\left(P_{l_j}^{S*}(\varpi)\right) + 2L_j^F Cov\left(\rho_j^L(\varpi), P_{l_j}^{S*}(\varpi)\right)\right)$$

The following first order necessary condition

$$\frac{\partial E\left[U_L^F\left(L_j^F\right)\right]}{\partial L_j^F} = E\left[P_{l_j}^{S*}(\varpi)\right] - P_{l_j}^F - A_L\left(L_j^F Var\left(P_{l_j}^{S*}(\varpi)\right) + Cov\left(\rho_j^L(\varpi), P_{l_j}^{S*}(\varpi)\right)\right) = 0$$

gives the expected utility maximizing LSE *j* 's forward market position being,

$$L_j^{F*} = \frac{E\left[P_{l_j}^{S*}(\varpi)\right] - P_{l_j}^F}{A_L Var\left(P_{l_j}^{S*}(\varpi)\right)} - \frac{Cov\left(\rho_j^L(\varpi), P_{l_j}^{S*}(\varpi)\right)}{Var\left(P_{l_j}^{S*}(\varpi)\right)} \tag{6.20}$$

where, $Cov\left(\rho_j^L(\varpi), P_{l_j}^{S*}(\varpi)\right) = Cov\left(\left(P_{l_j}^R - P_{l_j}^{S*}(\varpi)\right)L_j(\varpi), P_{l_j}^{S*}(\varpi)\right)$

$$= P_{l_j}^R Cov\left(L_j(\varpi), P_{l_j}^{S*}(\varpi)\right) - Cov\left(P_{l_j}^{S*}(\varpi)L_j(\varpi), P_{l_j}^{S*}(\varpi)\right)$$

And the second order sufficient condition satisfies,

$$\frac{\partial^2 E\left[U_L^F\left(L_j^F\right)\right]}{\partial L_j^{F\,2}} = -A_L Var\left(P_{l_j}^{S*}(\omega)\right) < 0$$

Similar to what is revealed in (6.15) for generators, the optimal forward position for LSEs consists of two components with the first reflects the position taken in response to the bias in the forward price as compared to the expected spot prices. Since $\rho_j^L(\varpi)$ is negatively correlated with $P_{l_j}^{S*}(\varpi)$ for $\forall l_j$, the second term of LSE *j* 's forward market position accounts for the effort to reduce the total profit's risk exposure to the spot market prices without forward hedging.

Therefore, taking (6.20) back to (6.9), the optimal position to take in the wholesale spot market by LSE *j* can be expressed as,

$$L_j^{S*} = L_j(\varpi) - \left(\frac{E\left[P_{l_j}^{S*}(\varpi)\right] - P_{l_j}^F}{A_L Var\left(P_{l_j}^{S*}(\varpi)\right)} - \frac{Cov\left(\rho_j^L(\varpi), P_{l_j}^{S*}(\varpi)\right)}{Var\left(P_{l_j}^{S*}(\varpi)\right)}\right) \tag{6.21}$$

Since GENs and LSEs take balanced forward and spot market positions in day-ahead and spot markets according to projected demand, the market risks imbedded are shared by the market participants. The retail price regulation prevents LSEs from transporting all of their market risk to end consumers who are vulnerable to price fluctuations due to the inelasticity of electricity consumption.

6.3. Market Equilibrium Prices

The equilibrium of the market can be reached when, in addition to every market participant choosing the optimal decision from each individual optimization problem given others' behavior strategies, the market reaches its coordination. In our case, it requires the balance of supply and demand with respect to transmission capability.

6.3.1 Theoretical formulations

In the forward wholesale market, the equilibrium requires,

$$\sum_{i=1}^{I} G_i^F = \sum_{j=1}^{J} L_j^F \tag{6.22}$$

In addition, according to the characterization of a $PTDF$ matrix, for the congesting flowgate k, we have,

$$\mathbf{F}_{\cdot,k}{}^T \left(\mathbf{G}^F - \mathbf{L}^F\right) = T_k \tag{6.23}$$

We get (see appendix B),

$$P_{\text{Ref}}^F = \frac{\kappa_2\left(\kappa_5 - \kappa_7 + T_k\right) - \kappa_3\left(\kappa_4 - \kappa_6\right)}{\kappa_2{}^2 - \kappa_1\kappa_3}$$

(6.24a)

$$\lambda_k^F = \frac{\kappa_1\left(\kappa_5 - \kappa_7 + T_k\right) - \kappa_2\left(\kappa_4 - \kappa_6\right)}{\kappa_2{}^2 - \kappa_1\kappa_3}$$

(6.24b)

$$P_n^F = \frac{\left(\kappa_2 - f_{n,k}\kappa_1\right)\left(\kappa_5 - \kappa_7 - T_k\right) - \left(\kappa_3 - f_{n,k}\kappa_2\right)\left(\kappa_4 - \kappa_6\right)}{\kappa_2{}^2 - \kappa_1\kappa_3}$$

(6.24c)

where, $\kappa_1 = \sum_{i=1}^{I} \frac{1}{A_G Var\left(P_{g_i}^{S*}(\varpi)\right)} + \sum_{j=1}^{J} \frac{1}{A_L Var\left(P_{l_j}^{S*}(\varpi)\right)}$

$$\kappa_2 = \sum_{i=1}^{I} \frac{f_{g_i,k^F}}{A_G Var\left(P_{g_i}^{S*}(\varpi)\right)} + \sum_{j=1}^{J} \frac{f_{l_j,k^F}}{A_L Var\left(P_{l_j}^{S*}(\varpi)\right)}$$

$$\kappa_3 = \sum_{i=1}^{I} \frac{\left(f_{g_i,k^F}\right)^2}{A_G Var\left(P_{g_i}^{S*}(\varpi)\right)} + \sum_{j=1}^{J} \frac{\left(f_{l_j,k^F}\right)^2}{A_L Var\left(P_{l_j}^{S*}(\varpi)\right)}$$

$$\kappa_4 = \sum_{i=1}^{I} \frac{E\left[P_{g_i}^{S*}(\varpi)\right]}{A_G Var\left(P_{g_i}^{S*}(\varpi)\right)} + \sum_{j=1}^{J} \frac{E\left[P_{Lj}^{S*}(\varpi)\right]}{A_L Var\left(P_{Lj}^{S*}(\varpi)\right)}$$

$$\kappa_5 = \sum_{i=1}^{I} \frac{f_{g_i,k^F} E\left[P_{g_i}^{S*}(\varpi)\right]}{A_G Var\left(P_{g_i}^{S*}(\varpi)\right)} + \sum_{j=1}^{J} \frac{f_{l_j,k^F} E\left[P_{l_j}^{S*}(\varpi)\right]}{A_L Var\left(P_{l_j}^{S*}(\varpi)\right)}$$

$$\kappa_6 = \sum_{i=1}^{I} \frac{Cov\left(\rho_i^G(\varpi), P_{g_i}^{S*}(\varpi)\right)}{Var\left(P_{g_i}^{S*}(\varpi)\right)} + \sum_{j=1}^{J} \frac{Cov\left(\rho_j^L(\varpi), P_{l_j}^{S*}(\varpi)\right)}{Var\left(P_{l_j}^{S*}(\varpi)\right)}$$

$$\kappa_7 = \sum_{i=1}^{I} \frac{f_{g_i,k^F} Cov\left(\rho_i^G(\varpi), P_{g_i}^{S*}(\varpi)\right)}{Var\left(P_{g_i}^{S*}(\varpi)\right)} + \sum_{j=1}^{J} \frac{f_{l_j,k^F} Cov\left(\rho_j^L(\varpi), P_{l_j}^{S*}(\varpi)\right)}{Var\left(P_{l_j}^{S*}(\varpi)\right)}$$

And the optimal day-ahead forward market positions G_i^{F*} and L_j^{F*} can be derived by combining (6.24c) with (6.15) and (6.20), respectively. The optimal forward positions derived are useful in evaluating which market participants have comparative advantage in participating as compared to being absent from forward transactions.

In the spot market, similar to (6.22), the coordination of the market requires the balance of supply and demand with respect to transmission capability as follows,

$$\sum_{i=1}^{I} G_i^{S*} = \sum_{j=1}^{J} L_j^{S*}$$

(6.25)

taking (6.16) and (6.21) into (6.25), it leads to,

$$P_{Ref}^F \left(\sum_{i=1}^{I} \frac{1}{A_G Var\left(P_{g_i}^{S*}(\varpi)\right)} + \sum_{j=1}^{J} \frac{1}{A_L Var\left(P_{l_j}^{S*}(\varpi)\right)} \right)$$

$$- \sum_{k \in \kappa} \lambda_k^F \left(\sum_{i=1}^{I} \frac{f_{g_i,k}}{A_G Var\left(P_{g_i}^{S*}(\varpi)\right)} + \sum_{j=1}^{J} \frac{f_{l_j,k}}{A_L Var\left(P_{l_j}^{S*}(\varpi)\right)} \right)$$

$$= \sum_{i=1}^{I} \frac{E\left[P_{g_i}^{S*}(\varpi)\right]}{A_G Var\left(P_{g_i}^{S*}(\varpi)\right)} + \sum_{j=1}^{J} \frac{E\left[P_{l_j}^{S*}(\varpi)\right]}{A_L Var\left(P_{l_j}^{S*}(\varpi)\right)}$$

$$- \sum_{i=1}^{I} \frac{Cov\left(\rho_i^G(\varpi), P_{g_i}^{S*}(\varpi)\right)}{Var\left(P_{g_i}^{S*}(\varpi)\right)} - \sum_{j=1}^{J} \frac{Cov\left(\rho_j^L(\varpi), P_{l_j}^{S*}(\varpi)\right)}{Var\left(P_{l_j}^{S*}(\varpi)\right)} + \sum_{i=1}^{I} \frac{\alpha_i^G}{\theta} P_{g_i}^S - \sum_{j=1}^{J} L_j(\varpi)$$

Combining (6.22) and (6.25), since the total generation should equal to the total demand, we have,

$$\sum_{i=1}^{I} \frac{\alpha_i^G}{\theta} P_{g_i}^S = \sum_{j=1}^{J} L_j = \sum_{l_j} d_{l_j} \tag{6.26a}$$

which equates the total generation production to total demand, we get,

$$\sum_{i=1}^{I} \frac{\alpha_i^G}{\theta} \left(P_{Ref}^S - f_{g_i,k} \lambda_k^S \right) = \sum_{n} d_n \tag{6.26b}$$

or, $$P_{Ref}^S \sum_{i=1}^{I} \alpha_i^G - \lambda_k^S \sum_{i=1}^{I} f_{g_i,k} \alpha_{g_i} = \theta \cdot L_j \tag{6.26c}$$

Also, according to the characterization of *PTDF* matrix and for the congesting flowgate k, corresponding to (6.23) in the day-ahead forward market, we have,

$$\mathbf{F}_{\cdot,k}{}^{T}\left(\left(\mathbf{G}^{F}+\mathbf{G}^{S}\right)-\left(\mathbf{L}^{F}+\mathbf{L}^{S}\right)\right)=T_k \tag{6.27a}$$

That is,

$$P_{Ref}^{S}\sum_{i=1}^{I}f_{g_i,k}\alpha_i^{G}-\lambda_k^{S}\sum_{i=1}^{I}\left(f_{g_i,k}\right)^2\alpha_i^{G}=\theta\cdot T_k+\theta\cdot\sum_{j=1}^{J}f_{l_j,k}L_j \tag{6.27b}$$

We get,

$$P_{Ref}^{S}=\frac{\nu_2\theta\left(T_k+\nu_4\right)-\nu_3\theta\sum_n d_n}{\nu_2{}^2-\nu_1\nu_3} \tag{6.28a}$$

$$\lambda_k^{S}=\frac{\nu_1\theta\left(T_k+\nu_4\right)-\nu_2\theta\sum_n d_n}{\nu_2{}^2-\nu_1\nu_3} \tag{6.28b}$$

$$P_n^{S}=\frac{\left(\nu_2-f_{n,k}\nu_1\right)\theta\left(T_k+\nu_4\right)-\left(\nu_3-f_{n,k}\nu_2\right)\theta\sum_n d_n}{\nu_2{}^2-\nu_1\nu_3} \tag{6.28c}$$

where, $\nu_1=\sum_{i=1}^{I}\alpha_i^{G}$

$$\nu_2=\sum_{i=1}^{I}\alpha_i^{G}f_{g_i,k}$$

$$\nu_3=\sum_{i=1}^{I}\alpha_i^{G}f_{g_i,k}{}^2$$

$$\nu_4=\sum_{j=1}^{J}f_{l_j,k}d_{l_j}$$

And the optimal spot market positions G_i^{S*} and L_j^{S*} can be derived by combining (6.28c) with (6.16) and (6.21), respectively.

6.3.2 Numerical examples

To illustrate the implications of economic determinants of the equilibrium forward prices as expressed in (6.24c), a series controlled experiments are designed and conducted on a 3-bus study system illustrated in figure 6-3.

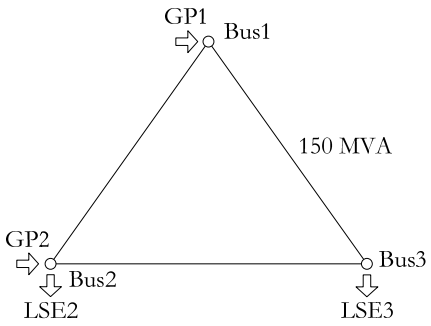

Figure 6-3 A 3-bus example system

The admittances of all transmission lines are assumed to be equal. Bus2 is the reference bus. There exist $I = 2$ generators (GEN1 and GEN2) located at bus 1 and 2, respectively, and $J = 2$ load serving entities (LSE 2 and LSE3) with respective franchised service territory whose demands are aggregated at bus 2 and 3, respectively. The ingoing and outgoing arrows illustrate power injections and ejections represented by GENs and LSEs, respectively. Transmission flowgate 1-3 is monitored for transmission congestion. We assume generation cost function parameters $\theta = 10$ and $\alpha_1^G = \alpha_2^G = 40$. All market participants have the same risk aversion. We also assume the regulated retail price by LSEs are 1.2 times the average spot market price.

Since the bus aggregated demands of end consumers are the most fundamental drivers for market price uncertainty and transmission flowgate congestions, we study the following scenarios by assuming different levels of aggregated demands at load buses 2 and 3. For simplicity, the demands are assumed to follow normal distribution $N(\mu, \sigma)$. The postulated parameters are as follows,

Scenario A: low demand

Scenario B: medium demand

Scenario C: high demand

In addition to the demand level, we study the impact of demand volatility as well by adding another scenario

Scenario D: medium demands with high volatility

The parameter of demands assumptions at bus 2 and 3 at each scenario are listed in table 6-1,

Table 6-1 Parameters of demand distributions (in $/MWh)

Load	Bus 2		Bus 3	
Parameter	μ	σ	μ	σ
Scenario A	250	250/9	200	200/9
Scenario B	275	275/9	225	225/9
Scenario C	325	325/9	250	250/9
Scenario D	275	275/6	225	225/6

When control over the explanatory variables is exercised through random assignments, since the randomization tends to balance out the effects of other variables that might affect the response variable, the resulting experimental data provide strong information about the cause-and-effect relationships than observational data. For each of the following experiment setup, the results are based on system dispatching conditions based on 100 load simulations.

The spot market prices, the day-ahead forward market prices, and the forward premiums in each scenarios are listed in tables 6-2 to 6-13 are listed as bellows,

Scenario A:

Table 6-2 Scenario A – Spot market prices (in $/MWh)

	Bus 1	Bus 2	Bus 3	Flow-gate Shadow Price
Mean	54.72	57.29	59.85	6.64
Variance	3.51	7.13	13.01	17.23

Table 6-3 Scenario A – Day-ahead forward market prices (in $/MWh)

Risk-aversion Coefficient	Bus 1	Bus 2	Bus 3	FG Shadow Price
0.05	54.87	56.73	58.60	5.60
0.005	54.79	57.08	58.74	5.18
0.0005	54.76	57.20	58.79	5.02

Table 6-4 Scenario A – Day-ahead forward premium (in $/MWh)

Risk-aversion Coefficient	Bus 1	Bus 2	Bus 3	FG Shadow Price
0.05	0.15	-0.56	-1.25	-1.04
0.005	0.07	-0.21	-1.11	-1.46
0.0005	0.04	-0.09	-1.06	-1.62

Scenario B:

Table 6-5 Scenario B – Spot market prices (in $/MWh)

	Bus 1	Bus 2	Bus 3	FG Shadow Price
Mean	54.78	69.67	84.56	23.22
Variance	20.05	160.78	812.10	1440.00

Table 6-6 Scenario B – Day-ahead forward market prices (in $/MWh)

Risk-aversion Coefficient	Bus 1	Bus 2	Bus 3	FG Shadow Price
0.05	52.57	55.11	57.65	44.30
0.005	54.56	68.21	81.87	40.97
0.0005	54.75	69.52	84.29	7.62

Table 6-7 Scenario B – Day-ahead forward premium (in $/MWh)

Risk-aversion Coefficient	Bus 1	Bus 2	Bus 3	FG Shadow Price
0.05	-2.21	-14.56	-26.91	21.08
0.005	-0.22	-1.46	-2.69	17.75
0.0005	-0.02	-0.15	-0.27	-15.60

Scenario C:

Table 6-8 Scenario C – Spot market prices (in $/MWh)

	Bus 1	Bus 2	Bus 3	FG Shadow Price
Mean	50.60	92.54	134.47	125.82
Variance	47.60	298.40	1650.00	4960.00

Table 6-9 Scenario C – Day-ahead forward market prices (in $/MWh)

Risk-aversion Coefficient	Bus 1	Bus 2	Bus 3	FG Shadow Price
0.05	44.33	104.42	164.50	180.25
0.005	47.47	98.48	149.49	153.03
0.0005	49.97	93.72	137.48	131.26

Table 6-10 Scenario C – Day-ahead forward premium (in $/MWh)

Risk-aversion Coefficient	Bus 1	Bus 2	Bus 3	FG Shadow Price
0.05	-6.26	11.88	30.02	54.43
0.005	-3.13	5.94	15.01	27.22
0.0005	-0.63	1.19	3.00	5.44

Scenario D:

Table 6-11 Scenario D – Spot market prices (in $/MWh)

	Bus 1	Bus 2	Bus 3	FG Shadow Price
Mean	52.93	71.23	89.52	48.04
Variance	39.20	322.50	1570.00	4300.00

T

Table 6-12 Scenario D – Day-ahead forward market prices (in $/MWh)

Risk-aversion Coefficient	Bus 1	Bus 2	Bus 3	FG Shadow Price
0.05	44.31	113.23	182.15	206.77
0.005	52.07	75.43	98.79	70.07
0.0005	52.85	71.65	90.45	56.40

Table 6-13 Scenario D – Day-ahead forward premium (in $/MWh)

Risk-aversion Coefficient	Bus 1	Bus 2	Bus 3	FG Shadow Price
0.05	-8.63	42.00	92.63	158.72
0.005	-0.86	4.20	9.26	22.03
0.0005	-0.09	0.42	0.93	8.36

According to experimental results illustrated above, the following observations can be made,

a. According to tables 6-4, 6-7, 6-10, and 6-13, the lower the risk aversion coefficients of market participants are, that is, the more risk-neutral the market participants become, the closer the forward prices, including on the reference bus, are to the expected spot prices

b. By comparing tables 6-2, 6-5, 6-8, and 6-11, the higher the demands, the more frequently the flow-gate gets congested in the spot market, and the higher the market prices at load buses and the lower the market prices at the generation buses are. Also, by comparing tables 6-3, 6-6, 6-9, and 6-12, similar results can be observed from the day-ahead forward market as well.

c. By comparing scenario B and scenario D results, for the same expected load level, the more volatile the load gets, the larger the forward prices at load buses and the lower the forward prices at the generation buses are.

6.4. Day-Ahead Forward Risk Premium

6.4.1 Theoretical formulation

By applying the relation of locational marginal prices as revealed by (6.5) to the day-ahead forward and spot markets, we get the following (6.29a) and (6.29b), respectively,

$$P_n^F = P_{Ref}^F - f_{n,k}\lambda_k^F \tag{6.29a}$$

$$E\left[P_n^S(\varpi)\right] = E\left[P_{Ref}^S(\varpi)\right] - f_{n,k}E\left[\lambda_{k^S}^S(\varpi)\right] \tag{6.29b}$$

Note that they reflect the effect of transmission capacity constraints on market clearing conditions. Following the forward market coordination (6.22), with the utility maximizing forward market positions of GENs and LSEs given in (6.15) and (6.20), respectively, we get

$$\sum_{i=1}^{I}\frac{P_{g_i}^{F}-E\left[P_{g_i}^{S*}(\varpi)\right]}{A_G Var\left(P_{g_i}^{S*}(\varpi)\right)}+\sum_{j=1}^{J}\frac{P_{l_j}^{F}-E\left[P_{l_j}^{S*}(\varpi)\right]}{A_L Var\left(P_{l_j}^{S*}(\varpi)\right)} \tag{6.30a}$$

$$=-\sum_{i=1}^{I}\frac{Cov\left(\rho_i^{G}(\varpi),P_{g_i}^{S*}(\varpi)\right)}{Var\left(P_{g_i}^{S*}(\varpi)\right)}-\sum_{j=1}^{J}\frac{Cov\left(\rho_j^{L}(\varpi),P_{l_j}^{S*}(\varpi)\right)}{Var\left(P_{l_j}^{S*}(\varpi)\right)}$$

which leads to (see appendix C),

$$\left(P_{Ref}^{F}-E\left[P_{Ref}^{S}\right]\right)\cdot\left(\sum_{i=1}^{I}\frac{1}{A_G Var\left(P_{g_i}^{S*}(\varpi)\right)}+\sum_{j=1}^{J}\frac{1}{A_L Var\left(P_{l_j}^{S*}(\varpi)\right)}\right) \tag{6.30b}$$

$$=\left(\lambda_k^{F}-E\left[\lambda_k^{S}\right]\right)\cdot\left(\sum_{i=1}^{I}\frac{f_{g_i,k}}{A_G Var\left(P_{g_i}^{S*}(\varpi)\right)}+\sum_{j=1}^{J}\frac{f_{l_j,k}}{A_L Var\left(P_{l_j}^{S*}(\varpi)\right)}\right)$$

$$-\left(\sum_{i=1}^{I}\frac{Cov\left(\rho_i^{G}(\varpi),P_{g_i}^{S*}(\varpi)\right)}{Var\left(P_{g_i}^{S*}(\varpi)\right)}+\sum_{j=1}^{J}\frac{Cov\left(\rho_j^{L}(\varpi),P_{l_j}^{S*}(\varpi)\right)}{Var\left(P_{l_j}^{S*}(\varpi)\right)}\right)$$

Equation (6.30b) connects the forward premium on the reference bus with the forward premium of transmission flowgate shadow prices $\left(\lambda_k^{F}-E\left[\lambda_k^{S}\right]\right)\ \forall k$, the covariance between the un-hedged profits of generators and load serving entities with their respective spot prices in the real-time spot market.

Model (6.30b) can be extended to the following more general form when the effect of multi transmission flowgates is taken into account,

$$\left(P_{Ref}^{F}-E\left[P_{Ref}^{S}\right]\right)\cdot\left(\sum_{i=1}^{I}\frac{1}{A_G Var\left(P_{g_i}^{S*}(\varpi)\right)}+\sum_{j=1}^{J}\frac{1}{A_L Var\left(P_{l_j}^{S*}(\varpi)\right)}\right) \tag{6.31}$$

$$=\sum_{k\in\mathcal{K}}\left(\lambda_k^{F}-E\left[\lambda_k^{S}\right]\right)\cdot\left(\sum_{i=1}^{I}\frac{f_{g_i,k}}{A_G Var\left(P_{g_i}^{S*}(\varpi)\right)}+\sum_{j=1}^{J}\frac{f_{l_j,k}}{A_L Var\left(P_{l_j}^{S*}(\varpi)\right)}\right)$$

$$-\left(\sum_{i=1}^{I}\frac{Cov\left(\rho_i^{G}(\varpi),P_{g_i}^{S*}(\varpi)\right)}{Var\left(P_{g_i}^{S*}(\varpi)\right)}+\sum_{j=1}^{J}\frac{Cov\left(\rho_j^{L}(\varpi),P_{l_j}^{S*}(\varpi)\right)}{Var\left(P_{l_j}^{S*}(\varpi)\right)}\right)$$

Note that the economic incentives of transmission network constraints as revealed by $\boldsymbol{\lambda}^{\{F,S\}}$ play an important role and consist a non-negligible component of the forward risk premium on the reference bus. Similarly, the effect on the forward risk premium on other buses can be derived by combining (6.5) and (6.31).

6.4.2 Empirical evidences

We start with an overview of the structure and functions performed by the New York independent system operator (NYISO). The NYISO is an outgrowth of the NYPOOL (New York power pool), which was created by New York's eight largest electric utilities to coordinate the statewide interconnection following the big Northeast blackout of 1965. In responding to the Federal Energy Regulatory Commission (FERC)'s acts and related state policies issued in mid 1990s intended to create more competition in the nation's wholesale electricity markets, the transmission system gradually became open and provide nondiscriminatory access to newly expanded non-utility generation. As the restructuring of the electric power industry evolved, NYPOOL was dissolved in 1998 and replaced with the not-for-profit NYISO. The NYISO's mission is to ensure the reliable, secure and efficient operation of the interconnected transmission system and to create and administer an open, competitive and nondiscriminatory electricity wholesale market, in which power is traded on the basis of competitive bidding. It enables the transactions to be settled at competitive prices, rather than regulated rates. Currently, the NYISO system oversees over 160,000 GWh energy transactions each year with a recorded summer load peak of over 32,075MW (July 26, 2005) and winter load peak of 25,540MW (December 20, 2004), which represent about $8 billion market value. Specifically, NYISO establishes and enforces market trading protocols, coordinates the transmission of electricity power from generation source to consumption centers, and clears the markets at settlement prices.

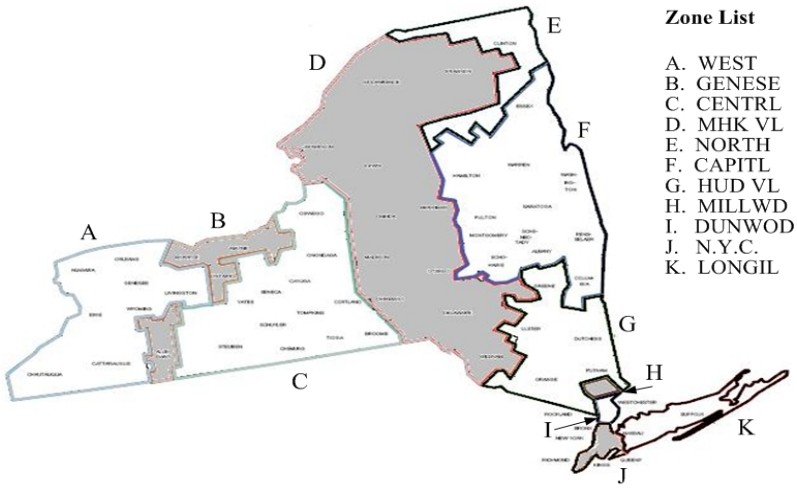

Figure 6-4 NYISO control area load zones

Compared with many other ISOs, where only partial, if any, markets have been created, the NYISO adopts a full, two-settlement system with comprehensive markets for a variety of energy-related contracts, including the day-ahead and real-time energy markets (balancing market).

In the day-ahead markets (DAM), a set of forward prices is determined on an hourly basis for each zone within the control area (and the neighboring areas) at a pre-specified time (11AM) by matching generation and energy transaction bids offered in advance to the ISO. The ISO runs a security constrained unit commitment and determines the amount of energy needed for each day. Transmission losses, congestion, shift factors, penalty factors and other system

mathematical quantities are calculated against a reference bus (physically located at the Marcy 345 kV substation in Marcy, New York). The DAM zonal locational based marginal prices (LBMPs) are obtained by adding the marginal costs of energy, losses and congestion and used as the basis for settlements. Generating units that can most economically satisfy the energy needed to supply customers' demand and allow a sufficient reserve for contingencies are scheduled. Typically, most (>90%) energy transactions processed by the NYISO occur in the DAM since market participants can hedge against the next day price risks.

In the real-time market (RTM), the ISO runs a security constrained dispatch (SCD) which determines the amount of energy needed on a continual basis. SCD makes adjustments to previous schedules to regulate generating units that can most economically satisfy the energy needed to supply customers' real-time demand and allow a sufficient reserve for contingencies. LBMPs are calculated at five-minute intervals throughout the day. Typically less (<10%) energy transactions processed by the ISO occur in the RTM. The settlements based on the RTM prices are intended to credit or charge market participants for energy transactions, due to variations in a power supplier's real-time dispatch quantity from what is pre-determined in the DAM. The total settlement is determined by the sum of balancing energy, incremental occurring losses, and created/eliminated congestion. There is actually a rolling hour-ahead market (HAM) intended to balance the most updated system situations with pre-schedules (sell excess and buy shortage). Since it serves the same function as the RTM as far as the proposed model is concerned, they are not distinguished here.

Note that the market settlements are based on LBMPs, which differ from the market-clearing prices determined at the New York Mercantile Exchange in that the spatial location of a power transaction matters even within a market.

We are interested in the following market participants, who can be categorized as follows based on their primary business functions,

a. Power producers that own generation units and sell to the wholesale markets

b. Load serving entities that buy from the wholesale markets and sell electricity at certain retail prices to end consumers via the distribution networks

c. End consumers that have access to electricity through load serving entities. They are generally immune to the market price risks since the prices are generally stable.

Although in reality most market participants are not exclusively electricity sellers or buyers but tend to appear on both sides of the market as the needs to fulfill contractual commitments or as the opportunities to generate extra profit come up, the primary business function of each market participant generally dominates its market activities and in our model, such subsidiary functions can be ignored without missing the major determinant factors for forward risk premium discovery.

One problem with empirical tests is the availability of market data. Since the market functions changed gradually following the conception of the deregulation, the historical data do not necessarily reflect the same market structure. Besides, market participants do not behave consistently due to the ever-evolving of the market design. Therefore, the historical market equilibrium prices over a long period of time bear discrete biases caused by regulatory adjustment. Taking the concerns listed above into consideration, we choose the time-horizon from February 1st 2005 to August 31st 2006 when the NYISO market structure was relatively

stable. The data used for this study consist of hourly LBMPs and flowgate shadow prices in day-ahead and spot markets, and hourly zonal loads as well. These data are acquired from NYISO website. The Zonal LBMPs are load-weighted LBMPs at all buses within the zone.

A summary of statistics for the electricity forward and spot prices on the system reference bus and in each zone is reported in table 6-14 as bellow.

Table 6-14 Statistics of forward and spot LBMPs (in $/MWh)

	Forward Market			Spot Market		
	Mean	Median	Volatility	Mean	Median	Volatility
Ref. Bus	66.99	63.21	21.95	63.67	58.56	40.72
CAPITL	74.67	70.42	25.11	69.82	64.32	45.43
CENTRL	63.72	59.80	21.95	61.46	56.22	41.29
DUNWOD	79.78	75.60	27.26	73.78	68.13	48.06
GENESE	60.48	56.33	21.30	58.89	53.04	41.64
HUD VL	78.38	74.37	26.64	73.17	67.52	47.87
LONGIL	82.76	78.33	27.88	76.26	70.87	48.76
MHK VL	68.19	64.40	22.67	65.79	60.49	43.35
MILLWD	79.79	75.73	27.35	73.58	67.93	48.03
N.Y.C.	83.42	78.68	29.25	76.24	70.19	49.85
NORTH	63.72	59.70	20.64	61.72	56.57	39.41
WEST	54.42	49.53	20.38	53.64	47.77	38.81

Table 6-14 shows that there is considerable forward premium for the reference bus and each individual zone. It also indicates the right-skewness of the electricity prices, which is consistent with the implication of the model presented in (Routledge, 2001). The forward premiums reflect market buyers' willingness to pay to secure the procurement of electricity.

Equation (6.31) describes a linear functional relationship between the forward premium on the reference bus $P_{Ref}^{F} - E\left[P_{Ref}^{S}\right]$ and the forward premium of shadow prices on the flowgates $\lambda_k^F - E\left[\lambda_k^S\right]$. The PTDF matrix **F** determines the effect of $\lambda_k^F - E\left[\lambda_k^S\right]$ on $P_{Ref}^{F} - E\left[P_{Ref}^{S}\right]$. However, since the topology of the NYISO transmission network is not accessible to the public, we can not derive a regression model between $P_{Ref}^{F} - E\left[P_{Ref}^{S}\right]$ and $\lambda_k^F - E\left[\lambda_k^S\right]$ to test the empirical data. To estimate the PTDF structure of the system, we resort to relationship between locational marginal prices and the reference bus price as revealed in (6.5). Given empirical data of hourly locational based marginal prices on the system reference and each zone, and shadow prices associated with transmission flowgates over the time horizon of $h = 1, \cdots, H$, the following multiple regression model can be constructed for all $n \in \mathcal{N}$ accordingly,

$$Y_{h,n} = \sum_{k=0}^{K} X_{h,k}\beta_{k,n} + \varepsilon_{h,n} \text{ with } X_{i0} \equiv 1 \tag{6.32a}$$

where, for, $k = 1, \cdots, K$, and $n = 1, \cdots, N$

$Y_{n,h}$ price difference between zone n and the system reference bus at hour h.

$X_{k,h}$ shadow price of transmission flowgate k at hour h.

$\beta_{n,k}$ regression coefficients representing the negative of PTDF $f_{n,k}$.

$\varepsilon_{n,h}$ independent error terms of the regression model with expectation 0 and variance σ^2

or, in the equivalent matrix form for each zone n ,

$$\underset{H\times 1}{\mathbf{Y}_n} = \underset{H\times K}{\mathbf{X}}\ \underset{K\times 1}{\boldsymbol{\beta}} + \underset{H\times 1}{\boldsymbol{\varepsilon}_n} \tag{6.32b}$$

We expect the observational $\mathbf{Y}_n$ to distribute around the regression surface (a hyper-plane in this case since it is more than 2 dimensions) $\mathbf{X}\boldsymbol{\beta}$. To set up interval estimates and make tests, the distributions of the residual terms ε_n are assumed to be normal. We have $\varepsilon_n \sim iid.N(0,\sigma_n^2)$

The normality assumption for the error terms is justifiable since the error terms represent the effect of random flowgate congestions omitted from model (6.32) that affect the response to some extend and that vary at random without reference to the modeled explanatory variables $\mathbf{X}$. Besides, as long as the distributions of error terms do not depart significantly from normality, the t-distribution based tests results are reliable. In equation (6.32b), components of $\boldsymbol{\beta}$ are the partial regression coefficients since they reflect the partial effect of one explanatory variable when other explanatory variables are held constant. Since the explanatory variables have additive effects, the effect of X_{k_1} on the mean response does not depend on the level of X_{k_2}, $k_1 \neq k_2$.

As indicated by the empirical data, in a large electric power system such as New York power pool, the system situation can be very complicated. To reduce the reality to a manageable proportion for the regression model (6.32), we choose an incomplete list of flowgates as explanatory variables for the spatial price differences. However, the flowgates enlisted are the most prominent ones for both day-ahead market and the real-time spot market and can make good sense for the purpose of the analysis. The major consideration for their choice is the extent to which the chosen flowgate contributes to reducing the remaining variation in the dependent spatial price difference after allowance is made for the contributions of other flowgate shadow prices as predictor variables that have tentatively been included in the regression model. Accordingly, in the formulation of the regression model (6.32), we restrict the coverage of the empirical data corresponding time intervals when the selected predictor variables are non-trivial. The shape of the regression function substantially outside this range should be treated differently.

Three prominent flowgates which experience transmission congestion most frequently in both the day-ahead and the real-time spot markets are picked. The corresponding ID's in the NYISO network are 25091, 23330, and 25546. They are denoted as FG1, FG2, and FG3 respectively hereinafter. The statistics of the shadow prices associated with the capacity constraints represented by them in the market dispatch model are reported in table 6-15 as follows.

Table 6-15 Statistics of forward and spot shadow prices of the flowgates (in $/MWh)

	Forward Market			Spot Market		
	Mean	Median	Volatility	Mean	Median	Volatility
FG1	16.20	11.96	23.12	23.79	10.47	48.61
FG2	1.10	0.00	5.39	5.53	0.00	143.52
FG3	3.02	0.00	17.19	3.48	0.00	54.30

As shown in table 6-15, FG1 is the most active transmission flowgate of the three. The time series of shadow prices associated with FG1 in the day-ahead and spot markets are illustrated in figure 6-5,

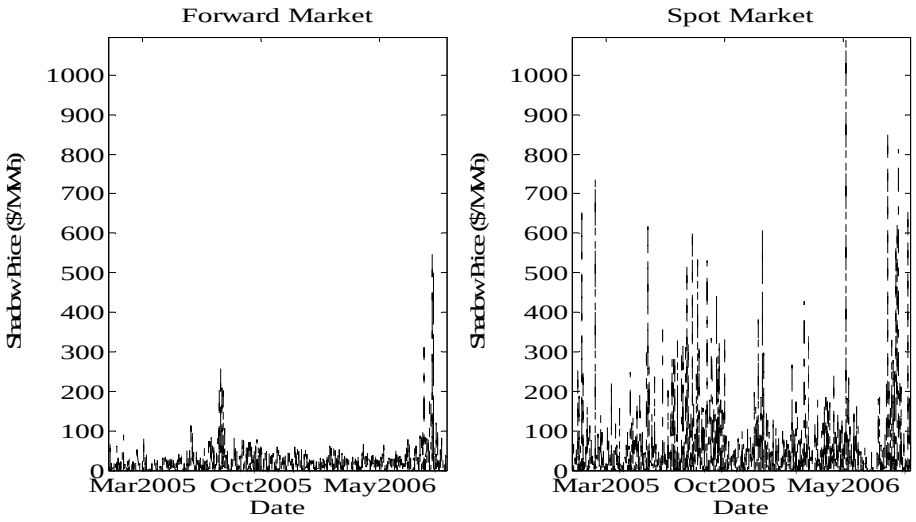

Figure 6-5 Hourly shadow prices on FG1 in forward and spot markets

According to table 6-10 and figure 6-5, it is observed that shadow prices of flowgates are generally less volatile in the forward market compared in the spot market, which conforms to the observation of electricity prices as revealed in figure 6-1. Besides, flowgate shadow prices take less extreme values in the day-ahead forward market and the averages are lower as compared with in the spot market.

The seasonality of electric load demands lead to similar pattern changes in market prices and system conditions. For instance, high market prices and frequent transmission congestions tend to be observed in summer and winter season. Transmission network topology may be changed by equipment maintenances which are usually scheduled in Springs and Falls when load demands are relatively low. Since later in the section, the inferred PTDF coefficients are used for the projection of out-of-sample (August 2006) market prices using model (6.31), we limit the historical data to be taken from June to August in 2005 and June to July in 2006 when the system structure is relatively stable and the explanatory variables' variation ranges are comparable to their counterparts in August 2006. Preprocessing of the data also includes getting ride of price spikes (we use 150$/MWh as the criteria for spikes) in locational market prices and shadow prices associated with selected flowgates.

According to the subset of active flowgates selected for the study of the imbedded statistical relation with the spatial price difference of electricity prices as modeled above, the unbiased maximum likelihood squares estimates of the set of PTDF coefficients **β**, denoted as **b** can be calculated and displayed in table 6-16.

Table 6-16 Estimation of PTDFs

	FG1	FG2	FG3
Zone-CAPITL	-0.1229	-0.1078	0.0045
Zone-CENTRL	-0.0376	0.0200	0.0782
Zone-DUNWOD	-0.1431	-0.2073	0.0276
Zone-GENESE	-0.0605	0.0615	0.2512
Zone-HUD VL	-0.1409	-0.1722	0.0170
Zone-LONGIL	-0.1493	-0.2172	0.0326
Zone-MHK VL	-0.0215	-0.0266	0.0331
Zone-MILLWD	-0.1513	-0.1775	0.0316
Zone-N.Y.C.	-0.1800	-0.3314	0.0183
Zone-NORTH	0.0791	0.0652	-0.0341
Zone-WEST	-0.0793	0.1264	0.2810

In regression model (6.32), the variance of the error terms ε_n indicates the variability of the probability distributions of Y. Its unbiased estimate error mean square (MSE) is calculated and displayed in the second column of table 6-17. The adjusted coefficients of multiple determinations shown in the third column of table 6-17 measure the proportionate reduction of total variation in **Y** associated with the use of the set of **X** variables, and in contrast to un-adjusted coefficient of multiple determinations, it takes the associated degrees of freedom of each sum of squares into consideration.

To test whether there is a regression relation between the response variable **Y** and the set of **X** variables $[X_k], k = 1,2,\cdots,K$, i.e., to test whether or not $\beta_k = 0$ for $\forall k$, an F test can also be conducted to determine between the alternatives:

$H_0: \beta_1 = \beta_2 = \cdots = \beta_K = 0$, $H_\alpha:$ not all $\beta_k = 0, k = 1,\cdots,K$

We use the test statistic:

$$F = \frac{MSR}{MSE}$$

with the decision rule to control the type I error at α as follows.

If $F^* \le F(1-\alpha; K, H-(K+1))$, H_0 is concluded, otherwise, H_α is concluded.

Apply regression model (6.32a) to all NYISO zones, the statistical measures including MSE, R^2, F, and p values, together with the serial correlation (ρ) of error terms of the regression model are shown in table 6-17:

Table 6-17 Statistics of regression

	MSE	R^2	F	p	ρ
Zone-CAPITL	8.7446	0.7051	4.3573	0.0055	0.0772
Zone-CENTRL	2.5466	0.7903	4.5583	0.0042	-0.0361
Zone-DUNWOD	12.7076	0.6564	3.7473	0.0121	0.0819
Zone-GENESE	12.8970	0.4678	3.2998	0.0217	0.0921
Zone-HUD VL	8.4994	0.6637	3.7299	0.0124	-0.0687
Zone-LONGIL	6.0739	0.6494	4.1753	0.0070	-0.0299
Zone-MHK VL	1.5187	0. 5413	3.2727	0.0225	0.0564
Zone-MILLWD	11.7480	0.7056	4.0583	0.0081	0.0478
Zone-N.Y.C.	15.6489	0.6728	2.9149	0.0358	-0.1141
Zone-NORTH	2.6171	0.573	3.8538	0.0106	0.0802
Zone-WEST	14.3732	0. 7393	3.1193	0.0275	-0.0744

Given the wide support of explanatory variables $\mathbf{X}$, together with moderate MSE values, high R^2 values imply good inference power. The p-value reported in table 6-17 is the probability of observing the given sample result under the assumption that the H_0 hypothesis of the F test is true, depends on assumptions about the independence and normality of the random disturbances ε_i in the model equation (6.32). Since all but one of the p-values are less than $\alpha = 0.05$ in general, this is a quite significant and strong indication that the null hypothesis can be rejected. F-statistic values as extreme as the ones reported in table 6-17 would rarely occur if the differences between a zonal price and the reference bus price are independent of the flowgate shadow prices.

To test whether there is a regression relation between the response variable $\mathbf{Y}$ and each of the $\mathbf{X}$ variables $[X_k]$, $k = 1,2,\cdots,K$, i.e., the tests whether or not $\beta_k = 0$ for each k, t tests can also be conducted to determine between the alternatives:

$H_0: \beta_k = 0$, $H_\alpha: \beta_k \neq 0$

We use the statistics $t^* = \dfrac{b_k}{s\{b_k\}}$

with the decision rule:

If $|t^*| \le t\left(1-\dfrac{\alpha}{2}; H-(K+1)\right)$, conclude H_0, otherwise, conclude H_α.

where $s(b_k)$ are square roots of the diagonal components of $\underset{(K+1)\times(K+1)}{\mathbf{s}^2\{\mathbf{b}\}} = MSE \cdot (\mathbf{X}'\mathbf{X})^{-1}$ and calculated and listed in table 6-18 as below,

Table 6-18 Value for the estimation of PTDFs

	FG1	FG2	FG3
Zone-CAPITL	0.0344	0.0573	0.0038
Zone-CENTRL	0.0369	0.0082	0.0409
Zone-DUNWOD	0.0539	0.0839	0.0258
Zone-GENESE	0.0375	0.0244	0.1093
Zone-HUD VL	0.0449	0.0772	0.0113
Zone-LONGIL	0.0537	0.0850	0.0200
Zone-MHK VL	0.0070	0.0369	0.0292
Zone-MILLWD	0.0470	0.0746	0.0277
Zone-N.Y.C.	0.0644	0.1173	0.0831
Zone-NORTH	0.0341	0.0499	0.0421
Zone-WEST	0.0483	0.0768	0.1538

The following table 6-19 shows the t-values of the PTDF regression estimations,

Table 6-19 t-Value for the estimation of PTDFs

	FG1	FG2	FG3
Zone-CAPITL	-3.5749	-1.8810	1.1886
Zone-CENTRL	-1.0178	2.4509	1.9125
Zone-DUNWOD	-2.6562	-2.4714	1.0695
Zone-GENESE	-1.6152	2.5175	2.2975
Zone-HUD VL	-3.1412	-2.2309	1.5074
Zone-LONGIL	-2.7794	-2.5545	1.6295
Zone-MHK VL	-3.0777	-0.7206	1.1319
Zone-MILLWD	-3.2180	-2.3803	1.1392
Zone-N.Y.C.	-2.7932	-2.8246	0.2201
Zone-NORTH	2.3206	1.3079	-0.8106
Zone-WEST	-1.6402	1.6466	1.8274

For most of the t-values associated with FG1 and FG2, the corresponding null hypothesis H_0's can be rejected at confidence level higher than 95%. Even for FG3, the H_α's are more favorable than the corresponding H_0's.

For the normal error regression model (6.32), we also have

$$\frac{b_k - \beta_k}{s(b_k)} \sim t\left(H - (K+1)\right),\ k = 0,1,\cdots,K$$

Note that if only the probability distributions of Y do not depart significantly from normality, the sampling distributions of estimates **b** are approximately normal and the t-distribution based tests can provide approximately the specified confidence coefficient. Even if **Y** departs seriously from normality, the estimators **b** have the property of asymptotic normality

and approach normality under the general conditions as the sample size increases. Therefore, the confidence intervals and the conclusions still apply. The confidence limits for β_k with $1-\alpha$ confidence coefficient are

$$b_k \pm t\left(1-\frac{\alpha}{2}, H-(K+1)\right)s(b_k),\ k=0,1,\cdots,K$$

Table 6-20 shows the confidence interval of PTDF estimates with 95% confidence level.

Table 6-20 Confident Interval of PTDFs estimation

	FG1	FG2	FG3
Zone-CAPITL	[-0.1908, -0.0550]	[-0.2209, 0.0053]	[-0.0030, 0.0120]
Zone-CENTRL	[-0.1105, 0.0353]	[0.0039, 0.0361]	[-0.0025, 0.1589]
Zone-DUNWOD	[-0.2494, -0.0368]	[-0.3729, -0.0417]	[-0.0233, 0.0785]
Zone-GENESE	[-0.1344, 0.0134]	[0.0133, 0.1097]	[0.0354, 0.4670]
Zone-HUD VL	[-0.2294, -0.0524]	[-0.3245, 0.0199]	[-0.0053, 0.0393]
Zone-LONGIL	[-0.2553, -0.0433]	[-0.3850, 0.0494]	[-0.0069, 0.0721]
Zone-MHK VL	[-0.0353, -0.0077]	[-0.0995, 0.0463]	[-0.0246, 0.0908]
Zone-MILLWD	[-0.2441, -0.0585]	[-0.3247, 0.0303]	[-0.0231, 0.0863]
Zone-N.Y.C.	[-0.3072, -0.0528]	[-0.5630, 0.0998]	[-0.1458, 0.1824]
Zone-NORTH	[0.0118, 0.1464]	[-0.0332, 0.1636]	[-0.1171, 0.0489]
Zone-WEST	[-0.1747, 0.0161]	[-0.0251, 02779]	[-0.0225, 0.5845]

Since the regression model (6.32) assumes that the congestion shadow prices are known constants, the confidence coefficient and risks of errors are interpreted with respect to taking repeated samples in which the congestion conditions are kept at the comparable levels as in the observed sample.

As it is illustrated in tables 6-11 and 6-12, although there exist variations across individual zones, the statistical measures provide evidence for a significant relation between the flowgate shadow prices and electricity price spatial differences. We conclude that the PTDF coefficients are estimated with satisfactory statistical significance. Note that the PTDF matrix as inferred above is different from what PTDF is defined in the traditional way since there does not exist a specific bus in a zone into which the power injection causes a portion of power flow indicated as the PTDF coefficient. Nevertheless, the PTDF matrix indicates the impact of aggregated power injection changes in one zone on a specific transmission flowgate. This is of special meaning when the locational based marginal prices are calculated for each zone of the NYISO system.

Previous research finds that the forward risk premiums in electricity forward prices vary systematically throughout the day and the forward premium manifests most significant during on-peak hours when spot market prices are most volatile. In Longstaff and Wang (2004), hour-by-hour forward premiums in PJM market tested show that the forward premium tends to be positive in on-peak hours but negative in off-peak hours.

By examining the empirical data with NYISO, we find a similar pattern in the forward risk premium on the reference bus as plotted in figure 6-6.

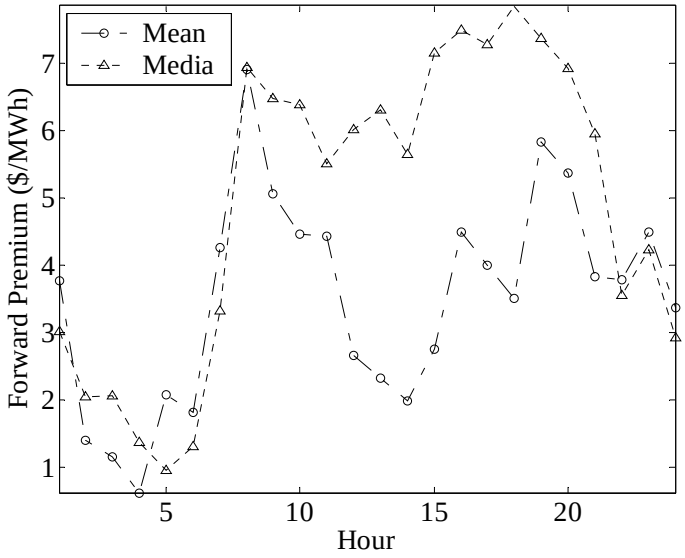

Figure 6-6 Forward premiums on the reference bus at each hour

Bessembinder and Lemmon (2002) note that the existence of large forward premiums reflects the lack of risk-sharing in electricity markets with market risk being borne by a subset of participants. The higher forward premiums during on-peak hours represent the time period within a day when the market participants face the greatest economic risks. Note that the period of high forward risk premium corresponds to the high load period. Taking the CENTRL zone as an example (and each zonal load has a similar daily pattern), the hour-by-hour loads are plotted in figure 6-7 as follows,

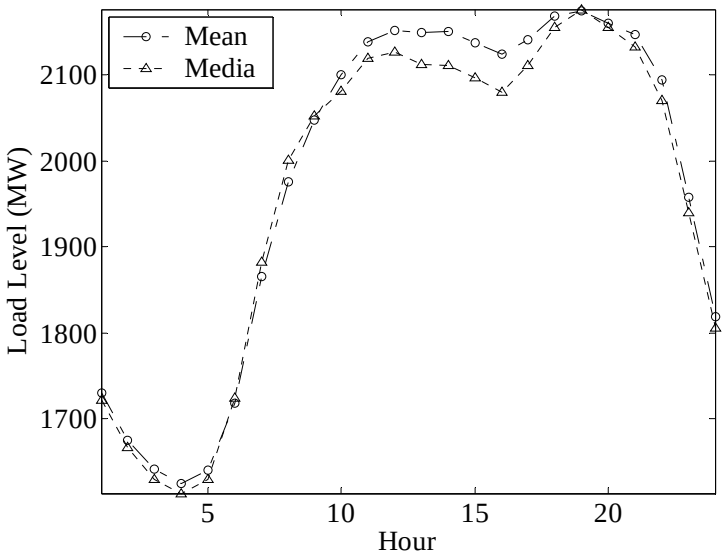

Figure 6-7 Load level in the CENTRL zone at each hour

One interesting observation is that the forward risk premium of the shadow prices on the transmission flowgate FG1 as plotted in figure 6-8 shows the opposite direction: the premium is high during off-peak hours while low during on-peak hours.

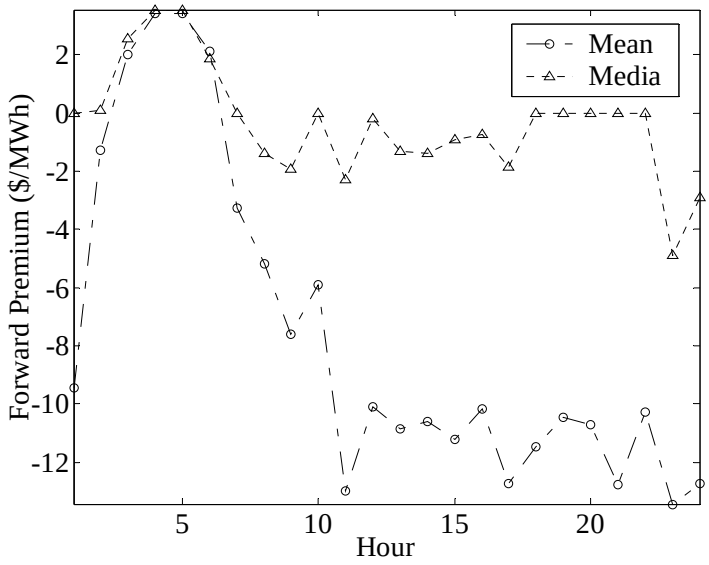

Figure 6-8 Forward premium of the shadow price on FG1 at each hour

This is not surprising if we look back at equation (6.31) and the estimated PTDF matrix illustrated in table 6-16. Since the power transfer distribution factors of most zones on the flowgate FG1 are negative numbers, the forward premium on the system reference bus is negatively correlated to the forward premium of flowgate shadow prices. This observation provides more insights to the forward premium in the electricity wholesale contracts. Actually, part of the premium can be attributed to the effect of having binding transmission capacity constraints.

To evaluate the forward risk premium determining model shown by (6.31), the same set of empirical data as used for system PTDF coefficient inference is used to test the following regression model,

$$Z_h = \sum_{p=0}^{5} \chi_{h,p}\tau_p + \varsigma_h \text{ with } \chi_{h0} \equiv 1$$

where, for $h = 1,\cdots,H$

Z_h system reference bus locational based marginal price forward premium term $\left(P_{Ref}^{F} - E\left[P_{Ref}^{S}\right]\right)\cdot\left(\sum_{i=1}^{I}\frac{1}{Var\left(P_{Gi}^{S*}(\varpi)\right)} + \sum_{j=1}^{J}\frac{1}{Var\left(P_{Lj}^{S*}(\varpi)\right)}\right)$ at hour h.

$\chi_{h,k}$ for $k = 1,2,3$, transmission flowgate shadow price forward premium term

$\left(\lambda_k^F - E\left[\lambda_k^S\right]\right)\cdot\left(\sum_{i=1}^{I}\frac{f_{Gi,k}}{Var\left(P_{Gi}^{S*}(\varpi)\right)}+\sum_{j=1}^{J}\frac{f_{Lj,k}}{Var\left(P_{Lj}^{S*}(\varpi)\right)}\right)$ at hour h.

$\chi_{h,4}$ the summation of covariance between GENs' un-hedged profit and the spot market price $\sum_{i=1}^{I}\frac{Cov\left(\rho_{Gi}^{*}(\varpi),P_{Gi}^{S*}(\varpi)\right)}{Var\left(P_{Gi}^{S*}(\varpi)\right)}$ at hour h.

$\chi_{h,5}$ the summation of covariance between LSEs' un-hedged profit and the spot market price $\sum_{j=1}^{J}\frac{Cov\left(\rho_{Lj}^{*}(\varpi),P_{Lj}^{S*}(\varpi)\right)}{Var\left(P_{Lj}^{S*}(\varpi)\right)}$ at hour h.

τ the regression coefficient vector.

ς_h independent error terms of the regression model with expectation 0 and variance σ^2

or, in the matrix form

$$\underset{H\times 1}{\mathbf{Z}} = \underset{H\times 6}{\boldsymbol{\chi}}\ \underset{6\times 1}{\boldsymbol{\tau}} + \underset{H\times 1}{\boldsymbol{\varsigma}} \tag{6.33}$$

We expect the observational $\mathbf{Z}$ to distribute around the regression surface (a hyperplane in this case since it is more than 2 dimensions) $\boldsymbol{\chi\tau}$. Since model (6.33) does not take all flowgates into consideration, beside, the empirical prices are subject to some exogenous factors which are not modeled in our model, we take normality assumption for the error terms ς_h to represent the effect of random factors that affect the response to some extend and that vary at random without reference to the modeled explanatory variables $\boldsymbol{\chi}$. We have $\varsigma_h \sim iid.N(0,\sigma^2)$

We used rolling average of corresponding empirical data at the specific hour in the previous 14 days for the conditional expectation measures $E\left[P_{Ref}^{S}\right]$ and $E\left[\lambda_k^S\right]$. For conditional variance and covariance measures, $Var\left(P_{Gi}^{S*}(\varpi)\right)$, $Cov\left(\rho_{Gi}^{*}(\varpi),P_{Gi}^{S*}(\varpi)\right)$, and $Cov\left(\rho_{Lj}^{*}(\varpi),P_{Lj}^{S*}(\varpi)\right)$ at hour h, we use the corresponding empirical data at the specific hour in the previous 14 days also. The regulated retail price at each zone is assumed to be 1.2 times the average of the spot market price throughout the interested time period. To distinguish the difference between on-peak and off-peak hours, we assume on-peak and off-peak retail prices and the averages are taken over on-peak and off-peak hours, respectively.

Since the parameters A_G and A_L in equation (6.31) are not directly observable based on the empirical data, we do not incorporate them explicitly in the regression function but keep in mind that they are positive numbers for risk-averse market participants as in the assumptions indicated above. Given that A_G and A_L should be comparable for the market participants modeled, the estimation of regression parameters τ_4 and τ_5 based on (6.33) as compared with (6.31) would reveal, approximately, the values of parameters A_G and A_L.

The estimates for the regression model coefficients are given in table 6-21,

Table 6-21 Estimation of regression coefficients

τ_1	τ_2	τ_3	τ_4	τ_5
0.4783	0.3658	0.2943	-0.0248	-0.0093

Based on the normality assumption of the error terms, to test whether there is a regression relation between the response variable $\mathbf{Z}$ and the set of $\boldsymbol{\chi}$ variables, i.e., to test whether or not $\boldsymbol{\tau}$ for each of its component, an F test can also be conducted to determine between the alternatives:

$H_0: \tau_1 = \tau_2 = \cdots = \tau_6 = 0$, $H_\alpha:$ not all $\tau_p = 0, p = 1, \cdots, 6$

with the decision rule to control the type I error at α:

If $F^* \le F(1-\alpha; K, H-(K+1))$, conclude H_0, otherwise, conclude H_α.

The statistical measures including the coefficient of multiple determinations R^2, the F value, and p-value, together with the serial correlation (ρ) of error terms of the regression model, are displayed in table 6-22 as follows,

Table 6-22 Statistics of regression coefficients

R^2	F	p	ρ
0.5021	3.5583	0.0053	0.1201

Since the p-values shows that a F statistic as extreme as the observed F would occur by chance close to once in 200 times if the forward premium term is independent of the flowgate shadow prices forward premium and the covariance between market participants' un-hedged profit and the spot market price, We conclude that H_0 can be rejected with significant confidence level.

Corresponding to the tests of whether there exists regression relation between the response variable $\mathbf{Z}$ and each of the $\boldsymbol{\chi}$ variables, i.e., the tests whether or not $\tau_p = 0$ for each p, $p = 1, \cdots, 5$,

$H_0: \beta_{\mathrm{p}} = 0$, $H_\alpha: \beta_{\mathrm{p}} \ne 0$

the t values corresponding to each partial regression coefficient τ_p are calculated and listed in table 6-23,

Table 6-23 t value of regression coefficients

	τ_1	τ_2	τ_3	τ_4	τ_5
t-Value	2.4352	1.9620	1.9703	1.4326	2.3801

The null hypothesis H_0's can be rejected with confidence as high as 95% for all τ_p's expect for τ_4. Given the small sample size and the difficulty of estimating the conditional measures, however, we think the results support the model in general.

Although the statistical significance varies according to individual regression coefficient, the statistical measures do suggest strong relations exist between the forward risk premium and the economic factors modeled. The estimates of $\boldsymbol{\tau}$'s are different from 1 as suggested by model (6.31). This can be attributed to the scale difference between A_G and A_L and to the fact that, as mentioned in earlier part of the section, the flowgate list as constructed is not a complete list of flowgates which affect the forward risk premium. The values of τ_4 and τ_5 also indicate that the risk-aversion coefficients A_G and A_L are of the magnitudes of $10^{-3} \sim 10^{-2}$, which are comparable to the values we adopted for the simulation study in section 6.3.1.

To further test the implications of the forward risk premium model, using the regression model based estimates of PTDF coefficients listed in table 6-19 and the reference bus forward premium regression coefficients listed in table 6-21, equation (6.33) is used to forecast spot market prices.

The out-of-sample spot price data and their projections are plotted in figure 6-9,

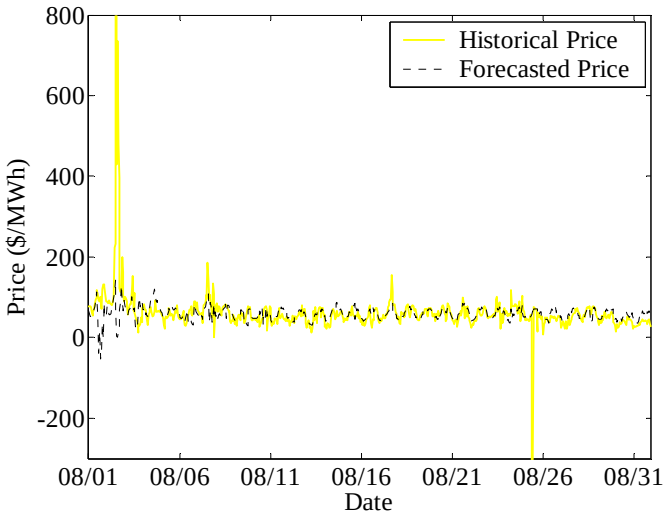

Figure 6-9 Historical and forecasted spot price at the reference bus in August 2006

Note that except for a few spikes of the spot market price and sags of the forecasted price, the rest sections of the curves fit quite closely. By looking at the shadow price on flowgate FG1 as illustrated in figure 6-10, we understand the sags come from the shadow price spikes.

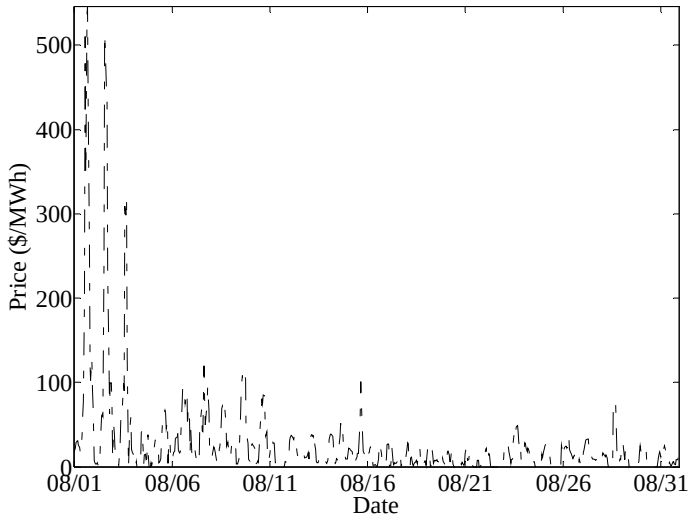

Figure 6-10 Historical day-ahead shadow prices of flowgate FG1 in August 2006

Assuming normality of the forecast error term (defined as the absolute deviation of forecasted prices from the realized spot prices), its distribution parameters and their confidence intervals (CI) are estimated in the table 6-24,

Table 6-24 Estimates of forecast error term Parameters ($/MWh)

μ	95% CI of μ	σ	95% CI of σ
10.22	[8.97, 11.47]	16.67	[15.85, 17.58]

By excluding the LBMP and flowgate shadow price (FGP) spikes (defined at certain quantiles of their corresponding distributions), the forecast error term's distribution parameters and their confidence intervals (CI) would be as follows,

Table 6-25 Estimates of forecast error term parameters by excluding LBMP and FGP spikes defined at different quantiles of their distributions ($/MWh)

Quantile	LBMP spike	FGP spike	μ	95% CI of μ	σ	95% CI of σ
95.0%	98.44	76.41	6.98	[5.92, 8.04]	12.96	[12.28, 13.70]
97.5%	120.17	131.45	7.03	[5.93, 8.13]	13.37	[12.67, 14.13]
99.0%	199.79	266.67	11.93	[10.65, 13.21]	17.04	[16.20, 17.97]

Empirical study with the NYISO data confirms the relations between the forward premium and the factors revealed in model (6.31). The functional relation is insightful for the understanding of how the forward premium can be affected by the market participants as well as the transmission network constraints. Although the statistics in tables 6-24 and 6-25 do not

indicate a price forecasting with high accuracy as compared with some existing models (for example, see Conejo et al., 2005), we expect the predictive power of the forward premium model can be greatly improved when we have more information about the transmission network topology. In that case, the PTDF coefficients can be calculated accurately without using the regression model for inference. At the same time, more transmission flowgates can be taken into account to determine the forward premium. With more accurate model coefficients and more explanatory variables, model (6.31) can be relied on for practical uses.

6.5. Conclusions and Discussions

We examine the risk premium present in the electricity day-ahead forward price over the real-time spot price. This study establishes a quantitative model for incorporating transmission congestion into the analysis of electricity day-ahead forward risk premium. Through simulations with a three-bus study-system, it is illustrated that the more frequently transmission congestion happens, the higher the forward prices get at the load buses. Consistent with the implications of the model, evidences from empirical studies with the New York electricity market data confirm that there exists a significant statistical relationship between the day-ahead forward risk premium and the shadow price premiums on transmission flowgates. When applied to the forecasting of next day spot prices, this model still has considerable room to improve its accuracy. One important factor is that the PTDF coefficients are inferred using historical market price data without the knowledge of the transmission network structure. However, for a long-term market participant in a specific power pool, who is more familiar with the system transmission conditions, these PTDF coefficients would be known. Furthermore, additional important transmission flowgates can be identified and the corresponding shadow price premiums can be added as explanatory variables in the regression model. With these enhancements, it is foreseeable that the forecasting accuracy of the model could be improved.

Given the encouraging empirical evidences from the New York electricity market, caution should still be exercised in generalizing the results to other markets where factors such as market power and regulators' price intervention may affect the market clearing process.

Future expansion of the model can be made to take into account the generation reserve markets in addition to the energy wholesale markets since market participants' decisions in these markets are interdependent. In addition, since the existence of non-zero forward risk premiums provide incentives for market speculators to take positions in the electricity derivatives markets, their behaviors and the impact on forward premiums need to be studies as well.

7. Inherent Inefficiencies of FTR Auctions Under Simultaneous Feasibility Constraints

Point-to-point financial transmission rights (FTRs) (see Bushnell and Stoft (1997) and Hogan (1992)) and flow-gate rights (FGRs) (see Chao and Peck (1996), (1997), and Chao, Peck Oren and Wilson (2000)) are two forms of Congestion Revenue Rights (CRRs) outlined in the Standard Market Design put forth by the Federal Energy Regulatory Commission (FERC) of the U.S. The purposes of the CRRs are two fold: a) Create a system of property rights to the transmission system that will offer economic signals for charging/compensating transmission usage/investment and facilitate the implementation of an economically efficient transmission congestion management protocol; b) Offer risk management capability to market participants entering into forward energy transactions so that they can hedge the uncertain congestion rents associated with such transactions. The allocation of FTRs can be done either on the basis of historical entitlements and use of the transmission system or through an auction whose proceeds are distributed to transmission owners or consumers who funded the construction of the system; or, through a combination of the two where unallocated FTRs and FTRs currently held by private parties are auctioned off through a centralized auction conducted periodically by an Independent System Operator (ISO). The latter approach is currently used by the three major ISOs in the northeastern US (New England, New York ISO and Pennsylvania-New Jersey-Maryland).

In this chapter we primarily focus on the risk management aspect of FTRs and the extent to which FTRs are efficient instruments for trading and mitigation of congestion risk. In evaluating a financial hedging instruments and its market performance, two questions must be addressed: How good is the hedge? Namely, to what extent does the payoff (or payout) of the instrument offset the fluctuations in the risky cash flow that the instrument is supposed to hedge. How efficient is the market for the instrument? That is, does the forward market price of the instrument reflect the expected risky cash flow hedged by the instrument with the proper risk premium adjustment.

Much of the discussion surrounding FTRs focuses on the first question and indeed FTRs provide a perfect hedge against real-time congestion charges based on nodal prices. A one Megawatt (MW) bilateral transaction between two points in a transmission network is charged (or credited) the nodal price difference between the point of withdrawal and the point of injection. At the same time (assuming that transmission rights are fully funded), a one MW financial transmission right (FTR) between two points is an entitlement (or obligation) for the difference between the nodal prices at the withdrawal node and the injection node. Thus regardless of how the system is dispatched, a one MW FTR between two nodes is a perfect hedge against the uncertain congestion charge between the same two nodes[10]. The hedging properties of FTRs make them ideal instruments for converting historical entitlements to firm transmission capacity into tradable rights that hold the owners of such entitlements harmless while enabling them to cash out when someone else can make more efficient use of the transmission capacity covered by these entitlements. In other words, FTRs make it relatively

10Some ISOs derate FTR settlements in order to cover congestion revenue shortfalls due to transmission contingencies not accounted for in the FTR auction. In such cases, depending on the derating approach, FTRs may not provide acceptable hedges.

easy to preserve the status quo while opening up the transmission system to new and more efficient use.

From the perspective of new transmission users who view the FTRs as a mechanism to hedge their exposure to congestion risk (as well as old users who are actively evaluating their commercial options with respect to FTR entitlements) the second question is as relevant as the first. A purchaser of FTRs must assess whether the forward price of the instrument indeed reflects the value that it provides in making the decision whether to purchase/hold the instrument or to face the exposure to the real-time congestion charges.

In typical financial and commodity markets, competition and liquidity push the forward prices to the expected spot prices with a proper (market based) risk premium adjustment. Such convergence is achieved through a process of arbitrage. Such arbitrage, however, may be more difficult when dealing with FTRs for several reasons. Most importantly, due to the large number of FTR types, the liquidity of these instruments is relatively low; and there is virtually no secondary market that enables reconfiguration and re-trading. In order to maintain financial solvency of the system operator who is the counter-party to FTRs, the configuration of FTR types must satisfy ``simultaneous feasibility conditions'' that are dictated by the system constraints. Consequently, pricing and trading of FTRs is done through a central periodic auction and the liquidity of the FTR depends on the frequency of that centralized reconfiguration auction. It is important to recognize that FTR liquidity cannot be measured in terms of the number of bids in the FTR auctions which merely reflect bid fragmentation. Indeed, the Pennsylvania-New Jersey-Maryland (PJM) ISO have experienced a large volume of FTR bids in their auction which may be misinterpreted as an indication of good liquidity. However, volume does not necessarily imply liquidity. True liquidity in a financial sense is reflected by the frequency of trading opportunities, bid-ask spreads and the ability to sell or buy FTRs for short time segment (e.g. one day or specific hours) which represent only small fractions of the time intervals between reconfiguration auction.

Furthermore, because of the interaction among the different FTR types through the simultaneous feasibility conditions, prices of the FTRs resulting from the FTR auction as well as the congestion charges hedged by these FTRs are highly interrelated. An efficient market (that correctly prices FTRs) must anticipate not only the uncertainty in congestion prices due to contingencies and load fluctuation but also the shift in the ``operating point'' within the feasible region which is determined by the economic dispatch procedure.

Empirical evidence reported by Adamson and Englander (2005), and Sinddiqui *et al* (2003), shows that the clearing prices for FTRs resulting from centralized auctions conducted by the New York Independent System Operator (NYISO) have differed significantly and systematically from the realized congestion revenues that determined the accrued payoffs of these transmission rights. Adamson, Noe and Parker (2008) argue that these diviations cannot be explained by risk aversion or by risk premium s for non-diversifiable risk. The question addressed by this chapter is whether such deviations are only due to transitory risk premiums and price discovery errors which will eventually vanish, or there are inherent inefficiencies in the auction structure itself that can explain the observed discrepancies. We address this question by presenting a theoretical analysis that can potentially explain the empirical findings cited above and then we demonstrate the implications of our theoretical results through numerical simulations and sensitivity analysis conducted on a DC-flow approximation model of a six-node system and the IEEE-24 bus Reliability Test System (see Sun, Deng and Meliopoulous (2004) for a general AC-flow

formulation) with known outage probabilities of each element and known statistical demand variability. In the example, we simulate the expected value of all point-to-point transmission rights taking into consideration all possible $n-1$ transmission contingencies and demand realizations. We then construct a hypothetical FTR auction in which all FTR bids equal the correct expected value of the corresponding congestion rents whereas the bid quantities are bounded by some multiple α of the corresponding average point-to-point transaction volume. In making the latter assumption we do not attempt to model bidding behavior in the FTR auction but rather to illustrate the effect of quantity limits on the bids and the order of magnitude by which bid quantities need to exceed average transaction volumes in order to eliminate price distortions in the FTR auction. The homogeneous scaling of bid quantities is simply convenient. Similar results can be obtained by assuming alternative patterns of bid quantity limits. In reality such quantity limits arise due to the desire of auction participants to match their FTR holdings to their hedging needs based on their expected use of the transmission system and due to credit limits faced by the bidders. The specific quantity limits on FTR bids and their relation to the expected transaction volume will, obviously, vary among FTRs and we do not attempt to predict those limits. In general, however, we anticipate that the ratios of FTR bid quantities to expected transaction volumes will be relatively low since excessive bid quantities relative to use, especially by regulated load serving entities, may be perceived as speculative behavior and frowned upon by regulators who are unlikely to pass through the downside risk of such activities to consumers. The results of our theoretical and computational analysis shed light on the observed discrepancies between realized FTR values and their auction prices.

The organization of this chapter is as follows. In section 7.1, we formulate an FTR auction model which incorporates the simultaneous feasibility conditions under postulated contingencies on transmission line availability and load variation. We then provide theoretical results on the potential systematic biases in market clearing nodal prices with respect to rational expectations. Numerical examples are presented in section 7.2 that confirm our theoretical findings. Finally, we conclude this chapter in section 7.3.

7.1. The Point-to-Point FTR Auction

We consider an FTR auction conducted by a system operator in an electric power grid with n buses and m transmission lines. The auction is cleared under the standard FTR auction rules that treat all FTR bids as simultaneous bilateral transactions that must satisfy all the line operating limits under all $n-1$ contingencies and load realizations. The auction is cleared so as to maximize FTR revenues and the prices are set to the marginal clearing bids for each FTR.

We first show that the FTR simultaneous feasibility auction can be represented by an equivalent virtual energy auction. We limit the proof to our case of interest where we assume that all bidders have perfect foresight of the expected value of the locational marginal price (LMP) for energy at all buses of a network. In this special case (assuming perfect competition and rational risk neutral bidders), all FTR auction participants bid only one price f_{ij} for FTR contracts with the same origin i and destination j. Furthermore, for each FTR from bus i to bus j, we can aggregate all bid quantities for this FTR into one single bid quantity $\bar{q}_{ij}$. [11] Let

11The result can be generalized to the more general case where there are multiple bids with different prices for each FTR but the mathematical representation of that general case is more complicated and will be omitted here for clarity.

$C \equiv (c_1, c_2, \cdots, c_n)^T$ denote the vector of expected LMPs at the n buses then $f_{ij} \equiv c_j - c_i$ (since the expected value of the difference between two random variables equals the difference of the respective expected values of these variables). Let $\{q_{ij}, \forall i, j\}$ denote the awarded FTR quantity from bus i to bus j and $Q \equiv (q_1, q_2, \cdots, q_n)^T$ denote the energy injection/withdrawal vector imputed from all awarded FTR quantities. Then $q_i \equiv \sum_{j \neq i} q_{ij} - \sum_{k \neq i} q_{ki}, \ \forall i \in N$ where N is the set of all buses. We adhere to the convention that a positive q_i represents injection while a negative q_i represents withdrawal. In an FTR auction market, participants are either hedgers who purchase FTRs to hedge the congestion charges of their energy transactions or speculators who trade FTRs for speculative profits subject to trading quantity limits set by risk control measures. None of these participants would bid for an unlimited amount of FTRs. Thus it is natural to assume that the aggregate bid quantity of the FTR from node i to node j is bounded by $\bar{q}_{ij}$ with all bids submitted at the expected settlement price for the corresponding FTR. The clearing mechanism for the FTR auction is formulated as follows. The system operator maximizes the as-bid value of awarded FTRs over all feasible FTR allocation quantities $\{q_{ij}, \forall i, j\}$ subject to the corresponding energy dispatch vector Q satisfying power flow constraints under all designated system reliability contingency scenarios. Let R denote the set of all plausible reliability contingencies. Each scenario $r \in R$ represents the outage of at most one transmission line. The FTR auction is cleared through solving the following optimization problem.

$$\begin{aligned} &\max_{\{q_{ij}, \forall i, j\}} \sum_{i \in N} \sum_{j \neq i} f_{ij} \cdot q_{ij} \\ &s.t.\ q_i = \sum_{j \neq i} q_{ij} - \sum_{k \neq i} q_{ki} \forall \ i \in N \\ &-L \leq G_r \cdot Q \leq L \forall \ r \in R \\ &0 \leq q_{ij} \leq \bar{q}_{ij} \forall i, j, \ and \ \ j \neq i \end{aligned} \tag{7.1}$$

where L is the vector of transmission line capacity limits and G_r is the power transfer distribution factor (PTDF) matrix with bus-n chosen as the swing bus in each contingency scenario r.

By re-arranging terms in the objective function of the FTR auction problem (7.1), we get the following:

$$\begin{aligned} &\sum_{i \in N} \sum_{j \neq i} f_{ij} \cdot q_{ij} \\ &\equiv \sum_{i \in N} \sum_{j \neq i} (-c_i + c_j) \cdot q_{ij} \\ &= -\sum_{i \in N} c_i \cdot (\sum_{j \neq i} q_{ij}) + \sum_{j \in N} c_j \cdot (\sum_{i \neq j} q_{ij}) \qquad (7.2) \\ &= -\sum_{i \in N} c_i \cdot (\sum_{j \neq i} q_{ij} - \sum_{j \neq i} q_{ji}) \qquad (7.3) \\ &= -\sum_{i \in N} c_i \cdot q_i \qquad (7.4) \end{aligned}$$

The term in (7.4) represents the merchandizing surplus in the network, (i.e. total purchase price minus sales price) for all transacted energy Q when all the awarded FTRs are exercised simultaneously. When the willingness-to-pay of all demands at a node and the generation cost at a node are constants (as assumed in our case) the merchandizing surplus equals the social surplus (i.e., the difference between demand willingness-to-pay and supply marginal cost).

Moreover, the constraints for the components of Q (i.e. q_i's) in (7.1) imply that Q is a balanced energy dispatch. Namely,

$$\begin{aligned} & e^T Q \equiv \sum_{i \in N} q_i \\ & = \sum_{j \in N} (\sum_{m \neq j} q_{jm} - \sum_{n \neq j} q_{nj}) = 0 \end{aligned} \tag{7.5}$$

where e is a row vector consisting of n ``1"s and a positive/negative q_i indicates an injection/ejection at node i.

Substituting (7.4) and (7.5) into the FTR auction problem (7.1), we have shown that (7.1) is equivalent to the following virtual energy auction conducted by the system operator to maximize the social surplus of all transacted energy. In particular, the constraints on the FTR bid quantities in (7.1) are implemented by converting the quantity bounds of FTR bids to quantity bounds of nodal energy in the virtual energy auction (7.6). Specifically the nodal demand/generation at node i is bounded from below by $\underline{q}_i = -\sum_{j \neq i} \overline{q}_{ij}$ and from above by $\overline{q}_i = \sum_{k \neq i} \overline{q}_{ki}$.

$$\begin{aligned} & \max_{Q} -\sum_{i \in N} c_i \cdot q_i \\ & s.t. \quad e^T Q = 0 \\ & \quad -L \leq G_r \cdot Q \leq L \forall r \in R \\ & \quad \underline{Q} \leq Q \leq \overline{Q} \end{aligned} \tag{7.6}$$

where L is defined in (1), G_r's are the same PTDF matrices as those in (7.1), and $\underline{Q}$ and $\overline{Q}$ denote the n-vectors of upper and lower quantity bounds whose elements are $\underline{q}_i$ and $\overline{q}_i$ $(\forall i \in N)$, respectively. The FTR award quantities for each pair of nodes (which must be subsequently allocated to all the bidders tied for each award) can be extracted from the optimal dispatch solution Q^* in the virtual optimal power flows by solving the equations:

$$\begin{aligned} & \sum_{k \neq i} q^*_{ki} - \sum_{j \neq i} q^*_{ij} = q^*_i, \ \forall \ i \in N \\ & 0 \leq q^*_{ij} \leq \overline{q}_{ij} \end{aligned} \tag{7.7}$$

The corresponding FTR auction prices are determined as the differences of the corresponding source and sink nodal prices in the virtual energy auction.

Remark Equations (7.7) always have a solution $\{q^*_{ij}, \forall \ i, j\}$ due to the number of variables being larger than the number of equations. Furthermore, $\{q^*_{ij}, \forall \ i, j\}$ is an optimal solution to the FTR auction problem (7.1).

Thus, an energy auction where energy bids and offers at all nodes equal the corresponding expected locational prices under all transmission contingencies and load scenarios is equivalent to an FTR auction where all FTR bids between two points are equal to their expected payoffs. Such an FTR auction where all market clearing bids for FTRs between any two nodes are identical to the respective expected payoffs of the FTRs over all transmission contingencies and load scenarios would represent a perfect price discovery in an auction market with risk-neutral bidders.

The above results can be summarized by the following statement:.

If market participants had perfect knowledge of the expected locational marginal prices for energy in an electricity grid and all bidderswere rational and risk-neutral price takers, then the FTR auction problem (7.1)would be equivalent to the virtual energy auction problem (7.6).

Since, according to the above, the FTR simultaneous feasibility auction can be represented by an equivalent virtual energy auction, in our subsequent analysis and numerical experiments, we represent the FTR auction as a virtual energy auction from which we can derive both the expected congestion rents and the FTR clearing prices. Under this scheme, the expected congestion rent between any two network locations is the expected difference of locational energy prices between the two points. Likewise, the FTR clearing price between any two points is the difference between the locational clearing prices for energy in the virtual energy auction. It follows that correct prediction of expected congestion rents between any two points is equivalent to correct prediction of the expected locational energy prices. Thus, an energy auction where energy bids and offers at all nodes equal the corresponding expected locational prices over all transmission contingencies and load scenarios is equivalent to an FTR auction where all FTR bids between two points are equal to their expected payoffs. The outcome of such an FTR auction where all market clearing bids for FTRs between any two nodes are identical to the respective expected payoffs of the FTRs over all transmission contingencies and load scenarios would represent a perfect price discovery when all bids exhibit rational risk-neutral price taking behaviors.

To identify the relationship between the bids/offers and the expected market clearing energy prices in the virtual energy auction, we show that the clearing prices in (7.6) depend on the upper and lower quantity bounds of energy bids. Let λ, (μ_r^+, μ_r^-), and (η^+, η^-) be the dual variables associated with the constraints in (7.6) where λ is a scalar associated with the energy balance constraint, (μ_r^+, μ_r^-) ($\forall r \in R$) are m-vectors associated with the transmission line capacity constraints and (η^+, η^-) are n-vectors associated with the bid quantity bound constraints. The dual problem of the linear programming (LP) problem (7.6) is as follows (see Luenberger (1984)).

$$\begin{aligned} \min_{\lambda,\mu_r^+,\mu_r^-,\eta^+,\eta^-} \quad & \sum_{r\in R}(\mu_r^+ + \mu_r^-)^T L + (\eta^+)^T \overline{Q} + (\eta^-)^T \underline{Q} \\ s.t. \quad & \lambda \cdot e^T + \sum_{r\in R}(\mu_r^+ - \mu_r^-)^T G_r + \eta^+ - \eta^- \geq C^T \\ & \mu_r^+, \mu_r^- \geq 0, \forall r \in R, \text{ and } \eta^+, \eta^- \geq 0. \end{aligned} \tag{7.8}$$

We can show that If none of the quantity bound constraints in (7.6) are binding, then the market clearing nodal prices resulting from the virtual energy auction are equal to the bid vector C.

However, if a bid quantity bound constraint at a bus i is binding, then the resulting market clearing nodal price P_i differs from the bid price c_i. Specifically, P_i is greater/less than c_i if bus i is a generation/load bus. This observation follows from the fact that the market clearing nodal price vector P of the FTR auction (7.6) is given by:

$$P \equiv \lambda \cdot e^T + \sum_{r \in R} (\mu_r^+ - \mu_r^-)^T G_r. \tag{7.9}$$

By the duality theory from linear programming (Luenberger (1984), the conclusions are drawn through inspecting the dual problem (7.8) and applying the strong duality result between the primal LP problem (7.6) and the dual problem (7.8).

When the nodal clearing price at a node in the virtual energy auction differs from the expected nodal price at that node under the various transmission contingencies and load scenarios, the resulting FTR clearing prices for FTRs involving that node also differ from their expected payoffs. In the following section we demonstrate this phenomenon by means of numerical examples.

7.2. Numerical Examples

We have argued above, on theoretical grounds that the FTR auction clearing prices deviate systematically from the ex ante FTR bids whenever the energy injection/ejection quantity bounds in (7.6), as implied by the FTR bid quantity bounds in (7.1), become binding. We now use two numerical examples to illustrate the impacts by the FTR quantity bounds on the deviation of the FTR market clearing prices. To compute the outcomes of an energy auction, the energy bid quantity bounds in (7.6) need to be specified.

For the ease of exposition, we assume that the bid quantity bound for each FTR type is given by a constant α times its expected transaction volume between the corresponding points. Consequently, the quantity of an energy bid at each node is bounded by the corresponding component of $\alpha \cdot \bar{Q}$ where $\bar{Q} \equiv (\bar{q}_1, \bar{q}_2, \cdots, \bar{q}_n)$ denote the expected quantities of energy transactions implied by the aggregate FTR transactions. Namely, $\overline{q_i} = \alpha \cdot \bar{q}_i$ and $\underline{q_i} = -\alpha \cdot \bar{q}_i$ ($\forall i \in N$) in (7.6). This characterization of the quantity bound enables simple sensitivity analysis by varying the multiplier α. Two test systems are considered in our simulation experiments. One is a 6-bus system and the other is the IEEE 24-bus Reliability Test System (RTS).

7.2.1 A 6-bus Example

First consider a 6-bus network example used by Chao and Peck (1998) and by Chao *et al* (2000) (see Fig. 1). Buses 1, 2 and 4 are generation nodes while bus 3, 5 and 6 are load nodes. The supply and demand functions at the 6 nodes are assumed to be linear in quantity q with parameters given in table 7-1.

Table 7-1 Bid Functions of Generation and Load

Bus-ID	Supply Bids	Bus-ID	Load Bids
Bus-1	$10 + 0.05 \cdot q$	Bus-3	$37 - 0.05 \cdot q$
Bus-2	$15 + 0.05 \cdot q$	Bus-5	$75 - 0.1 \cdot q$
Bus-4	$42 + 0.025 \cdot q$	Bus-6	$80 - 0.1 \cdot q$

The transmission line capacities (MW) and admittances (p.u.) are shown in figure. 7-1. Bus-6 is designated as the swing bus. We choose a set of 5 transmission reliability scenarios that are accounted for in the FTR auction: no line outage, line-13 out, line-45 out, line-16 out, and line-25 out.

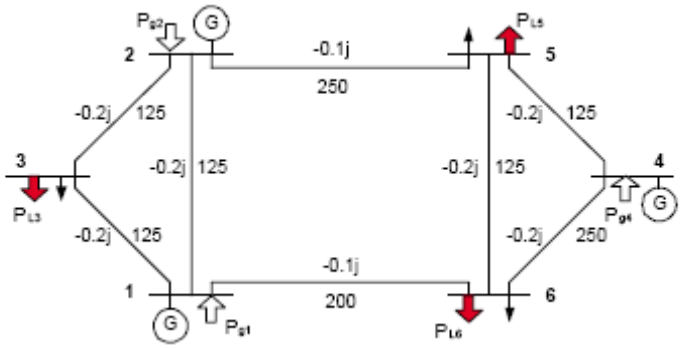

Figure 7-1 A 6-Bus Test System

7.2.1 Case 1: transmission line contingency but no load variation

We use the same supply and demand bid functions as in Chao *et. al.* (2000). The *ex post* nodal prices in each of the 5 contingencies are given in Table 7.2 (The quantity inside the parenthesis in the first column indicates the line on outage). The assumed probabilities of the contingencies are [0.6 0.1 0.1 0.1 0.1]. The expected nodal prices ($E[P]$) are given in the last row of table 7-2.

Table 7-2 *Ex Post* Nodal Prices and Expected Nodal Prices

Scenario	bus-1	bus-2	bus-3	bus-4	bus-5	bus-6
Normal	26.5	26.5	26.5	48.5	48.5	48.5
(L-13)	24.13	24.13	31.25	48.5	48.5	48.5
(L-16)	20.63	25	29.38	50	50	50
(L-25)	24.17	22.27	26.042	47.98	59.41	53.69
(L-45)	26.11	26.48	26.92	48.49	48.56	48.49
$E[P]$	25.40	25.69	27.26	48.60	49.75	49.17

Suppose the FTR market participants submit FTR bids that are equal to the expected payoffs over all contingencies. These bids are the differences in the expected nodal prices given in table 7-2. Then the corresponding nodal price bids c_i's in the equivalent virtual energy auction can be set to the expected nodal prices given at the bottom of table 7-2. The FTR bid quantity bounds are given by $-\alpha \cdot \bar{Q}$ and $\alpha \cdot \bar{Q}$ where the expected dispatch quantities $\bar{Q}$ obtained over all five reliability contingencies at all nodes are:

$\bar{Q}$ = (308.053, 213.733, 204.837, 243.855, 252.535, 308.320) MW.

From this data we compute the resulting market clearing nodal prices P_i's to examine whether $c_i = P_i$, $\forall i = 1, 2, \cdots, 6$. We vary the bounds for FTR quantity bids by varying the value of α. When $\alpha = 1$, none of the FTR bid quantity bounds is binding and the resulting P_i's, as reported in the second column of table 7-3, are the same as the c_i's (last column of table 7-3). When $\alpha = 0.7$ or $\alpha = 0.5$, some of the FTR bid quantity bounds reach the upper bounds thus resulting in market clearing prices P_i's (see table 7.3) that are different from the bid prices c_i's. In particular, Gen-1, Gen-4 and Load-5 reach their respective upper bounds when $\alpha = 0.7$ while Gen-1, Gen-2, Load-5 and Load-6 reach the upper bounds when $\alpha = 0.5$. The market clearing nodal energy prices for different α's are shown in table 7-3.

Table 7-3 FTR Auction Market Clearing Nodal Prices

	$\alpha = 1$	$\alpha = 0.7$	$\alpha = 0.5$	FTR Bids
bus-1	25.40	25.69	27.26	25.40
bus-2	25.69	25.69	27.26	25.69
bus-3	27.26	27.26	27.26	27.26
bus-4	48.60	49.17	48.60	48.60
bus-5	49.75	49.17	48.60	49.75
bus-6	49.17	49.17	48.60	49.17

Table 7-4 shows the sensitivity of FTR auction market clearing prices to bid quantities under the assumption that bid quantities are constant multiples of the average transaction volume between any two points. It provides a comparison of the FTR values for three different values of the multiplier α. The last column reports the *ex ante* FTR price bids.

Table 7-4 FTR Price Comparison under Transmission Contingencies Only

FTR \ α	$\alpha = 1$	$\alpha = 0.7$	$\alpha = 0.5$	FTR bids (ex ante)
FTR-12	0.28	0	0	0.28
FTR-13	1.86	1.57	0	1.86
FTR-14	23.19	23.48	21.34	23.19
FTR-15	24.34	23.48	21.34	24.34
FTR-16	23.77	23.48	21.34	23.77
FTR-23	1.57	1.57	0	1.57
FTR-24	22.91	23.48	21.34	22.91
FTR-25	24.06	23.48	21.34	24.06
FTR-26	23.48	23.48	21.34	23.48
FTR-34	21.34	21.91	21.34	21.34
FTR-35	22.49	21.91	21.34	22.49
FTR-36	21.91	21.91	21.34	21.91
FTR-45	1.15	0	0	1.15
FTR-46	0.57	0	0	0.57
FTR-56	-0.58	0	0	-0.58

7.2.1 Case 2: both transmission line and load contingencies

We then assume that under each transmission contingency there are three equally likely scenarios for loads: no change in loads, 25% more loads, and 25% less loads. Table 7-5 lists the load curves in all three scenarios at nodes 3, 5 and 6.

Table 7-5 Load Contingencies

	Node 3	Node 5	Node 6
no-load change	37.5-0.05q	75-0.1q	80-0.1q
load +25%	46.875-0.05q	93.75-0.1q	100-0.1q
load −25%	28.125-0.05q	56.25-0.1q	60-0.1q

The assumed joint probability distribution of the load and transmission line contingencies is given in Table 7-6.

Table 7-6 Joint Probability Distribution of Transmission and Load Contingencies

	Normal	(L-13)	(L-16)	(L-25)	(L-45)
Base Load	0.2	0.04	0.04	0.04	0.04
load +25%	0.2	0.03	0.03	0.03	0.03
load −25%	0.2	0.03	0.03	0.03	0.03

The computational results on market clearing nodal energy prices, energy quantities, and auction-clearing FTR prices are given in Tables 7-7 and 7-8. Specifically, Table 7-7 shows the nodal clearing prices and the dispatch quantities in the virtual energy auction as functions of the multiplier α, which is the ratio of the energy bid quantity bound to the expected dispatch quantity at each node. The first row in Table 7-7 contains the expected nodal energy prices and the expected dispatch quantities at the 6 buses over the 15 combined load and transmission line contingencies. We then assume that the FTR auction is conducted based on the price bids being set by the expected nodal energy prices (upper numbers in the first row) and the quantities of bids being bounded by α times the expected dispatch quantities (lower numbers in the first row), which corresponds to an FTR auction under the assumption of perfect price discovery. The rest of Table 7-7 contains the resulting nodal prices and the dispatch quantities at the 6 buses for α being 1.5, 1.0, 0.7, and 0.5.

Table 7-7 FTR Auction Bids and Market Clearing Prices and Quantities under Load and Transmission Contingencies

	bus-1	bus-2	bus-3	bus-4	bus-5	bus-6
P ($)	24.3	25.5	28.5	47.1	53.9	50.8
Q(MW) FTR	286.4	210.6	180.0	185.4	210.8	291.6
P ($)	24.3	25.5	28.5	47.1	53.9	50.8
Q(MW) α :1.5	250.0	75.0	125.0	241.7	133.3	308.3
P ($)	24.3	25.5	28.5	47.8	53.9	50.8
Q(MW) α :1.0	250.0	75.0	125.0	185.4	189.6	195.8
P ($)	25.5	25.5	28.5	50.8	50.8	50.8
Q(MW) α : 0.75	200.5	124.5	125.0	129.8	147.5	182.3
P ($)	28.5	28.5	28.5	47.1	47.1	47.1
Q(MW) α : 0.5	143.2	105.3	48.5	51.2	105.4	145.8

Comparisons of the FTR values in the 4 cases of different α's are shown in table 7-8.

Table 7-8 FTR Price Comparison under Both Load and Transmission Contingencies

α	1.5	1	0.7	0.5	*FTR Bids* (*exante*)
FTR-12	1.21	1.21	0	0	1.21
FTR-13	4.18	4.18	2.97	0	4.18
FTR-14	22.82	23.43	25.31	18.64	22.82
FTR-15	29.60	29.60	25.31	18.64	29.60
FTR-16	26.52	26.52	25.31	18.64	26.52
FTR-23	2.97	2.97	2.97	0	2.97
FTR-24	21.60	22.22	25.31	18.64	21.60
FTR-25	28.39	28.39	25.31	18.64	28.39
FTR-26	25.30	25.30	25.31	18.64	25.30
FTR-34	18.64	19.25	22.34	18.64	18.64
FTR-35	25.42	25.42	22.34	18.64	25.42
FTR-36	22.34	22.34	22.34	18.64	22.34
FTR-45	6.79	6.17	0	0	6.79
FTR-46	3.70	3.09	0	0	3.70
FTR-56	-3.09	-3.09	0	0	-3.09

7.2.2 An IEEE 24-bus RTS Example

Next, we consider the IEEE 24-bus RTS with system topology shown in figure 7-2. Generators are located at buses 1, 4, 7, 11, 13, 15, 17, 21, 22 and 23. The rest of the buses are loads. Generation and load are represented by linear supply and demand functions, respectively.

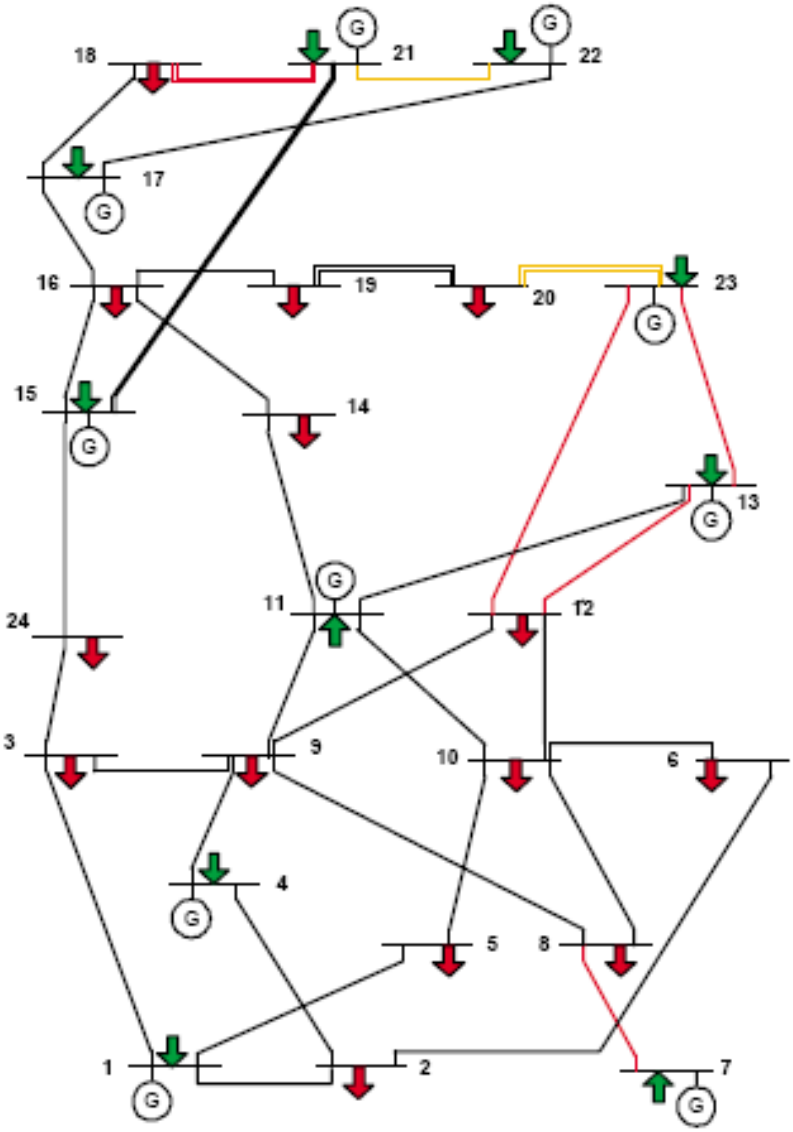

Figure 7-2 IEEE 24-Bus Reliability Test System

In the base case (or, the no-contingency case), the supply and demand bid functions are given in table 7-9.

Table 7-9 IEEE 24-bus RTS: Generation and Load Bid Functions

Bus-ID	Supply Bids	Bus-ID	Demand Bids
1	$15.483+0.0150q$	2	$65.000-0.0820q$
4	$20.000+0.0161q$	3	$75.517-0.1129q$
7	$12.555+0.0352q$	5	$63.000-0.0925q$
11	$29.000+0.0362q$	6	$42.289-0.0847q$
13	$39.859+0.1012q$	8	$62.517-0.1016q$
15	$29.678+0.0220q$	9	$50.517-0.0876q$
17	$23.180+0.0295q$	10	$59.517-0.0502q$
21	$30.031+0.0270q$	12	$45.289-0.0733q$
22	$20.966+0.0268q$	14	$64.517-0.0851q$
23	$35.330+0.0552q$	16	$58.289-0.1146q$
		18	$76.547-0.0792q$
		19	$72.517-0.0682q$
		20	$63.289-0.1033q$
		24	$72.289-0.0733q$

7.2.2 Case 1: transmission line contingency but no load variation

Following the same procedure as the one outlined in the 6-bus example, we first consider the transmission line outages over links connecting buses 10 and 11, 14 and 16, 15 and 21, as well as 19 and 20 in computing FTR price bids. The outage probability of each of the 4 lines is 0.1. We then compute the market clearing prices of FTRs with different multiple α. Table 7-10 provides a comparison of the FTR values for 4 different α values. The last column reports the *ex ante* FTR price bids. We observe that there are notable differences between the market clearing FTR prices and the FTR bids over buses 6, 9, 12 and 23 even when the multiple α is 8. The auction clearing FTR prices converge to the bids (which reflect correct expected settlement values) when α reaches a large value of 30.

Table 7-10 IEEE 24-bus with Line Contingency Only: FTR Auction Market Clearing Nodal Prices

Bus	$\alpha = 1$	$\alpha = 3$	$\alpha = 8$	$\alpha = 30$	FTR Bids
1	29.9	21.5	21.5	21.5	21.5
2	40.8	40.8	40.8	40.8	40.8
3	39.2	43.8	43.8	43.8	43.8
4	25.2	25.2	25.2	25.2	25.2
5	40.1	40.1	40.1	40.1	40.1
6	40.4	40.6	40.7	41.3	41.3
7	18.7	18.7	18.7	18.7	18.7
8	40.2	40.6	42.4	42.4	42.4
9	41.4	42.2	41.8	43.3	43.3
10	40.5	41.4	41.4	41.4	41.4
11	41.6	41.6	41.6	41.6	41.6
12	40.5	41.1	41.0	41.6	41.6
13	41.4	41.4	41.4	41.4	41.4
14	39.1	40.1	40.9	40.9	40.9
15	40.2	39.7	39.7	39.7	39.7
16	40.0	39.9	40.0	40.0	40.0
17	40.2	40.1	40.1	40.1	40.1
18	40.1	40.1	40.1	40.1	40.1
19	40.1	40.1	40.1	40.1	40.1
20	40.1	40.3	40.3	40.3	40.3
21	40.3	40.3	40.1	40.1	40.1
22	40.2	40.1	40.1	40.1	40.1
23	40.5	40.7	40.7	40.5	40.5
24	39.8	46.9	46.9	46.9	46.9

7.2.2 Case 2: both transmission line and load contingencies

As we incorporate load variation besides the line contingency in computing the *ex ante* FTR bids and then compute the FTR market clearing prices, we still find that the multiple α needs to be increased to 30 in order to achieve the convergence between the FTR auction clearing prices and the corresponding expected settlement values reflected by the bids (see table 7-11). Again, table 7-11 contains the market clearing FTR prices for 4 different α values and the FTR bids (the last column). A joint probability distribution (similar to the one defined by table 7-6 in the 6-bus example) on load variation (25% up or down) and line outages is assumed in computing the prices in table 7-11.

Table 7-11 IEEE 24-bus with Line Contingency and Load Variation: FTR Auction Market Clearing Nodal Prices

Bus	$\alpha = 1$	$\alpha = 3$	$\alpha = 8$	$\alpha = 30$	FTR Bids
1	21.6	21.6	21.6	21.6	21.6
2	42.7	41.4	42.7	42.7	42.7
3	38.3	45.8	45.8	45.8	45.8
4	24.9	24.9	24.9	24.9	24.9
5	34.0	41.8	41.8	41.8	41.8
6	40.7	40.9	41.2	41.2	41.4
7	18.7	18.7	18.7	18.7	18.7
8	40.1	40.7	42.7	42.7	42.7
9	41.5	42.5	40.9	43.5	43.5
10	39.7	42.0	42.0	42.0	42.0
11	41.7	41.7	41.7	41.7	41.7
12	40.3	40.2	40.8	41.6	41.6
13	43.2	43.2	43.2	43.2	43.2
14	37.1	41.1	41.1	41.1	41.1
15	40.1	39.4	39.4	39.4	39.4
16	39.8	40.0	40.0	40.0	40.0
17	39.8	38.8	38.8	38.8	38.8
18	39.3	39.3	39.3	39.3	39.3
19	40.0	40.0	40.0	40.0	40.0
20	39.9	39.9	39.9	39.9	39.9
21	40.6	40.8	39.5	39.5	39.5
22	40.3	39.1	39.1	39.1	39.1
23	40.6	40.6	40.6	40.6	40.6
24	39.4	49.5	49.5	49.5	49.5

7.3. Summary and Conclusions

We demonstrated in this chapter that FTR auctions enforcing the simultaneous feasibility constraints have inherent properties that result in a fundamental inefficiency in the FTR market. Specifically, the auction clearing prices do not converge to the expected payoffs of the auctioned instruments. Our analysis indicates that such divergence, which has been proved theoretically and demonstrated empirically, cannot be attributed just to lags in price discovery. It is indeed a convoluted effect of the current FTR auction clearing mechanism design and the bounded FTR bid quantities at all the network nodes. We show that even when bidders are risk neutral and have perfect foresight of expected payoffs (which they bid) the FTR auction would produce clearing prices that differ from the expected FTR payoffs. Based on our analysis, it is evident that the clearing prices depend on the natural quantity bounds of submitted FTR bids. When the FTRs serve primarily as hedging instruments, bid quantities for FTRs tend to track expected transaction volumes and FTR bids are spread over large number of node pairs. Such spread, however, has the effect of imposing quantity limits on certain FTR awards causing the clearing prices to deviate from the initial bid prices. In a more speculative market where FTR bid quantities exceed hedging needs, larger quantities of fewer FTR types would be awarded and

auction clearing prices are likely to better match their expected *ex ante* valuations. We conclude that price discovery alone does not remedy the discrepancy between the auction prices and the realized values of the FTRs. Such convergence is essential if the FTRs are to fulfill the need for efficient risk management and provision of correct price signal for transmission usage and investment. More liquidity in the FTR market through frequent reconfiguration auctions and the introduction of flowgate rights that can be traded in secondary markets are ways through which better convergence between forward prices and spot realization of the congestion rents can be achieved. Characteristics of a liquid secondary market for FTRs include the presence of a set of standardized trading quantities for FTRs and finer granularity in trading time intervals such as hours and days. To facilitate the computational analysis on the sensitivity of the price divergence with respect to the FTR bid quantity bounds, it is assumed that the bid quantities are fixed multiples of expected transaction volume. In reality the ratio of bid quantity to average transaction volume can vary across FTRs. Our theoretical analysis ensures that the qualitative conclusion is valid as long as the bid quantities are a relatively low multiple of the expected volume which is the case when FTRs are allocated or auctioned off as hedging instruments.

Finally, the above conclusions also suggest that from a property rights perspective it might be more appropriate to allocate the FTRs themselves based on historical entitlements leaving it to the recipients to re-trade these rights as opposed to auctioning the FTRs and allocating the auction revenues.

References

Project Publications

[1] Enzo Sauma and Shmuel Oren, “Proactive planning and valuation of transmission investments in restructured electricity markets”, Journal of Regulatory Economics, (2006) 30:358-387.

[2] Enzo Sauma and Shmuel Oren “Do generation firms in restructured electricity markets have incentives to support socially efficient transmission investments”, In review by Energy Economics, January, 2008.

[3] Mount, T. and Thomas, R. "Testing the Effects of Power Transfers on Market Performance and the Implications for Transmission Planning," Proceedings of the IEEE PES Conference, June 2006.

[4] Mount, T. and J. Ju, “Cost of Transmission Bottlenecks in New York”, Proceedings of the IEEE HICSS 40 Conference, Jan. 2006.

[5] Michaillat Pascal and Shmuel Oren, “A Probabilistic Graphical Approach to Computing Electricity Price Duration Curves under Price and Quantity Competition”, Proceeding of the 39th Hawaii International Conference on Systems Sciences HICSS40, Big Island, Hawaii, January 3-6, 2007.

[6] Shmuel Oren, “Transmission performance incentives trough active TO participation in FTR markets”, presented at the EUCI Conference on National Perspectives on Financial Transmission Rights, Arlington VA, March 20, 2007.

[7] S.J. Deng, J. Chen, and X. Huo (2007). “Electricity Price Curve Modeling by Manifold Learning,” submitted to IEEE Transactions on Power Systems, 2006

[8] Deng Shijie, Shmuel S. Oren and Sakis Meliopoulous, “The Inherent Inefficiency of the Point-to-Point Congestion Revenue Right Auction”, Proceeding of the 37th Hawaii International Conference on Systems Sciences HICSS 37. Big Island, Hawaii, January 5-8, 2004.

[9] Siddiqui, Afzal S., Emily S. Bartholomew Chris Marnay and Shmuel S. Oren, “On the Efficiency of the New York Independent System Operator Market for Transmission Congestion Contracts”, Journal of Managerial finance, Vol 31, No. 1, (2005) pp. 1-45.

References

[1] “ABB, New Concepts for the Transmission Grid”, DOE Workshop on Analysis and Concepts to Address Electric Infrastructure Needs, 2001

[2] Adamson, S. and S. Englander (2005). ``Effiency of the Transmission Congestion Contract Auction." *Procedings of the Hawaii Interanational Conference on System Science (HICSS38)*, Big Island, Hawaii.

[3] Seabron Adamson,Thomas Noe and Geoffrey Parker, “Efficiency of Financial Transmission Rights Markets in Centrally-Coordinated Periodic Auctions, Presented at UKERC workshop on Financial Methods in Electricity Markets, Oxford UK, July 9-10, 2008

[4] Alomoush, M. and Shahidehpour, S., “Fixed transmission rights for zonal congestion management”, IEE Proceedings of Generation, Transmission, and Distribution, Vol. 146, pp. 471- 476, September 1999.

[5] Alonso, J., Trias, A., Gaitán, V., and Alba, J. (1999), Thermal plant bids and market clearing in an electricity pool: minimization of costs vs. minimization of consumer payments, IEEE Trans. Power Syst., 14(4): 1327-1334.

[6] Alvarado, F., “Converting system limits to market signals”, IEEE Trans. Power Syst., vol. 18, no. 2, pp. 422-427, May. 2003

[7] Arroyo, J. and Conejo, A. (2000), Optimal response of a thermal unit to an electricity spot market, IEEE Trans., Power Syst., 15(3): 1098-1104.

[8] Audet, N., Heiskanen, P., Keppo, J., and Vehvilainen, I., Modelling Prices in Competitive Electricity Markets. London: John Wiley & Sons, 2004, ch. Modeling Electricity Forward Curve Dynamics in the Nordic Market.

[9] Belkin, M., and Niyogi, P., “Laplacian eigenmaps for dimensionality reduction and data representation,” Neural Computation, vol. 15, no. 6, pp. 1373–1396, June 2003.

[10] Bessembinder, H. and Lemmon, M. (2002), Equilibrium pricing and optimal hedging in electricity forward markets, The Journal of Finance, LVII(3): 1347-1382.

[11] Billinton, R. and Li, W., “Reliability assessment of electric power systems using Monte Carlo methods”. New York: Plenum, 1994.

[12] Bloyd, C., Bharvirkar, R., and Burtraw, D., “Investment in Electricity Transmission and Ancillary Environmental Benefits”, March 2002

[13] Bobo, D., Mauzy, D., and Trefny, F., “Economic generation dispatch with responsive spinning reserve constraints”, IEEE Trans. Power Syst., vol. 9, no. 1, pp. 555-559, Feb. 1994

[14] Bohn, R., Caramanis, M., and Schweppe, F., “Optimal pricing in electrical networks over space and time”, Rand J. Economics, vol. 15, pp. 360-376, 1984.

[15] Borestein, S., Busnhell, J., Kanh, E., and Stoft, S., “Market power in California electricity markets”. Utilities Policy, 5:219–236, 1995

[16] Borenstein, S., Busses, M., and Kellogg, R. (2006), Security of Supply and forward price premia: evidence from natural gas pipeline rates, working paper, University of California.

[17] Borg, I., and Groenen, P., Modern Multidimensional Scaling: Theory and Applications. New York: Springer-Verlag, 1997

[18] Bushnell, J. (1997). ``Transmission Rights and Market Power." The Electricity Journal, 12(8): 77-85.

[19] Bushnell, J. and S.E. Stoft (1997). ``Improving Private Incentives for Electric Grid Investment." Resource and Energy Economics, 19:85-108.

[20] Chao, Hung-po and Stephen Peck (1996). ``A Market Mechanism for Electric Power Transmission." Journal of Regulatory Economics 10(1): 25-60.

[21] Chao, Hung-po and Stephen Peck (1997). ``An Institutional Design for an Electricity Contract Market with Central Dispatch." The Energy Journal 18(1): 85-110.

[22] Chao, H., Peck, S., Oren, S., and Wilson, R. (2000). ``Flow-based transmission rights and congestion management." Electricity Journal, 38-58, Oct. 2000.

[23] Chao, Hung-po and Stephen Peck (1998). ``Reliability Management in Competitive Electricity Markets." Journal of Regulatory Economics 14: 189-200.

[24] Conejo, A., Plazas, M., Espínola, R., and Molina, A. (2005), Day-ahead electricity price forecasting using the wavelet transform and ARIMA models, IEEE Trans., Power Syst., 20(2), 1035-1042.

[25] Chen, J., Thorp, J., Thomas, R., and Mount, T., "Locational Pricing and Scheduling for an Integrated Energy-Reserve Market", Proceedings of the 36th Hawaii International Conference on System Sciences (HICSS'03)

[26] Chao, H., Peck, S., Oren, S., and Wilson, R., "Flow-based transmission rights and congestion management", The Electricity Journal, pp. 38-58, October 2000.

[27] Dahlgren, R., Liu, C., and Lawarree, J., "Risk assessment in energy trading". IEEE Trans. Power Syst., vol. 18, no. 2, pp. 503-511, May. 2003

[28] Davison, M., Anderson, L., Marcus, B., and Anderson, K., "Development of a hybrid model for electricity spot prices," IEEE Transactions on Power Systems, vol. 17, no. 2, pp. 257–264, 2002.

[29] Deng, S., "Pricing Electricity Derivatives under Alternative Stochastic Spot Price Models", Proceedings of the Thirty-Third Hawaii International Conference on System Sciences, Hawaii, January, 2000.

[30] Deng, S. J., "Stochastic models of energy commodity prices and their applications: Mean-reversion with jumps and spikes," UCEI POWER Working Paper P-073, 2000.

[31] Deng, S., and Oren, S., "Priority Network Access Pricing for Electric Power", Journal of Regulatory Economics, 19(3) July 2001: 239-270.

[32] Deng, S., and Oren, S., "Valuation of Electricity Generation Assets with Operational Characteristics", Working Paper, Georgia Institute of Technology.

[33] Deng, S., Johnson, B., and Sogomonian, A., "Exotic Electricity Options and the Valuation of Electricity Generation and Transmission Assets", Decision Support Systems, (30)3, pp.383-392, 2001.

[34] Denton, M., Palmer, A., Masiello, R., and Skantze, P., "Managing market risk in energy", IEEE Trans. Power Syst, vol. 18, no. 2, pp. 494-502, May. 2003

[35] Donoho, D. L., and Grimes, C., "Hessian eigenmaps: new locally linear embedding techniques for high-dimensional data," Proceedings of the National Academy of Sciences, vol. 100, pp. 5591–5596, 2003.

[36] Endrenyi, J., "Reliability Modeling in Power Systems", John Wiley & Sons, 1978.

[37] Eydeland, A., and Geman, H. (1998), Pricing power derivatives, Risk, October, 71–74.

[38] Gedra, T., and Varaiya, P., “Markets and pricing for interruptible electric power”, Power Systems, IEEE Transactions on, Volume 8, Issue 1, Feb. 1993 Page(s):122 – 128.

[39] Hastie, T., Tibshirani, R., and Friedman, J., The elements of statistical learning. Springer, 2001.

[40] Hirst, E., U.S. “Transmission Capacity: Present Status and Future Prospects”, June, 2004.

[41] Hogan, William (1992). ``Contract Networks for Electric Power Transmission." Journal of Regulatory Economics 4(3): 211-242.

[42] Hogan, W. (1997), A market power model with strategic interaction in electricity networks, The Energy Journal, 18(4): 107–141.

[43] Hull, J., “Options, Futures, & Other Derivatives”, Prentice Hall, 2002.

[44] Huo, X., Ni, X., and Smith, A. K., Mining of Enterprise Data. Springer, 2005, new york Ch. A survey of manifold-based learning methods, invited book chapter, to appear, also available at http://www2.isye.gatech.edu/statistics/papers/06-10.pdf.

[45] Huo, X., and Chen, J., “Local linear projection (LLP),” in First IEEE Workshop on Genomic Signal Processing and Statistics (GENSIPS), Raleigh, NC, October 2002, http://www.gensips.gatech.edu/proceedings/.

[46] Huo, X. , “A geodesic distance and local smoothing based clustering algorithm to utilize embedded geometric structures in high dimensional noisy data,” in SIAM International Conference on Data Mining, Workshop on Clustering High Dimensional Data and its Applications, San Francisco, CA, May 2003.

[47] Jiang W. (2000), Some simulation-based models towards mathematical finance, Ph.D Dissertation, University of Aarhus.

[48] Johnson, B. and Barz, G., Energy Modelling and the Management of Uncertainty. Risk Books, 1999, ch. Selecting Stochastic Processes for Modeling Electricity Prices, London.

[49] Joskow, P. and Tirole, J., “Merchant Transmission Investment”, 2004

[50] Kamat, R. and Oren, S., “Exotic options for interruptible electricity supply contracts”, PSERC Working Paper, University of California, Berkeley, 1999.

[51] Kang, S. and Meliopoulos, A., “Analytical approach for the evaluation of Actual Transfer Capability in a deregulated environment”, Proceedings of 32st Annual North American Power Symposium, October 1999.

[52] Kang, S., “A New Approach for Power Transaction Evaluation and Transfer Capability Analysis”. PhD Thesis, Georgia Institute of Technology,2001

[53] Kruskal, J. B., “Multidimensal scaling by optimizing goodness of fit to a nonmetric hypothesis,” Psychometrika, vol. 29, pp. 1–27, 1964.

[54] Leite da Silva, A., Lima, M., and Anders, G., “Available transmission capability-sell firm or interruptible, Power Systems”, IEEE Transactions on, Volume 14, Issue 4, Nov. 1999 Page(s):1299 – 1305

[55] Levina, E., and Bickel, P. J., “Maximum likelihood estimation of intrinsic dimension,” in Advances in Neural Information Processing Systems 17 (NIPS2004). MIT Press, 2005.

[56] Li, Z. and Shahidehpour, M. (2005), Security-constrained unit commitment for simultaneous clearing of energy and ancillary services markets, IEEE Trans., Power Syst., 20(2): 1079-1088.

[57] Longstaff, F., and Wang, A (2004), Electricity forward prices: a high-frequency empirical analysis, The Journal of Finance, LIX(4): 1877-1900.

[58] Lora, A. T., Santos, J. M. R., Exp´osito, A. G., Ramos, J. L. M., and Santos, J. C. R., “Electricity market price forecasting based on weighted nearest neighbors techniques,” Working Paper, University of Sevilla, Spain, 2006.

[59] Lucia, J. J. and Schwartz, E. S., “Electricity prices and power derivatives: Evidence from the Nordic power exchange,” Review of Derivatives Research, vol. 5, no. 1, pp. 5–50, 2002.

[60] Luenberger, D.G. (1984). Linear and Nonlinear Programming, 2nd Edition, Addison-Wesley, Reading, MA.

[61] McCalley, J., Dorsey, J., Qu, Z., Luini, J., and Filippi, J., “A new methodology for determining transmission capacity margin in electric power systems”, IEEE Trans. Power Syst., vol. 6, no. 3, pp. 944-951, Aug. 1991.

[62] Meliopoulos, A., “Power System Modeling, Analysis, and Control, Class Notes for ECE 6320”, Georgia Institute of Technology (to be published by Marcel Dekker), 2001.

[63] Meliopoulos, A., Kovacs, R., Reppen, N., Contaxis, G., and Balu, N. “Power System Remedial Action Methodology”, IEEE Transactions on Power Systems, vol. 3, no. 2, pp. 500-509, May. 1988.

[64] Meliopoulos, A., Cheng, C., and Xia, F., “Performance Evaluation of Static Security Analysis Methods”, IEEE Transactions on Power Systems, vol. 9, no. 3, Aug. 1994.

[65] Meliopoulos, A., Cokkinides, G., and Chao, X., “A new probabilistic power flow analysis method”. IEEE Trans. Power Syst, vol. 5, no. 1, pp. 182-190, Feb. 1990.

[66] Mount, T. and Ethier, R., “Estimating the Volatility of Spot Prices in Restructured Electricity Markets and the Implications for Option Values”, PSERC Working Paper, Cornell University, 1998.

[67] Nadler, B., Lafon, S., Coifman, R. R., and Kevrekidis, I. G., “Diffusion maps, spectral clustering and reaction coordinates of dynamical systems,” Applied and Computational Harmonic Analysis: Special issue on Diffusion Maps and Wavelets, vol. 21, pp. 113–127, July 2006.

[68] Ong, J. (1996), New paradigms for electric power, Derivatives Strategy, Dec./Jan. 1996.

[69] Oren, S. and Spiller, P., “Wild prices out west: What can be done?”, Public Utilities Fortnightly, November 2000.

[70] Otero-Novas, I., Meseguer, C., Battle, C., and Alba, J. (2000), A simulation model for a competitive generation market, IEEE Trans. Power Syst., 15(1): 250–256.

[71] Plazas, M., Conejo, A., and Prieto, F. (2005), Multimarket optimal bidding for a power producer, IEEE Trans. Power Syst., 20(4): 2041-2050.

[72] Rotger, J. and Felder, F., “Promoting Efficient Transmission Investment: The Role of the Market in Expanding Transmission Infrastructure”, November, 2001.

[73] Routledge, B., Seppi D., and Spatt, C. (2000), Equilibrium forward curves for commodities, Journal of Finance, 55, 1297–1338.

[74] Routledge, B., Seppi D., and Spatt, C. (2001), The “spark spread:” an equilibrium model of cross-commodity price relationships in electricity, Working paper, Carnegie Mellon University.

[75] Ruff, L., Flowgates, “Contingency-Constrained Dispatch and FTRs”, October, 2000

[76] Saul, L. K., and Roweis, S. T., “Think globally, fit locally: unsupervised learning of low dimensional manifolds,” Journal of Machine Learning Research, vol. 4, pp. 119–155, 2003.

[77] Saul, L. K., and Roweis, S. T., “Nonlinear dimensionality reduction by locally linear embedding,” Science, vol. 290, pp. 2323–2326, 2000.

[78] Schweppe, F., Tabors, R., Kirtley, J., Outhred, Jr.H., Pickel, F., and Cox, A. (1980), Homeo-static utility Control, IEEE Trans. Power Syst., PAS-99(3): 1151-1163.

[79] Siddiqi, S. and Baughman, M., “Reliability differentiated real-time pricing of electricity”, IEEE Trans. Power Syst., vol. 8, no. 2, pp. 548-554, May. 1993.

[80] Siddiqui, A.S., E.S. Bartholomew, C. Marnay, and S.S. Oren (2003). ``The New York Transmission Congestion Contract Market: Is It Truly Working Efficiently." Electricity Journal, vol.16(9):1-11.

[81] Sun, H., “Integrated Modeling of Electric Power System Operations and Electricity Market Risks with Applications”, Ph. D. thesis, Georgia Institute of Technology, Dec. 2006.

[82] Sun, H., Deng, S., and Meliopoulos, A. (2005), Impact of market uncertainty on congestion revenue right valuation, Journal of Energy Engineering, 131(2): 139-156.

[83] Sun, Haibin, Shi-Jie Deng, A.P. Sakis Meliopoulos, George Cokkinides, George Stefopoulos, and Timothy D. Mount. ``A Probabilistic Analysis of Transmission Right Valuation under Market Uncertainty." Working Paper, Georgia Institute of Technology.

[84] Tarjei Kristiansen, “Allocation of long-term financial transmission rights for transmission expansion”, European Journal of Operational Research, vol. 184(3), pp. 1122-1139, 2008.

[85] Tenenbaum, J. B., Silva, V. de, and Langford, J. C., “A global geometric framework for nonlinear dimensionality reduction,” Science, vol. 290, pp. 2319–2323, 2000.

[86] Tim Mount and Jaeuk Ju, “Auctions for Transmission Congestion Contracts: a Market or a Money Machine?”, 26th Annual Eastern Conference: Advanced Workshop in Regulation and Competition, May 16-18, 2007.

[87] Verveer, P., and Duin, R., “An evaluation of intrinsic dimensionality estimators,” IEEE Transactions on Pattern Analysis and Machine Intelligence, vol. 17, no. 1, pp. 81–86, 1995.

[88] Zhang, J. and Anderson, M., “A Comprehensive Dynamic Pricing Method for the Use-of-Transmission-System Charges in the Context of Power Systems Deregulation”, Presentation at the University of Missouri-Rolla and the Frontiers of Power Conference, 1999

[89] Zhang, Z., and Zha, H., “Principal manifolds and nonlinear dimension reduction via tangent space alignment,” SIAM Journal of Scientific Computing, vol. 26, no. 1, pp. 313–338, 2004.

Appendix A: Procedures of Sensitivity Coefficient Calculation

According to equation (7.11), we have

$$a_{k,n}^{h,s} = \frac{d}{d(s_n)} h_k = \frac{\partial h_k}{\partial s_n} + \hat{\mathbf{x}}_{\mathbf{Q}}{}^{T} \boldsymbol{\Phi}(\mathbf{x}_{\mathbf{Q}}) \tag{A.1}$$

Assuming flowgate k is a transmission line $m-n$, we have

$$h_k = \sqrt{(P_{mn})^2 + (Q_{mn})^2} \tag{A.2}$$

where: $P_{mn} = G_{mn}\left(V_{mr}^2 + V_{mi}^2 - V_{mr}V_{nr} - V_{mi}V_{ni}\right) + B_{mn}\left(V_{mr}V_{ni} - V_{mi}V_{nr}\right) + G_{smn}\left(V_{mr}^2 + V_{mi}^2\right)$

$$Q_{mn} = G_{mn}\left(V_{mr}V_{ni} - V_{mi}V_{nr}\right) + B_{mn}\left(V_{mr}V_{nr} + V_{mi}V_{mi} - V_{mr}^2 - V_{mi}^2\right) - B_{smn}\left(V_{mr}^2 + V_{mi}^2\right)$$

$$V_{mr} = v_m \cos(\theta_m),\ V_{mi} = v_m \sin(\theta_m)$$

Since h_k is not an explicit function of s_n, we have $\frac{\partial h_k}{\partial s_n} = 0$.

Therefore, equation (A-1) becomes

$$\frac{d}{d(s_n)} h_k = \frac{\partial h_k}{\partial \mathbf{x}_{\mathbf{Q}}} \cdot \left(\frac{\partial \mathbf{g}_{\mathbf{Q}}(\mathbf{x}_{\mathbf{Q}}, \mathbf{u})}{\partial \mathbf{x}_{\mathbf{Q}}} \right)^{-1} \boldsymbol{\Phi}(\mathbf{x}_{\mathbf{Q}}) \tag{A.3}$$

$$= \frac{1}{h_k} \left(P_{mn} \frac{\partial P_{mn}}{\partial \mathbf{x}_{\mathbf{Q}}} + Q_{mn} \frac{\partial Q_{mn}}{\partial \mathbf{x}_{\mathbf{Q}}} \right) \left(\frac{\partial \mathbf{g}_{\mathbf{Q}}(\mathbf{x}_{\mathbf{Q}}, \mathbf{u})}{\partial \mathbf{x}_{\mathbf{Q}}} \right)^{-1} \boldsymbol{\Phi}(\mathbf{x}_{\mathbf{Q}})$$

where the non-zero components of the partial differential vector corresponds to the $[V_{kr}, V_{ki}, V_{mr}, V_{mi}]$ in the state vector $\mathbf{x}_{\mathbf{Q}}$.

$$\frac{\partial P_{mn}}{\partial \mathbf{x}_{\mathbf{Q}}} = \begin{bmatrix} 0 \\ \vdots \\ G_{mn}(2V_{mr} - V_{nr}) + B_{mn}V_{ni} + 2G_{smn}V_{mr} \\ G_{mn}(2V_{mi} - V_{ni}) - B_{mn}V_{nr} + 2G_{smn}V_{mi} \\ -G_{mn}V_{mr} - B_{mn}V_{mi} \\ -G_{mn}V_{mi} + B_{mn}V_{mr} \\ 0 \\ \vdots \\ 0 \end{bmatrix}, \frac{\partial Q_{mn}}{\partial \mathbf{x}_{\mathbf{Q}}} = \begin{bmatrix} 0 \\ \vdots \\ G_{mn}V_{ni} + B_{mn}(V_{nr} - 2V_{mr}) - 2B_{smn}V_{mr} \\ -G_{mn}V_{nr} + B_{mn}(V_{ni} - 2V_{mi}) - 2B_{smn}V_{mi} \\ -G_{mn}V_{mi} + B_{mn}V_{mr} \\ G_{mn}V_{mr} + B_{mn}V_{mi} \\ 0 \\ \vdots \\ 0 \end{bmatrix}$$

Appendix B: Solving for Equilibrium Forward and Spot Prices

According to the characterization of *PTDF* matrix in the day-ahead forward wholesale market, take equations (7.15) and (7.20) into (7.23), we get the following,

$$\sum_{i=1}^{I} f_{Gi,k}\left(\frac{P_{Ref}^{F}-f_{Gi,k}\lambda_{k}^{F}-E\left[P_{Gi}^{S*}(\varpi)\right]}{A_{G}Var\left(P_{Gi}^{S*}(\varpi)\right)}+\frac{Cov\left(\rho_{Gi}^{*}(\varpi),P_{Gi}^{S*}(\varpi)\right)}{Var\left(P_{Gi}^{S*}(\varpi)\right)}\right)$$

$$-\sum_{j=1}^{J} f_{Lj,k}\left(\frac{E\left[P_{Lj}^{S*}(\varpi)\right]-P_{Ref}^{F}+f_{Lj,k}\lambda_{k}^{F}}{A_{L}Var\left(P_{Lj}^{S*}(\varpi)\right)}-\frac{Cov\left(\rho_{Lj}^{*}(\varpi),P_{Lj}^{S*}(\varpi)\right)}{Var\left(P_{Lj}^{S*}(\varpi)\right)}\right)=T_{k} \tag{B.1}$$

Taking (7.5a) into (B.1), we have,

$$P_{Ref}^{F}\left(\sum_{i=1}^{I}\frac{f_{Gi,k}}{A_{G}Var\left(P_{Gi}^{S*}(\varpi)\right)}+\sum_{j=1}^{J}\frac{f_{Lj,k}}{A_{L}Var\left(P_{Lj}^{S*}(\varpi)\right)}\right)$$

$$-\lambda_{k}^{F}\left(\sum_{i=1}^{I}\frac{\left(f_{Gi,k}\right)^{2}}{A_{G}Var\left(P_{Gi}^{S*}(\varpi)\right)}+\sum_{j=1}^{J}\frac{\left(f_{Lj,k}\right)^{2}}{A_{L}Var\left(P_{Lj}^{S*}(\varpi)\right)}\right)$$

$$=\left(\sum_{i=1}^{I}\frac{f_{Gi,k}E\left[P_{Gi}^{S*}(\varpi)\right]}{A_{G}Var\left(P_{Gi}^{S*}(\varpi)\right)}+\sum_{j=1}^{J}\frac{f_{Lj,k}E\left[P_{Lj}^{S*}(\varpi)\right]}{A_{L}Var\left(P_{Lj}^{S*}(\varpi)\right)}\right)+T_{k^{F}}$$

$$-\left(\sum_{i=1}^{I}\frac{f_{Gi,k}Cov\left(\rho_{Gi}^{*}(\varpi),P_{Gi}^{S*}(\varpi)\right)}{Var\left(P_{Gi}^{S*}(\varpi)\right)}+\sum_{j=1}^{J}\frac{f_{Lj,k}Cov\left(\rho_{Lj}^{*}(\varpi),P_{Lj}^{S*}(\varpi)\right)}{Var\left(P_{Lj}^{S*}(\varpi)\right)}\right) \tag{B.2}$$

Combined with market balancing condition (7.22), we have (7.24a-c)

Appendix C: Solving for Forward Risk Premium

According to the market balancing conditions in the day-ahead forward markets

$$\sum_{i=1}^{I} Q_{Gi}^{F} = \sum_{j=1}^{J} Q_{Lj}^{F} \tag{C.1}$$

Taking (7.15) and (7.20) into (C.1)

$$\sum_{i=1}^{I}\left(\frac{P_{Gi}^{F} - E\left[P_{Gi}^{S*}(\varpi)\right]}{A_G \cdot Var\left(P_{Gi}^{S*}(\varpi)\right)} + \frac{Cov\left(\rho_{Gi}^{*}(\varpi), P_{Gi}^{S*}(\varpi)\right)}{Var\left(P_{Gi}^{S*}(\varpi)\right)} \right)$$

$$= \sum_{j=1}^{J}\left(\frac{E\left[P_{Lj}^{S*}(\varpi)\right] - P_{Lj}^{F}}{A_{Lj} \cdot Var\left(P_{Lj}^{S*}(\varpi)\right)} - \frac{Cov\left(\rho_{Lj}^{*}(\varpi), P_{Lj}^{S*}(\varpi)\right)}{Var\left(P_{Lj}^{S*}(\varpi)\right)} \right) \tag{C.2}$$

Based on

$$E\left[P_{n}^{S}(\varpi)\right] = E\left[P_{Ref}^{S}(\varpi)\right] - f_{n,k^S} \cdot E\left[FG_{k^S}^{S}(\varpi)\right] \tag{C.3}$$

(C.2) can be rewritten as,

$$\sum_{i=1}^{I} \frac{\left(P_{\mathrm{Ref}}^{F} - f_{Gi,k}\lambda_{k}^{F}\right) - \left(E\left[P_{Ref}^{S}(\varpi)\right] - f_{Gi,k}E\left[\lambda_{k}^{S}(\varpi)\right]\right)}{A_G Var\left(P_{Gi}^{S*}(\varpi)\right)} + \sum_{i=1}^{I} \frac{Cov\left(\rho_{Gi}^{*}(\varpi), P_{Gi}^{S*}(\varpi)\right)}{Var\left(P_{Gi}^{S*}(\varpi)\right)}$$

$$= \sum_{i=1}^{I} \frac{\left(E\left[P_{Ref}^{S}(\varpi)\right] - f_{Lj,k}E\left[\lambda_{k}^{S}(\varpi)\right]\right) - \left(P_{\mathrm{Ref}}^{F} - f_{Lj,k}\lambda_{k}^{F}\right)}{A_L Var\left(P_{Lj}^{S*}(\varpi)\right)} - \sum_{j=1}^{J} \frac{Cov\left(\rho_{Lj}^{*}(\varpi), P_{Lj}^{S*}(\varpi)\right)}{Var\left(P_{Lj}^{S*}(\varpi)\right)} \tag{C.4}$$

Reorganize the items of (C.4) leads to (7.30b)